VYSOKÉ UČENÍ TECHNICKÉ V BRNĚ

FAKULTA CHEMICKÁ

P.H.D. Thesis

Characterisation of the Physical Chemical Processes using the Fractal and Harmonic Analysis

Basel, Kroměříž 2009 Ing. Jan Haderka

Brno University of Technology
Faculty of Chemistry
Purkyňova 464/118, 61200 Brno 12

Dissertation Thesis Assignment

Number of dissertation thes	**FCH-DIZ0022/2008**	Academic year: **2008/09**
Institute:	Institute of Physical and Applied Chemistry	
Student:	**Haderka Jan, Ing.**	
Study programme:	Physical Chemistry (P1404)	
Study field:	Physical Chemistry (1404V001)	
Head of thesis:	**prof. Ing. Oldřich Zmeškal, CSc.**	
Supervisors:		

Title of dissertation thesis:

Characterisation of the Physical Chemical Processes
using the Fractal and Harmonic Analysis

Dissertation thesis assignment:

Study of the kinetics of the yeast cell division and its growth
Determination of the count and size based distribution of the yeast cells

Deadline for dissertation thesis delivery: 30.9.2009

Dissertation thesis is necessary to deliver to a secretary of institute in three copies and in an electronic way to a head of dissertation thesis. This assignment is enclosure of dissertation thesis.

Haderka Jan, Ing. Student	prof. Ing. Oldřich Zmeškal, CSc. Head of thesis	prof. Ing. Miloslav Pekař, CSc. Head of institute

In Brno, 3.10.2009

doc. Ing. Jaromír Havlica, DrSc.
Dean

Abstract

Existuje mnoho různých způsobů jak analyzovat disperzní systémy a fyzikálně chemické processy ke kterým v takových systémech dochází. Tato práce byla zaměřena na charakterizaci těchto procesů pomocí metod fraktální analýzy. Obrazová data sledovaných systémů byla analyzována pomocí waveletové analýzy. V průběhu práce byly navrženy různé optimalizace samotné analýzy, převážně zaměřené na odstranění manuálních operací během analýzy a tyto optimalizace byly také zakomponovány do programového vybavení pro Harmonickou a Fraktální Analýzu (HarFA), který je vyvíjen na Fakultě chemické, VUT Brno.

Summary

There are many different ways to characterize the dispersed systems and processes occuring in such systems. This work focuses on use of Fractal properties of such systems to describe the physical and chemical processes occuring in such systems. The Fractal properties are calculated from the image data of the systems under the observation using the Wavelet analysis. Since the Fractal Analysis can be relatively easily automated, the work also focuses on algorithmisation of the analysis and the removal all manual steps from the process. The automation have been performed by incorporating all the findings into the software for Harmonic and Fractal Analysis (HarFA) developed at the Faculty of Chemistry, BUT.

Klíčová slova

aggregace, predikce, experimentální studie, mikrobiologie, buňky, kvasinky, fraktály, geometrie, kolonie buněk, distribuce velikostí, fraktální dimenze, fraktální míra, wavelety, Fourierova transformace, harmonická analýza

Keywords

aggregation, prediction, experimental studies, microbiology, cells, yeast, fractals, geometry, populations, size distribution, fractal dimension, fractal measure, wavelets, Fourier transform, harmonic analysis

Haderka, J. *Characterisation of the Physical Chemical Properties using the Fractal and Harmonic Analysis* Brno: Brno University of Technology, Faculty of Chemistry, 2009. 80 p. Headed by prof. Ing. Oldřich Zmeškal, CSc.

DECLARATION

I declare that the diploma thesis has been worked out by myself and that all the quotations from the used literary sources are accurate and complete. The content of the diploma thesis is the property of the Faculty of Chemistry of Brno University of Technology and all commercial uses are allowed only if approved by both the supervisor and the dean of the Faculty of Chemistry, BUT.

.....

student's signature

Contents

1. ACKNOWLEDGEMENTS

I would like to thank to Prof. Ing Oldřich Zmeškal, CSc. for supervising my doctoral study. Seven years ago he convinced me to work on this thesis in the department of Physical Chemistry and I never regretted my choice.

I would also like to thank to my family and specially to my wife Renata for all the support and graceful handling of all the time I have taken from the family while studying and working on the thesis.

2. INTRODUCTION

This work describes the current understanding and possibilities of the application of fractal geometry and methods for describing properties defined by it for classification and description of coarsely grained systems such as groups of living organisms. Living organisms of same family have fundamental properties very close to each other therefore they naturally fit the description of fractals as self similar sets of finite points. Single organism or its description in form of image could be thought of as single set and colony of such organisms could be then described as fractal. The use of fractal properties for data analysis is not completely novel. However the methods used to obtain the fractal properties of the systems and their individual components are still evolving. The fractal properties of the systems can be also put into a wider picture and used to capture and describe the processes happening in the systems if the data are collected over a time. In following pages the attempt had been made to describe use of fractal analysis to provide such a description and the findings and optimisations of the method made during the work have been incorporated into the software for harmonic and fractal analysis HarFA, developed at the Faculty of Chemistry, Brno University of Technology.

3. INITIAL STATE OF THE RESEARCH

Physical chemical processes are participants of all experiments and their characterisation is a mean of describing the experiment and our understanding of it. While this process is easy in simple and straightforward experiments, the characterisation of processes becomes quite difficult with increasing complexity of the experiments. The difficulty arises from the fact that many sub-processes are present and affect each other. This is specially true in experimenting with heterogeneous systems in which elements act independently and affects each other only indirectly. One such example are heterogeneous disperses of living organisms like bacteria or cells. This works attempts to show how Fractal and Harmonic Analytical methods can help in characterisation and understanding of such systems. More precisely the way of use of Fractal and Harmonic analysis to classify the changes in yeast cell colonies under different conditions will be described.

The main benefit of using Fractal and Harmonic analysis methods in comparison to more classic approaches is the intrinsic property of such analysis – looking at the whole experimental area as whole rather then examining each piece and its effect separately. This property of Fractal and Harmonic analysis methods makes them very well suited for examining heterogeneous unstable systems with complex interactions such as living cell colony.

3.1 Classification of researched systems

3.1.1 Coarsely Disperse Systems

Disperse system or shortly dispersion is a physical system containing two distinct parts. Those are *dispersed particles* and *dispersion environment*. Distinct physical properties of each part are then crucial for the system properties as whole.

Disperse systems are commonly classified based on some of their properties. Most often based on those properties that are in particular interest to experiment involving such system.

Homogeneity is one of the often used classifications of disperse systems. Based on homogeneity systems are recognized as *homogeneous* and *heterogeneous*. Homogeneous systems are single physical phase systems. They are *true solutions* and tend to be very stable. The degree of dispersion is constant (except when changing phase). Heterogeneous systems on the other hand have each of the participants in different state and are divided by physical boundary. Such systems tend to be less stable, and unless kept in the dispersion state by force (e.g. mixing) they will separate freely over time[1].

Type of dispersion based classification divides disperse systems based on size distribution of dispersed particles in the system. U*niform* or *mono-disperse* and *non-uniform* or *poly-disperse* systems are then recognized based on size distribution. Mono-disperse systems have all particles of approximately same size while size of particles of poly-disperse systems vary.

Granularity is the property of disperse systems recognized only for heterogeneous system. As such granularity is a function of the size particles dispersed in the system. Smaller particles are the finer granularity system has. Granularity can be also expressed as a *degree of dispersion*, which is then defined as

$d = x^{-1}$, where x is an average size of particles.

Degree of dispersion based classification of disperse systems introduces following different systems:

Macro coarse grained dispersions with degree of dispersion $d > 10^{-5}$ m

Micro coarse grained dispersions with 10^{-6} m < d < 10^{-5} m

Colloid dispersions with 10^{-9}m < d < 10^{-6}m

Analytical dispersions – true solutions, uniform, $d < 10^{-9}$m

Yet another classification of dispersions is divides systems based on the shape of their particles. Dispersions can be then divided on *isometric dispersions* whose particles are roughly same in all three axes and an-isometric *dispersions* whose particles are significantly different at least in one of the axis [2].

The nomenclature and exact definition of different possible dispersed systems can be found for example at [3] or [4].

3.1.2 Dynamic dispersed systems

Dynamic coarsely dispersed systems are the systems fitting the above mentioned description which are not in stable state. The instability of the system can be caused by many different factors. In organic or inorganic coarsely dispersed system the common factor is gravity causing separation of the particles in the system by process known as sedimentation. Another such factor can be for example introducing electric current in the system and causing the flux by forcing particles to orient or move in direction of their charge. Hereby described and analysed coarsely dispersed systems are in dynamic state by their nature as the described systems are living cells in their respective living environment or sets and colonies of such cells. The dispersity of the living systems is achieved by each of the living cells maintaining membrane separating the organism from its environment throughout the life time. The study of such systems is normally concern of the field of Microbiology, or more precisely, Microbiology is a study of micro-organisms that can be either unicellular or cell-clustered [5].

3.2 Analysis methods used in Microbiological studies

Each of the micro-organisms studied is generally separated from the environment by a membrane. Therefore micro-organisms and their living environment form coarsely dispersed systems and can be analysed by method similar to those used to study coarsely dispersed systems.

The common subjects of study in the field of microbiology are static and dynamic properties of living systems. Static studies concern themselves with the characterization of micro-organisms based on their size, shape, when living in clusters also the properties of the clusters as a whole are studied. Dynamic or kinetic properties of systems are then observed and described as functions of grow, life span, multiplication or degradation of single organisms or those of the clusters. When studying clusters also the maximum and minimum sizes of the clusters and the maximum sizes of the individual cells relative to their position in the cluster, survival factors and colony forming properties [7] are studied.

Although microbes are commonly associated with illnesses and degradation processes they are also responsible for many other processes specially those widely employed in food processing and pharmaceutical industry. Such processes are for example fermentation, brewing, waste water treatment, antibiotic production, enzyme and protein productions. Industrial use requires use of various analytical method to quantify those processes and provide prediction and verification of production line output and quality.

In order to provide industrial scale and quality analysis and characteristics of various microbiological systems and those of microbe behavioural changes in various kinds of environments many different analytical methods have to be employed. Industrial use also predicates needs of accuracy and precision.[7] Classical methods of analysing microbiological systems are for example cell enumerations, turbidity based cell growth measurement and others.

3.2.1 Cell concentration measurements

There are many experiments in which it is necessary to determine the cell concentration. For example in microbiology, the cell culture and many other experiments that require use of the colonies of the cells. One way to determine the density of such cell suspension is spectrophotometrically, however this method doesn't allow an assessment of the viability of the single cells in the suspension nor does it make possible to distinguish the individual cell types.

The number of cells per unit of the volume is often determined by the device called a counting chamber. The device evolved in a general use from a more specialized device called a *hemocytometer*, that was originally used for performing the blood cell counts (hence the “hemo” in the name).

One of the conditions necessary to satisfy in order to be able to use counting chamber to obtain a count of cells is a need to dilute the solution enough so the single cells or other solid particles in the solutions do not overlap. It is also necessary for the cells in such diluted state to be uniformly distributed throughout the solution. To perform the cell count, magnification of the observation instrument need to be set so the desired cell type can be easily recognized. Once set, the the cells are counted in the selected squares so the total count is around 100 cells. Such a high number is necessary to obtain a statistically significant count. When performing a count of large cells, this usually means that four large corner squares and the middle square have to be counted. When counting dense suspensions of small cells, it is usually enough to count cells in the four 1/25 mm^2 corners and the middle square in the centre. To avoid a bias the specific counting pattern has to be selected. For example for overlapping cells ruling is made that they are counted as being inside when they overlap the top right, and considered outside when they overlay at the bottom or left.

Lets take counting using Neubauer hemocytometer as an example. Supposing the count have been performed using the rules describe above, and the total of 175 particles was found in the five small squares and each square area is of the 0.04 mm^2 (or 1/25 mm^2) with a depth of 0.1 mm, then the total volume in each square would be 0.004 mm^3 (0.04 × 0.1). The 5 squares that have been counted is then 5 times 0.004 mm^2 or 0.02 mm^3. Since the total count have been 175 cells in a 0.02 mm^2 the cell concentration is then 175 divided by 0.02 or 8750 cells per µl or 8 750 000 cells per ml.

Quite many experiments however works with larger cells and are therefore in need of counting cells over larger surface area. Such count can be the total number of cells in the middle square plus the four large corner squares together. Each large square has a surface area of 1 mm^2 and a depth 0.1 mm, which gives a total volume of 0.1 mm^3. Suppose the total of 140 cells have been counted in the selected squares. Since the 5 squares have been counted, the total of 140 cells per 0.5 mm^3 or 280 cells/mm^3 have been found. To get the value in ml simply multiply by 1000 obtaining total of 280 000 cells/ml.

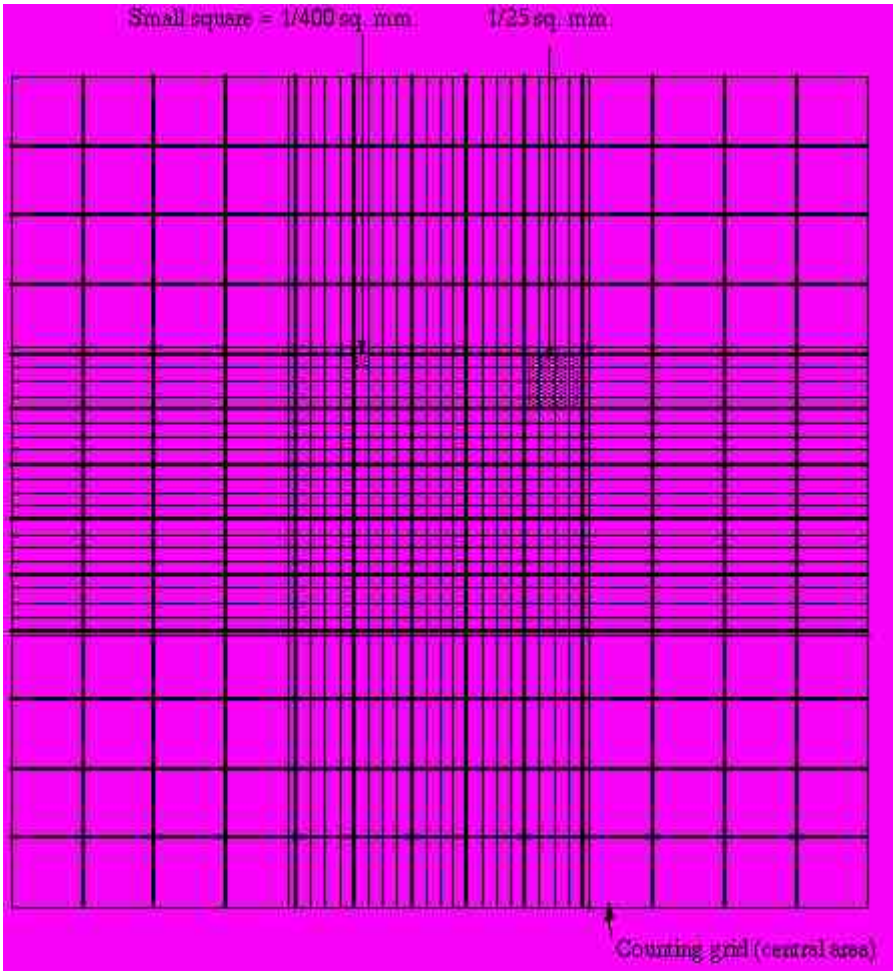

Figure 1: Counting Chamber grid [38]

Another method similar to conventional plate counting using the chamber grid is for example a spiral plate counting method. In this method a mechanical plater inoculates a rotating agar plate with liquid sample. [38] The sample volume concentration decreases from the centre to the edge of the plate. Similarly to the conventional method, the agar plate is divided in the segments (see Figure 2) and the concentration is determined by counting the colonies on the parts of the dish that are easily countable and dividing this by the volume of given section. One inoculation is used to determine volumes between 500 to 500 thousands of micro-organisms. The method is in details described for example at [31],[32] and [33].

The spiral counting method is often used for counting bacteria in milk and diary products. The detailed comparison of different methods of counting for yeast cells can be found at [34].

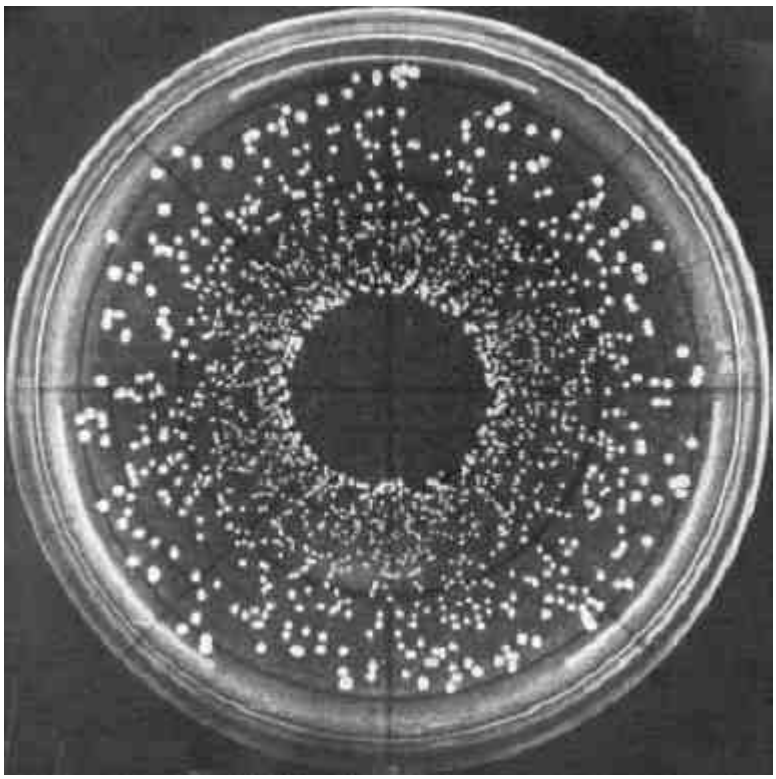

Figure 2: Spiral Plate Counting Method; Agar plate divided in segments.

3.3 Dynamic experiments - Microbial growth

Microbes have different phases during their growth cycle. Dynamics of those phases are tell-tale signs of the quality of the environment as well as indicating health and strength of particular micro-organism. Due to its relative simplicity and wide range of properties that can be observed or deduced from the experiment is phase of growth observation commonly executed kind of experiment.

Once an organism is introduced into a growth medium of choice this medium is inoculated with the particular organism of choice. However, the growth of the inoculum doesn't begin immediately, it takes a little while before the organism adapts to the new environment. This period of the adaptation is called the lag phase. Once the lag phase is over, the rate of the growth of the organism increases steadily for a time period usually called log or exponential phase. When the exponential phase is over, the rate of the growth slows down. The slow down is due to concentration of nutrients continuously falling while the concentration of toxic substances in the proximity of the organism is increasing. The phase during which the increase of the rate of the growth is checked is called the deceleration phase. After the deceleration phase the growth ceases completely and the culture enters a steady state or a stationary phase. The chemical constitution remains unchanged unless other micro-organisms contaminate the culture. Another possible source of contamination can also be the mutation of the organism itself. Such source of contamination is then called internal contamination. Otherwise the biomass of the experimental environment remains constant, except for when certain accumulated chemicals in the culture lyse the cells (a process called chemolysis).

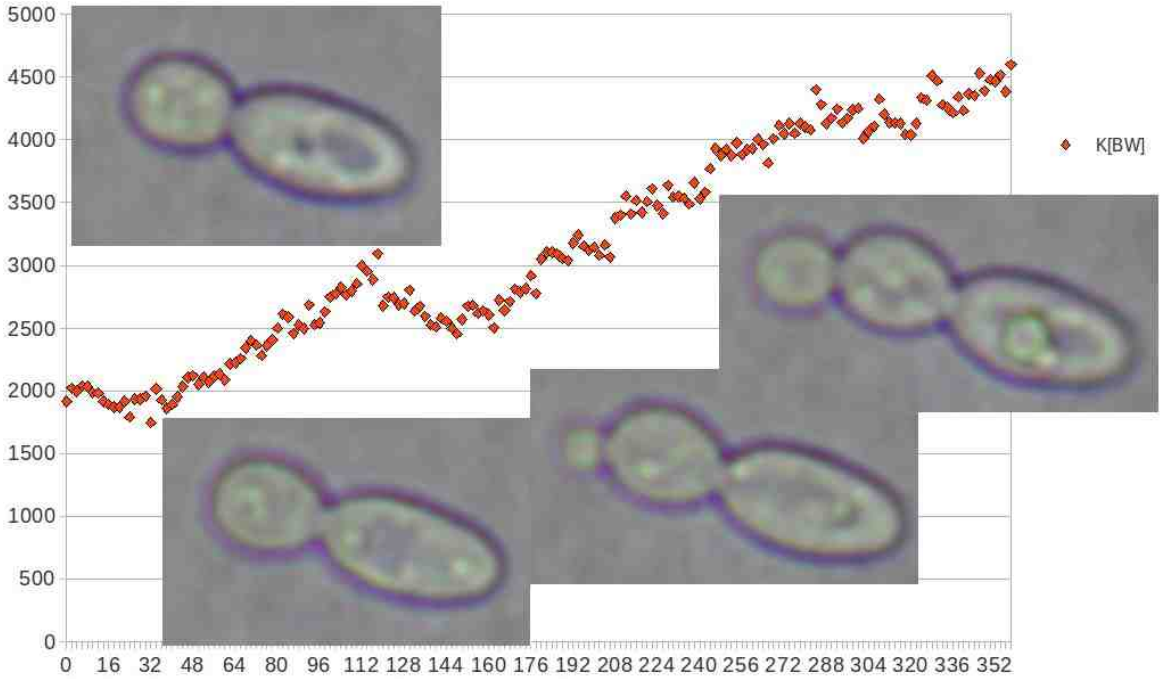

Figure 3: *Candida vini*, cell growth observation, Fractal Measure of the cellular wall

The experimental goal of observing of growth phases of microbial organisms is to quantify its dynamics. This can be done by measuring change in properties like, size of the organism, amount of multiplication cycles during fixed period of time, length of the adaptation, steady growth phase and deceleration phase. Common setup requires fixing of the plate with media and observed culture to prevent accidental mixing of the media which would affect growth dynamics. Another complication arising during experiment is tendency of some of the micro organisms to move around in their environment and putting therefore constrains on the observable area under the microscope.

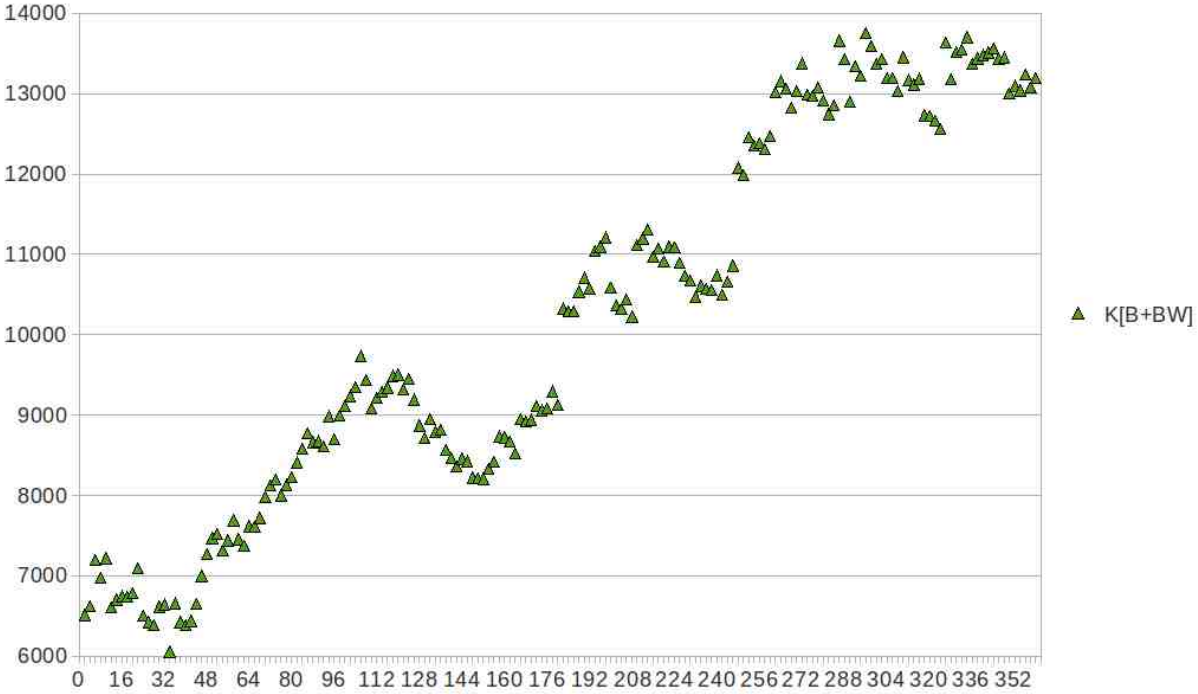

Figure 4: *Candida vini*, cell growth, Fractal Measure of cellular walls and the boundaries

The example of *Candida vini* yeast cell growth experiment in Figure 3 shows the changes in the Fractal Measure values proportional to the size of the cell measured as a mass of the cellular wall of the observed cell. See the chapter 3.4.1.3 for more detailed explanation of the Fractal Measure and its significance. The small drop in the Fractal Measure values just before cell starts dividing is caused by the thinning of the wall in the place where dividing will take the place just before it occurs. The mentioned drop is becoming even more pronounced when Fractal Measure of the cellular wall including the boundary between the wall and cell inside and between the wall and the surrounding media is taken in the account as shown in Figure 4.

3.3.1 Analytical methods in growth experiments

Classic examples of analysing growth experiment data are for example quantification techniques based on measurements of changes in turbidity of media during experiment [35]. While this technique allows for observation of changes in the media caused by microbial growth it lacks of ability to exactly quantify the cells in experiment. Only relative changes can be measured or calibration curve for given media and micro-organism must exist obtained by other means.

Another example of technique used for growth analysis is cell/colony enumeration. Variations of this technique are used at industry for example to quantify amount of micro organisms in milk [33] Cell/Colony enumeration is used very often even thought counting of individual cells or colonies is very tedious. This technique provides absolute numbers and is therefore well suitable for standards and controling of the processes. Commonly used variations of this technique are for example Conventional plate counting[36] and Spiral plate counting[37].

3.3.2 Commonly faced problems in cell/colony enumeration

Due to the size of micro-organisms, magnification is needed and observation of the experiment is normally done using microscope. Under microscopic view counting of visible separate elements, be it cells or colonies is difficult. This issue is normally overcome by use of grids covering visible field. A counting chamber, for example Burker counting chamber shown in (Figure 5) is commonly used to facilitate cell counting or semi automatic counters such as Quebec colony counter (Figure 6) is used to simplify colony counting.

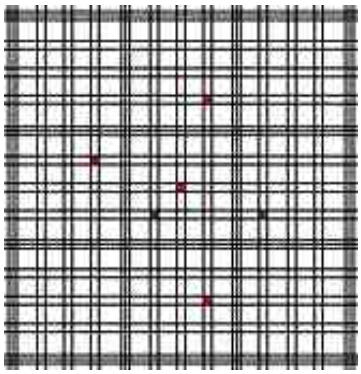

Figure 5: Burker Counting Chamber. In red are highlighted the random grid cells selected to estimate the total count and concentration of cells in the media.

Use of the counters simplifies the process of experiment, yet is doesn't completely remove the tedious work of counting cells or colonies over whole grid. Not only is such process cumbersome it is also error prone. To provide better results and to allow for re-evaluation of the experiment results it is beneficial to record images of the experiment and analysed observed data separately.

Figure 6: Quebec Colony Counter

3.4 Image Analysis

Image analysis is a method using recorded image data as a source for the analysis rather then live experiment. The main advantage of this indirect analytical approach is the ability to run multiple different sub analysis on the same data set and possibility to re-evaluate results for as long as the captured images are kept. Traditionally, the use of image analysis have been limited by the resolution of images captured, long and slow processing of the classic photography and the minimum amount of computing power necessary to analyse image in acceptable time frame. With the continuous rapid increase in available computing power of available computers and the resolution of available CCD cameras as well as their speed, the main obstacles of using image analysis to indirectly analyse the experimental data have been removed and more complex methods can be used to perform the analysis. The Fractal and Harmonic analytical methods belong to this category of more computationally expensive methods as they use the whole image to provide a complex view of analysed data.

Another advantage of using the image data for the analysis is an increased possibility of automating the experiment, which is specially useful in long running experiments such as observation of cell or cellular colonies growth. Problems faced with autonomous, unattended experiment runs is often a premature termination of the experiment due to movement of observed cell/ colony from the visual area of the camera backed microscope. Such problem doesn't occur when whole plate is in the visible field, but in many circumstances only part of the plate is of interest during experiment and keeping whole plate in visual field reduces maximum allowable magnification in the experiment and thus the amount of interesting data that can be captured and analysed later. Due to this fact it is necessary to provide computing techniques intelligent enough to be able to extrapolate further movement of observed cells from available data and to instrument positioning data to the plate holder. While not shown here, the methods and algorithms for observing the cell growth can be also used to provide

such information simply by including the x-y positional data in the analysis rather then discarding them.

3.4.1 Fractal image analysis

3.4.1.1 Fractal Theory (FT)

Fractal theory is set of theorems and lemmas defining fractals as finite closed compact and bounded subsets of fractal space. Due to the special properties of the fractal spaces and fractal metrics new properties of the set can be measured. Those are so called fractal properties. However not every group of points forms necessarily fractals. In order to become fractal, group has to fulfil on its content requirements described by the fractal theorems (like compactness, completeness, bounded, etc.) [9].

Fractals as such can be and are commonly divided into two distinct groups. First of such groups are so called deterministic fractals that are created by repeated self projection of some simple mathematical function on defined subspace [9]. Example of such fractals would be Cantor set (1D) or Sierpinsky Triangle or Sierpinsky Carpet (both 2D). Sierpinsky Carpet is shown in Figure 10. The other group of so called non-deterministic fractals is a group of objects that are usually rules by laws too complex to be defined in exact mathematical terms, but whose show fractal properties of self similarity. Such objects are of special interest as fractal geometry and theory gives us right tool in order to define those systems in exact terms or at least closely estimate what their definition may look like.

Most commonly shown example of non-deterministic fractals in every day environment are a coast line, trees, snow flakes [9]. In case of a coast line fractal group of points is defined as a δS – a group of the border points of the land (or of the sea, since both land and sea groups are defined as open, they do not contain their own boundary). In other examples the requirements of the fractal space definition are satisfied by grouping single objects into the sequence and achieving requirements of continuity by defining f continuous for all points from one tree to another or from one flake to another. The transformations is then defined as

$f(x)=A(x)+t$ generally,

or more exactly, in 2D Euclidean space $\begin{vmatrix} f_1(x,y) \\ f_2(x,y) \end{vmatrix} = \begin{vmatrix} a & b \\ c & d \end{vmatrix} \begin{vmatrix} x \\ y \end{vmatrix} + \begin{vmatrix} e \\ f \end{vmatrix}$

The partial equations then look as $x_{i+1}=ax_i+by_i+e$ and $y_{i+1}=cx_i+dy_i+f$

Apart from the common properties characteristic and defined for any kind of group, for fractals there are defined few more properties. The most basic one is the Hausdorff distance defined as $h(A,B)$ where A and B are two closed, compact and bounded sets [9]. $h(A,B)$ itself is then defined as

$$h(A,B)=d(A,B)\vee d(B,A)$$

However most commonly used properties are Fractal Dimension and Fractal Measure. Those properties are not concerned with distance between single sets but with the continuity

of the fractals. Each of them can be obtained by number of different ways and those properties describe amount of (or lack of) self-similarity between 2 fractals as well as the "size" of the fractal. As it is true for other properties it is true also for the fractal properties that meaning of the property in connection to the defining space stays same over various transformation of the space as long as the transformation is metrically equivalent and reversible homomorphism describing the transformation can be defined [9].

Over past few years the various methods for calculation of fractal properties and their use for obtaining other characteristics of measured objects have been developed. The recent development of techniques for calculation of fractal properties and their use was driven mainly by advances in the computational power of current computers and their ability to perform complex calculations in near real time. This in turn allowed for use of the fractal calculation in characterization of other experiments as an addition to the classical characteristics defined.

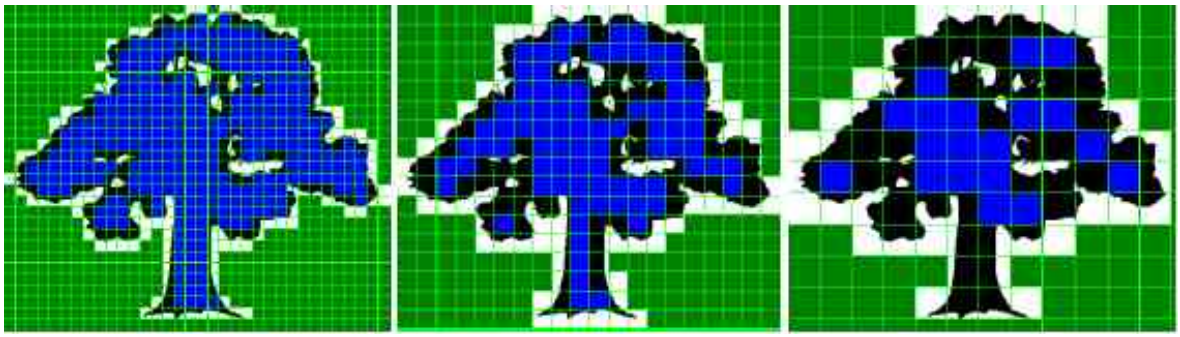

Figure 7: Box counting method - coverage of the tree by boxes of different size.[11]

3.4.1.2 Fractal Dimension

Fractal dimension is a number describing character of the fractal. There are various methods for calculating such a number; some of them producing numbers more useful then others. Fractal dimension is used to deterministically compare two fractals without need to evaluate them point by point [9]. By simplest of all the methods of obtaining the Fractal Dimension – Box Counting method, it is defined and calculated as a trend of changes of amount of squares necessary to cover the fractal based on changes in size of the squares.

The fractal dimension is an extended non-negative real number (that is a number in the closed infinite interval [0, ∞]) associated to any metric space [11]. It was introduced in 1918 by the mathematician Felix Hausdorff [13]. Many of the technical developments used to compute the Fractal dimension for highly irregular sets were obtained by Abram Samoilovitch Besicovitch [14]. For those reasons fractal dimension is often referred to as Hausdorff dimension or as Hausdorff-Besicovitch dimension. Less frequently it may is called in some literature as the capacity dimension due to its ability to quantify fractal space [15],[16].

Fractal Dimensions are the attempts to quantify how densely fractal occupies metric space in which it lies [9].

Importance of the Fractal Dimension arises from its ability to characterize fractal as a whole rather then in terms of point by point connection as in real word experiments we are often faced with the objects and sets which due to their complexity can be only approximately measured (aggregates of sand or dust, snow flakes, cell colony, feathers, tree nodes, etc.). The

fractal dimension is often the only way how to quantitatively compare such sets in reasonable amount of time.

One of the possible ways of describing fractal dimension is to think of the dimension of the set as a similar to the topological dimension of the set. However there are some very fundamental differences between the two for highly irregular sets. For example topological dimension of Cantor Set (1D, Euclidean metric) is a zero while it behaves like a set of a higher dimension. This is taken into account when fractal dimension is calculated by incorporating a level of self projection of the set into itself in the dimension definition. The fractal dimension for the Cantor Set is approximately 0.63 or more precisely ($\frac{\ln ۲}{\ln ۳}$).

The exact mathematical description can be found for example at [9],[10], for purpose of this introduction it will suffice to state that:

$\dim_{fra} \geq \dim_{top}$, and

$\dim_{fra}(X) = \dim_{top}(X')$, for all X and X' that are homomorphic.

3.4.1.3 Fractal Measure

Fractal measure, also called Hausdorff Measure was defined by the Hausdorff during his studies of the fractals. When fractal is defined in a metric space[3D, Euclidean metric], it is possible to find its measure by counting the number of balls of a given radius needed to completely cover the set defined in a metric space [9]. This definition leads to the so called *box-counting theorem* and *box-counting method.* Hausdorff approached problem of defining fractal measure differently and using a measure theory [10] he defined a fractal measure on subsets of *X*, one for each possible dimension $s \in <0,\infty)$.

Figure 8:

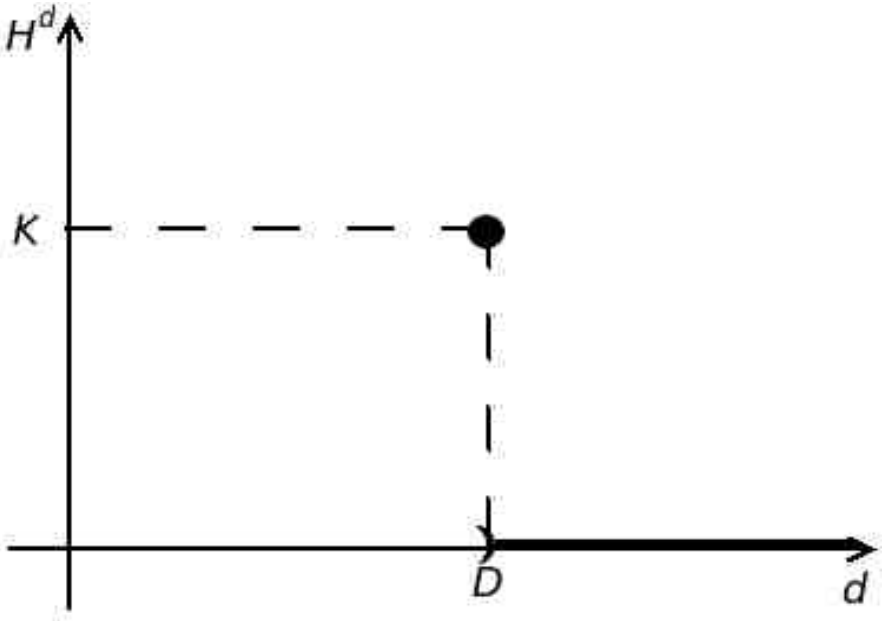

Hausdorff's *d*-dimensional measure, *D*-Hausdorff-Besicovitch (fractal) dimension, *K*-Hausdorff-Besicovitch (fractal) measure [12]

D-dimensional measure H^d is then defined on all the subsets of the spaces with same or lower dimensions. For example for $\Re^3$ that would be defined over the line (d = 1), plane (d = 2) and cube (d =3).

Other definition (using the coverage of the space by balls) would be [9]:

$H_\delta^d(E)$

In other words fractal measure is an infinitum of all $h>0$, such that for all $\delta>0$ E can be covered by countably many closed sets with diameter less or equal to δ and the sum of the d^{th} powers of such diameters is less then or equal to h.[9]

There are also different definitions of the fractal measure described at [18],[19],[20],[21], [22], some of which maps it to the rescaled Borel's measure λ and some of which makes fractal measure coincide exactly with Borel's measure in Euclidean space. With the current level of understanding of the fractal geometry and laws which governs it, both of the latter above mentioned approaches seem to be valid and useful each for their own purposes. In the end, the exact mapping can be described as rescaling with a factor 1 which makes a second approach special case of the first one.

3.4.2 Methods for calculation of the fractal properties

The previous works of for example [8],[11],[29] have suggested a few different optimisations of methods for calculation of fractal properties and using a Fractal Dimension and Fractal Measure to obtain a quantifiable information about the image data.

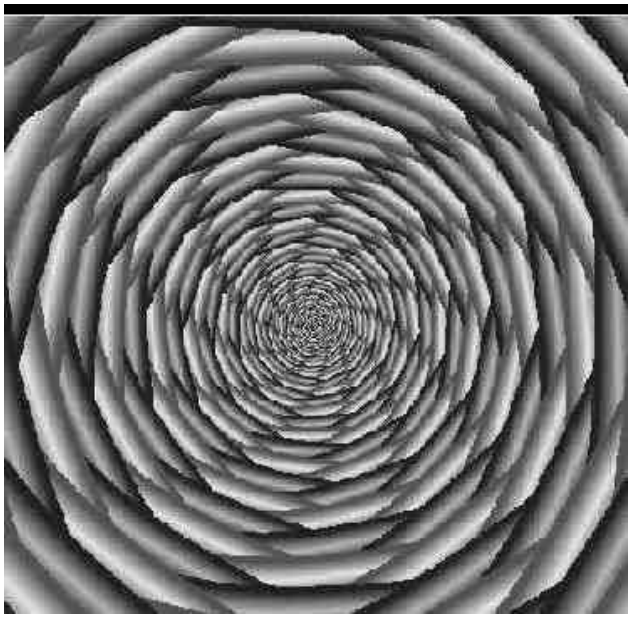

Figure 9: Deterministic Carlson Fractal (© Carlson Fractal Collection)

The main benefit of such optimizations have been increased speed of calculation of the properties without loss of precisions. The optimisations are based around the fact that it is possible to use a Haar transformations on the image data to obtain fractal properties of the analysed image (or image set) giving the exactly same results as the classic Box Counting method.

3.4.2.1 Box Counting Method

The box counting method is based on dividing the analysed area into the boxes by laying grid over the analysed image data. Let's say the analysed image is a black drawing of some shape on white background, and the N_B is a number of boxes of a linear size s_B necessary to cover the whole object. The Fractal dimension D_B is then given by

$$N_B = s_B^{-D_B}$$

By measuring the distribution of N for different box sizes, the D_B can be then obtained by a power law fit for the obtained distribution.

3.4.2.2 Periodic analysis – Discrete Fourier transformation

The base of the periodic transformations can be either the harmonic (sin, cos) or orthogonal (e.g. sign) function. During the transformation, all singular functions are made by repeating the function executing while varying the measure [23].

For the purposes of image analysis, the most often used periodic analysis functions are discrete Fourier transformation, cos transformation and Walsh-Hadamar transformation. The discrete Fourier transformation is a linear orthogonal transformation changing analysed image $f(m,n)$, where $m = 1, 2, \ldots M-1$ and $n = 1, 2, \ldots N-1$ are the coordinates of the image of the size $M \times N$ on a discrete spectra pre-set by complex function $F(k, l)$, where $k = 1, 2, \ldots M-1$ and $n = 1, 2, \ldots N-1$

$$F(k,l) = \sum_{m=0}^{M-1} \sum_{n=\cdot}^{N-1} f(m,n) \mathrm{e}^{-2\pi \mathrm{j}\left(\frac{mk}{M}+\frac{nl}{N}\right)}$$

where $j = \sqrt{-1}$. Since the calculation is computationally expensive and therefore bit slow for practical use it is quite often replaced by so called Fast Fourier Transformation (FFT) which imposes additional condition of $N = M = 2^i$, where i is a whole number.

Applying the transformation on real image data, the real part becomes an even function and the imaginary part becomes an odd function. For analysis is then used so called Modulation Transfer Function (MTF) also known as a spatial frequency response. The MFT is symmetric along the axis[25][26].

$MTF = \mathrm{Re}[F(k, l)] + \mathrm{Im}[F(k, l)]$

Fourier transformation preserves the symmetry, or more precisely the even (respectively odd) function is after the transformation still even (odd). This property of the Fourier transformation is derived from the properties of the base function which can be divided in the even real (cos function) and imaginary odd (sin function) part [23].

Fourier transforms is commonly used to find the frequency components of a signal buried in a noisy time domain signal. It is also often used as a helper function when solving differential equations on both end open ended straight lines where the independent variable is used as a coordinate on the line. In image analysis and image processing, the MFT is often used in modern digital photography to establish the sharpness of obtained images [27], and by comparison of MFT the overall quality of images can be found[23][25].

3.4.2.3 Wavelet analysis – Haar Transformation

Similar to periodic transformations, the wavelet transformations can also have base made of harmonic (sin, cos) or orthogonal (sign) functions. However in difference to the periodic

transforms the singular sub-functions are in this case made by translation and change of measure[25]. Such function results can be then organized in a tree structure, based on the coefficients used for translation and measure changes. The use of tree hierarchy allows then to show the advantage of the wavelet transformation – the possibility to analyse the signal in different resolutions[28].

When performing the wavelet transformations in image analysis, the most often variation of the transformation called Haar transform is being used. Haar transform provides results nearly identical to the output of the box counting method. It is a linear orthogonal transform with the rectangular base function. The transform changes original image data $f(m,n)$ into a discrete spectra pre-set by a real function $F(k,l)$.

$$F(k,l)=\sum_{m=0}^{M-1}\sum_{n=0}^{N-1} f(m,n)h_{m,k}h_{n,l}$$

where $h_{m,k}$ and $h_{n,l}$ are the coefficients of the Haar Matrix H_N

$$H_0=1, H_1=\begin{bmatrix}1 & 1\\ 1 & 1\end{bmatrix}, H_2=\begin{bmatrix}1 & 1 & 1 & 1\\ 1 & 1 & -1 & -1\\ 1 & -1 & 0 & 0\\ 0 & 0 & 1 & -1\end{bmatrix}$$

Wavelets can be thought of as a functions with pre-set properties which allow (similarly to Fourier Transforms) describing the different functional dimensions. In difference to the Fourier, the wavelet theory is more general and its use often results in more precise results. The wavelet theory is based on the idea of use of the orthonormal base of given space for all whole number translations and some of the whole number dilatations of one and only one function, sometimes referred to as mother-wavelet. There are infinitely many of such functions and each can be constructed by use of various mathematical solutions. One important condition for the mother-wavelet is fast decrease in infinity. In difference to sin and cos functions are therefore wavelets localized in space.

The spacial localization of wavelets brings another of their advantages – due to compactness of the carrier of wavelet coefficient matrix the representation of function or data is sparse and therefore simplifying all coefficient based operations, which further speeds up the calculations.

Wavelets are most often used to process and analyse the signals (1D) or two or three dimensional image data. They are also often used to compress and clean up the data[28].

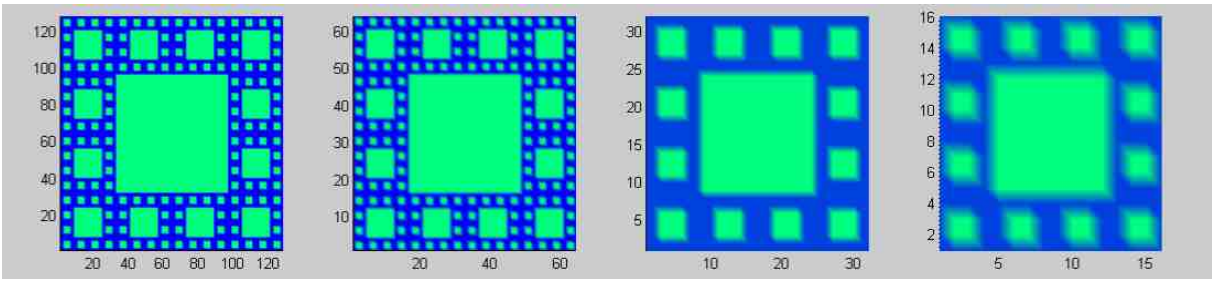

Figure 10: Sierpinki carpet and transformed carpet image with filtered details[11]

4.4.4. Comparison of measurement methods

In the light of the methods described above the comparison of the wavelet transformation using Haar function can be made with the box counting method, periodic methods represented by discussed discrete Fourier transformation (DFT) or by for example Walsh-Hadamar periodic transformation.

Box counting method Since for the B&W images both of the discussed methods delivers exactly same results, and both suffer from the same limitation (size of the image has to be power of 2), main advantage of the box counting method could be considered to be its simplicity. The main advantage of the wavelet Haar Transform would be a flexibility that allows it to operate on the bigger space in respect to the dimension represented by image colour.

Discrete Fourier Transformation – DFT. DFT and its modification FFT are known for very long time (basis were defined by Gauss as early as 1805 and later on formalized by Cooley and Tukey (1965) and by Gergkand (1969) and Strang (1993).[10] The FT has been also used in various application like removing signal interference, signal (1D) and image (2D) data compression and decompression and so on. That resulted in relatively good understanding of its internal working and limitation. Main limiting factors in connection to the fractal image analysis are the computational expense of the method and sometimes hard to predict erroneous results. The advantage would be the understanding of the method inner workings and availability of tools for performing such analysis.

In difference to the Haar transform FT cannot be simplified to just counting of the pixels and the both direct and reverse transformations have to be performed because the results are affected also by surrounding pixels. Pixels are transformed into a Fourier space during the analysis creating the analysis data matrix. Analysed image of size of power of the given number (2^i) is transformed into the spectral space, where the spectra is sequentially filtered by the lower bound of size of the square of 2^i, where $I = 1, 2, 4, \ldots n-1$. In the images created by the reverse transformation the total count of black, white and black&white pixels can be found. The result will be again the Fractal Dimension for black, white and black&white areas and Fractal Measures for the same areas. The fractal properties will be different from those found by box counting or wavelet transformation, since they depend also on the pixels surrounding the analysed area. The weight by which the surrounding pixels affects the analysis results is falling with their distance from the analysed area.

Walsh-Hadamar transformation – WH. WH transform is another example of periodic function with orthogonal sign function. In essence WH transform gives same results as the Haar transform and suffers from the same limitations.

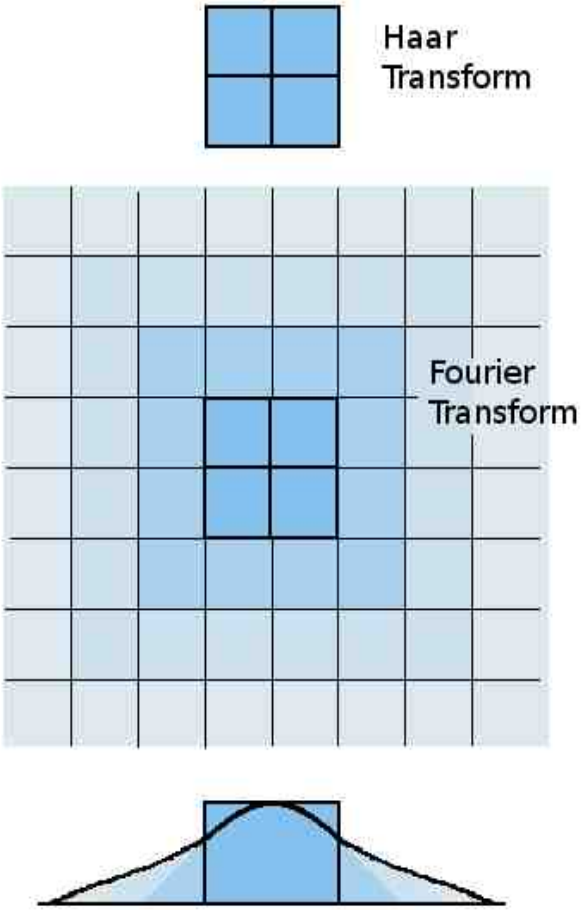

Figure 11: The influence of the pixels surrounding the analyzed area in Haar and Fourier transforms on determined fractal parameters

The most visible problem of periodic transforms in comparison to the wavelet ones is higher dependency of the results provided by them on the pixels surrounding the analysed area. While wavelet transform using Haar function is distributes the value on the squares of size of 2 (making the dependency matrix of 4 pixels in total), the periodic transforms tends to be influenced by wider area (for example matrix of size of 4 for FT).

The comparison of the surrounding pixels effect is visually described in Figure 11. The dark blue colour shows the effect of the analysed pixel and the lighter shade of blue highlights surrounding pixels that affect the results in given transform. Towards the bottom is shown the effect of surrounding pixels shown on the curve created by the function used in Fourier transform with the darkness of the colour indicating amount of influence.

4. EXPERIMENTS AND METHODS

The target of this work is an observational study of the cell growth and division and determination of the cell count and size distributions. The data for studying the cell growth and distribution have been performed on the five different species of the yeast cells. The methods for the count and size distributions of the cells have been also performed on the colonies of the yeast cells that were also in addition exposed to the radiation and colour marked.

4.1 The used species of the yeast cells

The species used for growth experiments have been obtained from the culture “CCY - Zbierka kultúr kvasiniek” of the Academy of Sciences, Bratislava, Slovakia

4.1.1 *Saccharomyces fragilis* CCY 51-1-1

SF is an ellipsoid to cylindrical vegetative cell growing to sizes between 2-6 μm × 3-10 μm. The size to which the cells grow depends on number of external and internal factors such as an age, health of the cell or the amount of nutrition and toxins in the environment. Cells are usually living alone or in pairs and exceptionally can form chains. The pseudomycelium is easily formed, but the true mycelium is not. This specie is able to survive long term in environment with temperatures up to 47 °C. It can live in the warm blooded animals and be a cause of various diseases. In can be also found in a diary products and is an unwelcome contaminant there. The cells reproduce by budding and ferments the lactose, galactose, sucrose, raffinose[30].

4.1.2 *Candida vini* CCY 29-39-3

CV are elliptical to tubular cells growing to sizes between 3-4.5 μm × 3-10 μm. The size to which the cells grow again depends on number of external and internal factors. Pseudomycelium is tree-like made of the elongated cells, budding into an elliptical blastokonids. Can be found to form on the top of the wine containers if those are not protected against the access of air. The specie is able to utilize ethanol, glycerol and acetic acid and break them into the carbon dioxide and water. When present in wine, species usually reduces the amount of alcohol by half. Apart from that the specie is also able to utilize malic, lactic and succinic acids. From sugars, it ferments the glucose. Its optimal living temperature is approximately 23 °C, but is able to survive in range from 1 to 30 °C. The specie is also known to cause beer cataracts and changes in taste[30].

4.1.3 *Kloeckera apiculata* CCY 25-6-22

Cells in vegetative state are sized between 1.5-5 μm × 2.5-11 μm. The cells shape is bears similarity to the shape of lemons. The budding occurs in the top narrow part of the cell. The specie forms tree-like pseudomycelium. This specie is known to inhibit growth of some bacteria like Lactobacillus plantarum or Bacillus megatherium. The specie produces deadly toxin. In is present in soil and sea water, but can be found also in pressed fruit juices or picked cucumbers[30].

4.1.4 *Geotrichum candidum* CCY 16-1-16

GC multiplies using arthokonids. The two different types are known: the cylindrical, growing to sizes 3.5 μm × 17 μm and elliptical, growing to sizes 5 μm × 14 μm. On agar

soil forms soft fur like colonies. The specie is the fastest growing from the whole Geotrich family. The specie is multiplying by somatic division. Cells assimilates xylose and cellulose. The specie is present in everyday human food, waste waters and other places. Most of the time is not harmful, but in some special cases can become a pathogen.

4.1.5 *Dipodascus magnusii* CCY 25-6-22

The grown cells are tubular, often elongated with sizes between 3.5-5 μm × 7-20 μm. In some cases the length of the cell can be up to 40 μm. The specie is not very common. Usually grows into a big colonies. Similar to GC this specie multiplies by somatic division. The specie ferments glucose and sucrose. It is also able to assimilate raffinose, xylose and cellulose. Metabolic processes of the specie results in creation esters with the fruit like smell, acetic acid and anaerobically also small amounts of alcohol.

4.1.6 Rhodotorula glutinis

The cells are elongated with sizes between 2.5-5 μm × 6-13 μm. In some cases the length of the cell can be up to 16 μm. On agar has the brownish, to pink to orange colour. Colonies tend to close up around the edges, the primitive pseudomycelium is rare. The specie ferments maltose, lactose, glucose and sucrose. It is also able to assimilate raffinose, xylose and cellulose. The cells are relatively common and not very sensitive to the living conditions and are able to survive long term in the environment lacking nitrogen rich compound.

4.1.7 Hansenula anomala

The cells grow circular to ellipsoid with sizes between 2-4 μm × 2-6 μm. Grows into white powder like colonies. Pseudomycelium is rich and structured. The specie ferments maltose, lactose and sucrose. It is also able to assimilate raffinose, xylose and cellulose. The specie is one of the most common yeasts in food.

4.1.8 Saccharomyces pastorianus

The cells grow ellipsoid to circular with sizes between 3.7-9.7 μm × 2.6-6.4 μm. Occasionally can grow into a cylindrical shape. Colonies tend to have creamy to brownish colour with flat shiny surface. The specie ferments maltose, lactose and sucrose. It is also able to assimilate raffinose, xylose and cellulose. The specie is often used during beer fermentation processes.

4.2 Nutrients

Two different nutrients have been used in experiments.

Media 1 – carbohydrate

- glucose 4 g
- pepton 0.5 g
- yeast extract 0.5 g

Media 2 – wort

- wort Starobrno, pH 6.5, 75 ml
- glucose 3 g
- nicotinic acid 20 mg
- aminobenzoic acid 20 mg
- pyridoxin 20 mg

- thiamin 20 mg
- distilled water 50 ml

4.3 Measuring equipment

4.3.1 Microscope Nikon Eclipse E400

Magnification range is 10 to 1500 times for direct observation or 2 to 500 times for connected 35 mm camera. Parfocal distance is 60 mm with diameter of visible field 22 mm. Backlight is provided by centred, focused 100 W bulb, centred and focused. Fine focusing is 0.1 mm per round and rough focusing is 12.7 mm per round. High quality of the optical of the microscope together with its great stability make it ideal instrument for long-term experiments.

Figure 12: Nikon E200

4.3.2 Microscope Nikon Eclipse E200

Nikon E200 is a first microscope with the new infinite focus optical system CFI60. The new optical system keeps view focused and clear over all magnifications. The chromatic error is correlated in the whole viewable area. Microscope uses special lenses CFI E Plan Achromat. The configuration elements are placed so the one hand manipulation is possible. Microscope comes with the binocular tube. The triocular tube is also supported and is used usually in connection with the classic photographic or digital camera. The angle of the tube is 30°. Microscope also supports use of up to two filters of a diameter 45 mm. It also contains adapters for the Nikon Coolpix and Nikon Eclipse digital cameras. All other specifications are same as for the Nikon E 400.

Figure 13: Nikon E400

4.3.3 Digital camera Nikon Coolpix 990

Coolpix 990 compact camera has one 1/1.8 inch CCD with 3.34 mega pixels on silica. That allows for effective 3.14 mega pixels resolution and format of images 2 048 × 1 536 pixels. The camera comes with 3 times zoom capable lenses with focal length between 8 – 24 mm. The auto focus mode allows for different modes with the most effective “best of 5”, matrix based 5 point focus calculation algorithm with minimal focusing distance being 20 mm. The camera also supports 256 segment matrix measurement and matrix white colour adjustment.

Figure 14: Nikon Coolpix 990

4.4 Cell growth experiment

The selected yeast specie have been cultivated in agar for 17 to 24 hours. Then the selected cells have been transferred in the nutrition media where they were left cultivating for at least another hour. After that the sample have been transferred using sterile instrument to the Bürker counting chamber and put under the microscope. The use of the chamber was not a strictly necessary since no manual counting have been performed in this experiment. However the chamber itself allowed to keep the sample alive under the observation for the amount of time necessary for the experiment by keeping extra nutrient media in the excess channels of

the chamber. Even then it was necessary to maintain special conditions in the lab in which the experiment have been performed. The special conditions in this case means the higher then usual humidity of the air to prevent nutrient media and sample in the counting chamber from drying out during the experiment. In the initial stages of the experiment it have been found that it is not possible to mitigate the effect of drying out by adding extra water or nutrient media in the counting chamber excess channels as this resulted in the higher then usual movement of the cells under observation and effectively led almost always to the termination of the experiment.

Another condition that affected the experiment was changing background light during the day time. To prevent it's effect an artificial background light source have been used during the experiment. The effect of the changing background light have also been partially mitigated by using automatic white balancing features of the digital camera used to capture the images.

It have been also necessary to constantly refocus the cells under observation during the experiment due to drying out of the nutrient media and due to changes in the size of the cells themselves. It has been found that using lens with low magnification (40x) it had became impossible to focus the whole cell including its bud when their position differed. Due to those instrument limitations, the best image data have been obtained when cell budding happened in the plane parallel to the chamber walls, rather then parallel to the angle of observation. Budding in direction other then parallel to the chamber walls usually led to the termination of the experiment.

When focusing the cells it have been possible to choose between focusing on the outer wall of the cell or focusing on the cells internals. While the second approach provided more precisely bounded cell outlines, it has also obscured the cell inner area by the artefacts like the cells own organelles. For this reason only the images of the cells made with focus on the outer cellular wall have been further analysed.

Due to cell movement, it have been also necessary to adjust the position of the counting chamber in the microscope to keep the cells under observation in the visual field. The most of the movement have been attributed to the small cells in a low viscosity nutrient media. When the cells grew up or the viscosity of the nutrient media was higher, very little or no movement at all have been observed.

While this experiment concerns itself with the grow of the single cells, it is possible to capture images of multiple cells at once as long as they are in the visual field of the microscope and that of the digital camera used to capture the images.

In the experiment the images of the cells have been taken in the regular interval (usually 2 minutes) and stored in the lossless TIFF format without compression. Such a raw images have been then directly analysed in the Harmonic and Fractal Analyser software – HarFA[42]. The area of interest selected in the software have been then applied on the whole image sets and such cut-off over whole set then stored as an AVI video (using lossless codec without compression). This is an difference in comparison to older similar experiments like [29] where the additional preprocessing steps have been necessary.

The size of the analysed area have been 512 × 512 pixels or alternatively 256 × 256 pixels, depending on the initial and final size of the observed cell(s).

Figure 15: *Candida vini*, from left to right: no threshold, threshold levels 105, 126, 134

During the analysis HarFA software have been used to determine the optimal level of the thresholding for the given set of images. The different threshold levels for single frame showing the single cell of *Candida vini* are shown in Figure 15. While from this frame it appears that the most suitable thresholding level would be that of 105, it is not true. This is due to the fact that despite the best effort in the open lab settings the lightening conditions could not be kept absolutely same throughout the experiment and the difference in the background lights affects the image data adversely, causing some of the captured images to be under exposed (i.e. not showing whole cell). The second shown thresholding level (126) have provided reasonably good results throughout the whole image set. The third thresholding level have been too high, effectively hiding the cell in the surrounding noise. While the second thresholded image contains some noise, coming from the dirt on either the lens of the microscope or that of the camera or from the dirt or scratches on the counting chamber, this error have been shown to be insignificant for the analysis. This is mainly due to the comparative nature of the performed study. The target of the experiment have been observation of the cell growth and the noise is same in all the captured images therefore not contributing to the measured growth and only offsetting the initial value. If necessary the effect of the noise can be completely canceled by producing the image of the empty chamber prior to the experiment and discounting the value of all data found at given thresholding level from all subsequently taken images.

4.4.1 Analysis Description

While in the past the main focus of the automation of image analysis and use of computational resources in the process was towards the preprocessing of the data in terms of clean and simple repetitive tasks, progress made in the computational power of modern computers allows for more sophisticated uses and solutions. The progress is not only due to ever increasing computational power, but also due to advances in algorithmisation of the solutions to known problems, our understanding of the problems and specifics of image analysis and new approaches and methodologies in software development.

To demonstrate this, let us compare similar work performed 5 years ago. [29] The software used at the time was also performing image analysis using wavelet fractal analysis, but higher homogeneity of the data have been necessary to achieve reasonable quality of the analysis results, therefore images used for such analysis had to be manually pre-processed.

- The thresholding had to be performed manually, with additional removal of the artefacts introduced during the analysis (most often dirt on the camera lens or on the microscope lenses or on the glass of the used container itself.

– All the image data showing the analysed cell had to be manually centred to ensure same cell had to appear at same position for the whole duration of the experiment.

In this work we show that such work can be avoided with the advances made to the analytic method algorithm and with computationally obtained calibration curve for analysed image data.

On top of the simplification of the analysis process, additional, more specialized uses of the method are now possible. It is actually possible to train the software (currently still with the help of the operator, but already technically possible to introduce self learning mechanism into the whole analysis process), to perform repetitive tasks automatically for the data coming from similar experiments in form of replaying pre-recorded actions. It is also possible to train the software, not only analyse the data, but also to recognize and alert operator to found discrepancies during preparation of the data for analysis and while performing analysis. For example let's have a look at the set of the image data recorded while running experiment observing growth speed of the cell depending on the living environment conditions.

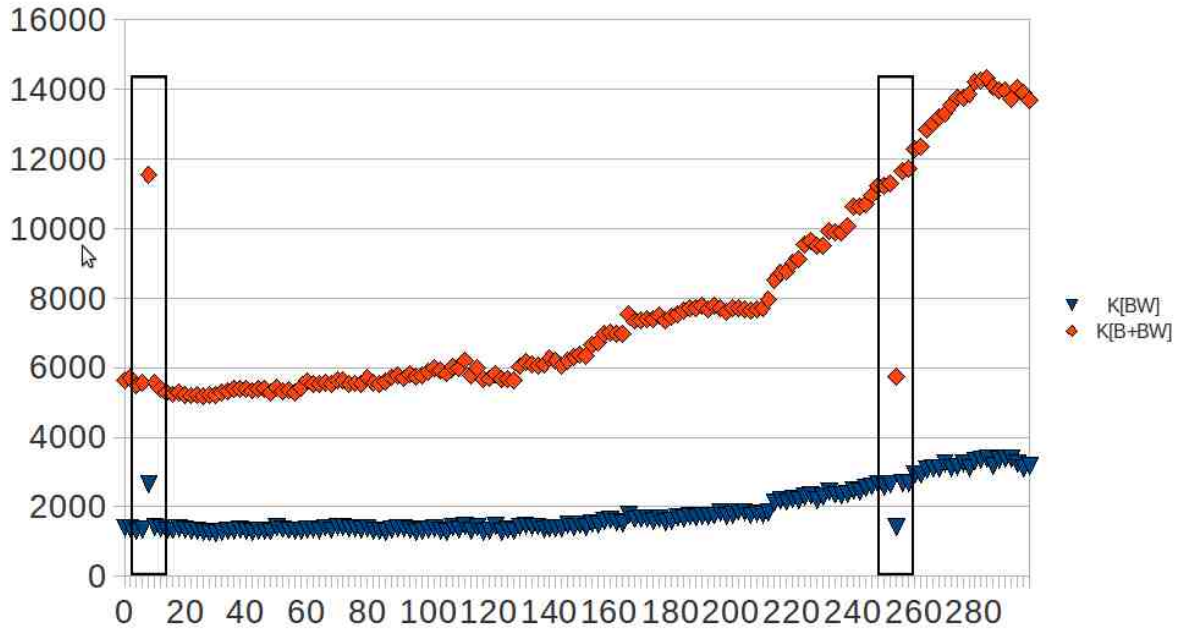

Figure 16: *Geotrichum Candidum*, growth curve with inserted incorrect data frames

While changing the conditions of the experiment might lead to changes in the speed with which cells are growing (or dying), under no circumstances can this experiment result in discontinuous changes in the growth data about the cell. Having known that, it is easy to set the continuity requirement for the analysed data and have a software to raise alert should such condition not be met. This is exactly what the Figure 16 above is showing. The image data have been intentionally mixed here by inserting incorrect frames at positions 5 and 128 as shown in Figure 17. The introduced error is clearly visible in the resulting fractal measure curve and can be filtered out during the analysis by simple application of the statistical methods for removing the erroneous data from the sets.

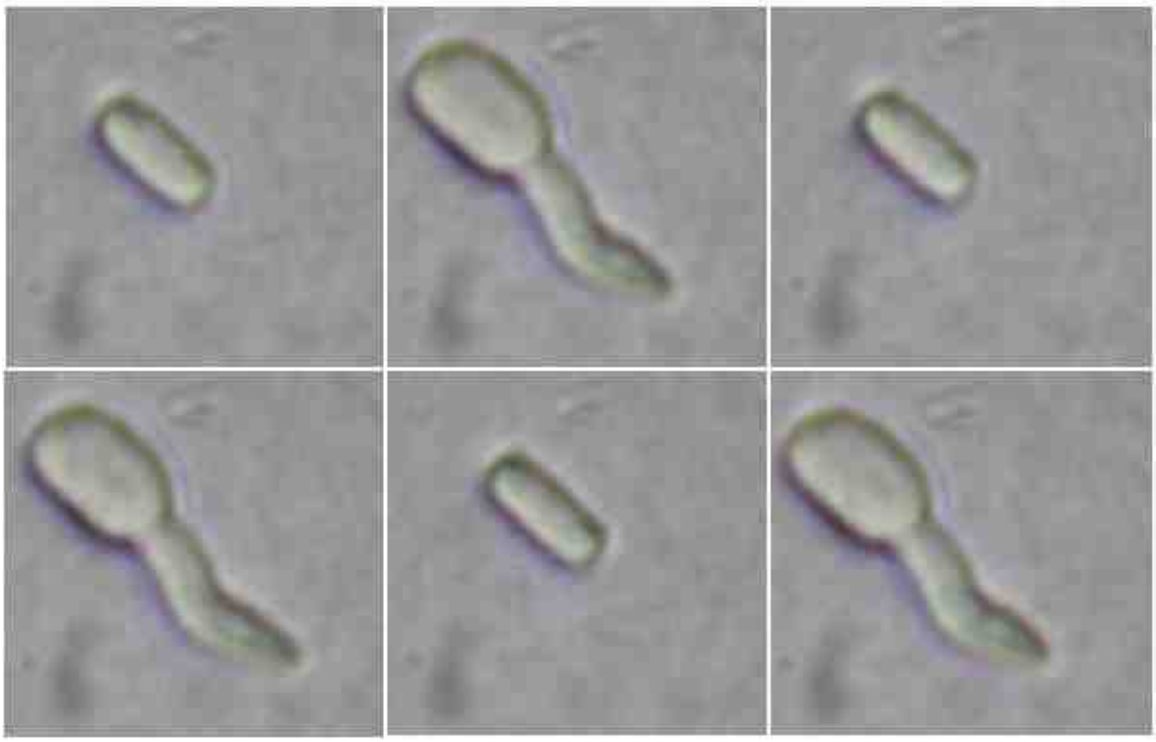

Figure 17: *Geotrichum Candidum*, inserted mixed frames, matching the highlighted areas in Figure 16, from left to right, top to bottom: position 3, 4, 5, 127, 128, 129

Application of such statistical method can be easily introduced in the analysis operation chain as another post-processing step and can optionally automatically discard such data or alert the operator to the presence of incorrect data. While not shown in this paper, it is also possible to obtain original and reordered video data, showing all frames as they were as well as when correctly ordered automatically. It have been confirmed by inspecting each of the frames of reordered data set video, that indeed software have made order of the single frames correctly.

Of course there are limitations to such solutions, like reordering would not be possible for experiments producing data with oscillating curves or other in cases where condition of continuity cannot be met. However using now a days very common modular architecture for the further software development of the Harmonic Fractal Analyser, it is possible to provide such more specialized extensions in form of pluggable modules allowing users to easily customize and enhance software for any given experiment, without sacrificing any of the general purpose functionalities already provided in the system.

Another example of how redefined algorithm and use of wavelet fractal analysis can help to quantify experimental data is by providing extra safety net for recognition of external influences on the experiment. The data show below, show the detection of the changes in data illumination causes be running the experiment in day light, which is naturally changing during the day, instead of choosing controlled conditions of artificial illumination. While not significant in this case, in many other scenarios, the light conditions may have very high impact on the kinetics of growth of the organism under the observation.

4.4.2 Error handling during the analysis

There are various errors that might appear in the image data and although previously this kind of errors meant that the data have to be either thrown out or have to be manually processed to remove the errors, it is increasingly possible to automate such preprocessing data validation and clean up.

4.4.2.1 Systematic Errors Handling

One of such errors is the caused by presence of various other then analysed objects in the visual field of the camera. Such objects might be for example dirt on the camera lens or on the microscope lens. Importance of such error diminishes with the analysis method described in this work. Since the error is fixed in size and appears on all images it can be safely ignored if not covering significant (more then 10% of the visual field).

Figure 18: Thresholded *Candida vini* cell with a dirt visible in a visual field after the thresholding

In case of occurrence of more significant consistent errors, it is possible to adjust whole calibration curve up or down (depending on whether black or white error is present) to mitigate its effect. The amount by which such adjustment is necessary can be calculated from empty image containing no measured data, only the erroneous areas.

4.4.2.2 Non Systematic, identifiable error handling

More significant problem is the occurrence of such objects that is random. As a sample of this can be visible part of the scratched net on the glass chamber used throughout the experiment and it's random appearance due to cell movements. The only way to avoid such problem would be to use clean containers without any visible marks. This however was not possible in the experiment that called for the test of automatic method by classic manual cell count per net cell. This problem have been mitigated in some other works [29] by manual preprocessing and removal of such visual artefacts from the images after thresholding.

However since we have the intimate knowledge of the shapes of objects of interest in the experiment, it is possible to use software methods to identify and remove such artefacts automatically. This can be done for example using algorithm described below.

- Send the four probes parallel to the edges of the image and two on diagonal lines.
- When running into black points, grow the region and see if it is growing linearly in any direction, while keeping constant in the other.
- If the conditions are met remove whole region and replace it be the background colour.

The schema below shows the lines on which the probes will be working through the image data. While this approach doesn't cover 100% of the image area it is fast enough not to slowdown whole processing and successful enough to uncover majority of big artefacts. The small artefacts can be safely ignored since they contribute little to the total measured values. Usage of such algorithm to uncover edges and artefacts in the images have been already successfully applied in other imaging techniques and is used in the industrial scale[40][41].

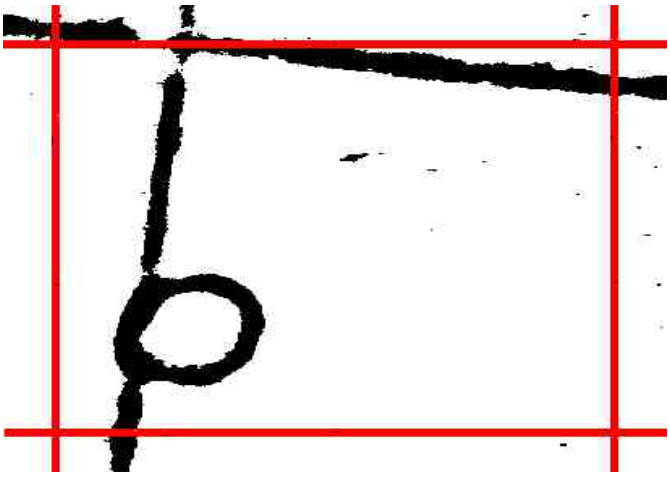

Figure 19: Cell obscured by the visible grid boundaries. In red path of the probes used to detect such anomaly.

Such method can be of course used only in the experiments where straight lines can't occur as a part of the experiment. Even though use of this algorithm is limited by the conditions described above, it can be present in the software in form of pluggable module used only for experiments where its use is of benefit, like the one described in this work. However, it should be noted that further work is possible to provide detection of other shapes then the linear ones and use the same module in different configurations (e.g. when measuring interferences or waves forming straight lines, the method can be used to remove accidentally appearing drops of condensed water vapour or similar).

5. RESULTS AND DISCUSSION

5.1 Kinetic studies

As described above the main purpose of the kinetic experiments is to gauge the cells growth potential and allow for comparison of the quality and strength of different species or different growth environments. There are many more possible applications, but for the purpose of this work the above types of kinetic experiments have been chosen.

5.1.1 Algorithms

The following algorithm attempts to describe process of cell growth kinetics measurement analysis.

1. Select area of interest so that it covers cells of interest over whole range of the image set.
2. Decide on most suitable colour space for the analysis
3. Find out most suitable thresholding level, so that the analysed cells are clearly visible over the whole analysed image set
4. Perform 2D Wavelet Analysis of the area of interest (ROI) in the image
5. Create graphs of changes of Fractal Measure K values over the ROI over the whole set.

Depending on the analysed data the K_B, K_W or K_{BW} is of interest. In this concrete case the K_B or K_{B+BW} have been of particular interest since the captured images are thresholded so the cellular wall is visible in the analysed data rather then whole cell.

5.1.2 Programing

The functionality to perform two dimensional wavelet analysis over image data have been incorporated in the latest version of Harmonic Fractal Analyser (HarFA) software building on the previously implemented, more general wavelet and harmonic analysis functionality. The programing language used for implementation is Delphi. HarFA can be therefore now used to generate distribution data sets from analysed images as well as the sets from calibration data. The output from the analysis is suitable for further processing in the common spreadsheets such as Excel.

5.1.2.1 Data processing Optimizations

The various possible optimizations of the existing software have been considered and discussed. The main proposed changes are described below.

The image analysis process itself consists of many little tasks that were traditionally executed in sequence for each image. With the penetration of multi core computers however, the new approach to the analysis and paralleling of the tasks and processing multiple images at once have to be considered. The processing sequence should be coupled in such a way that allows for maximal use of the available computing power on different cores.

The typical tasks of which analysis of cell images consists:

- ROI determination,
- colour space reduction,
- thresholding,
- artefact (glass net, dirt on lenses, etc.) removal,
- fractal properties calculation.

5.1.3 Data Processing

The result of performing the data processing according to the algorithm above have been as series of graphs for each of the experiments. The steepness of the curve in the graphs and changes in the steepness during the experiment run allows for comparison of the speed of growth of different species or the same species in the different conditions (e.g. when using different nutrient media or different temperature), but also comparison of different phases of growth and identification of the cell division points.

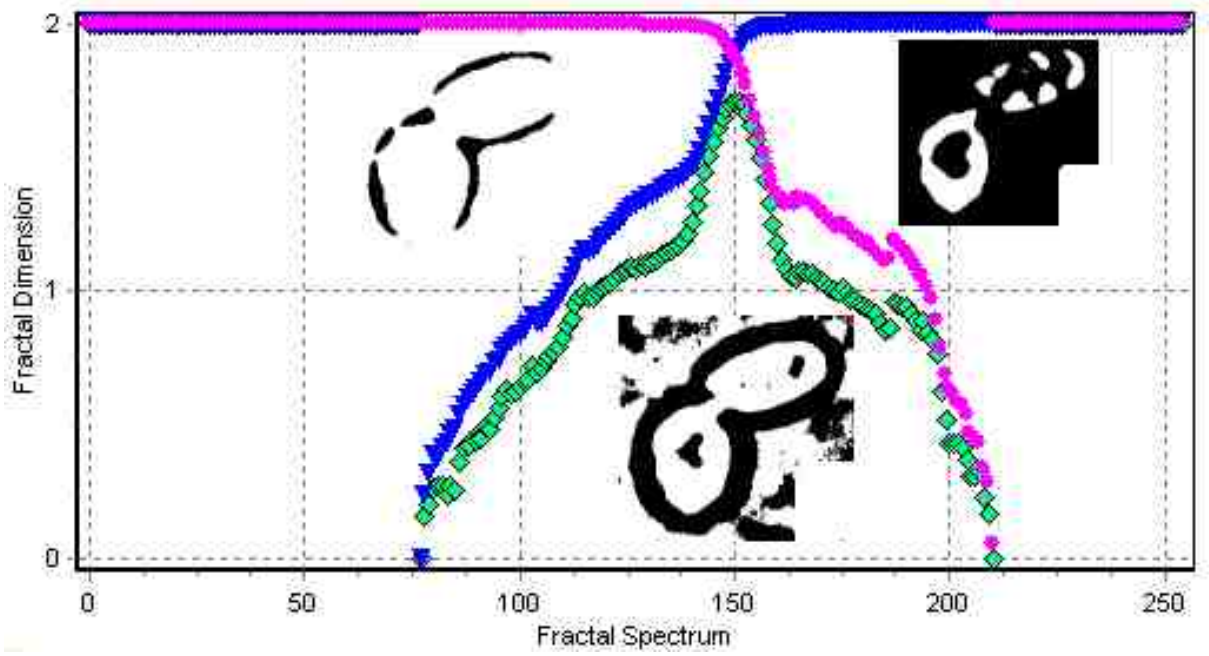

Figure 20: Fractal Dimension values at different thresholding levels in the intensity color space with images of the cell at levels 120, 150, 170 (left to right)

For the analysing the data itself it is of high importance to decide on the thresholding level for the image set. As previously mentioned, due to slight inconsistencies in the lightening conditions the optimal level can't be decided from analysing the single image, but whole data set has to be processed. Apart from finding the optimal thresholding level, it is also necessary to find out most suitable colour space for analysing the given image.

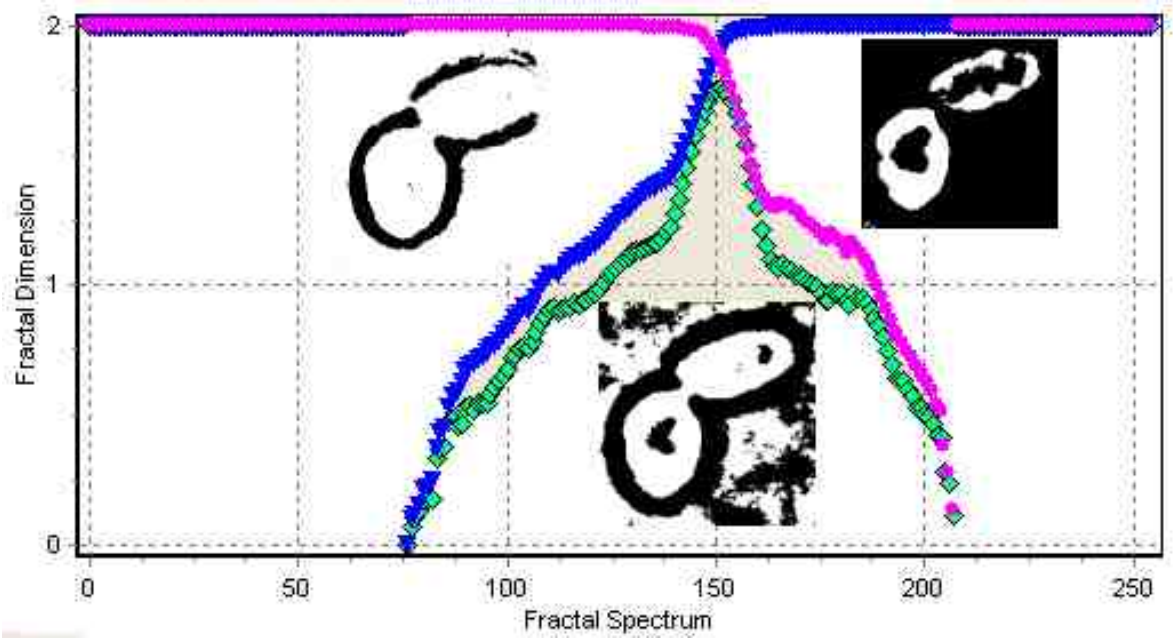

Figure 21: Fractal Dimension values at different thresholding levels in the red color space with images of the cell at levels 136, 151, 165 (left to right)

When comparing the curves in Red colour space shown in Figure 21 and the RGB shown in Figure 24 it can be found that those are nearly identical. This is due to the way of storing the colours in RGB space. The colours in 24bit RGB colour space are stored in the separate bytes. The Red colour is stored in the first byte, the Green colour in the second byte and the Blue colour in the third byte. The bytes are then combined together to create one integer like number. The final number is not made by the simple sum, but by shifting the bytes instead therefore value representing Red is 2^{16} times higher and value for Green is 2^{8} times higher then the value for Blue. So it can be stated that in the RGB space the influence of the Red

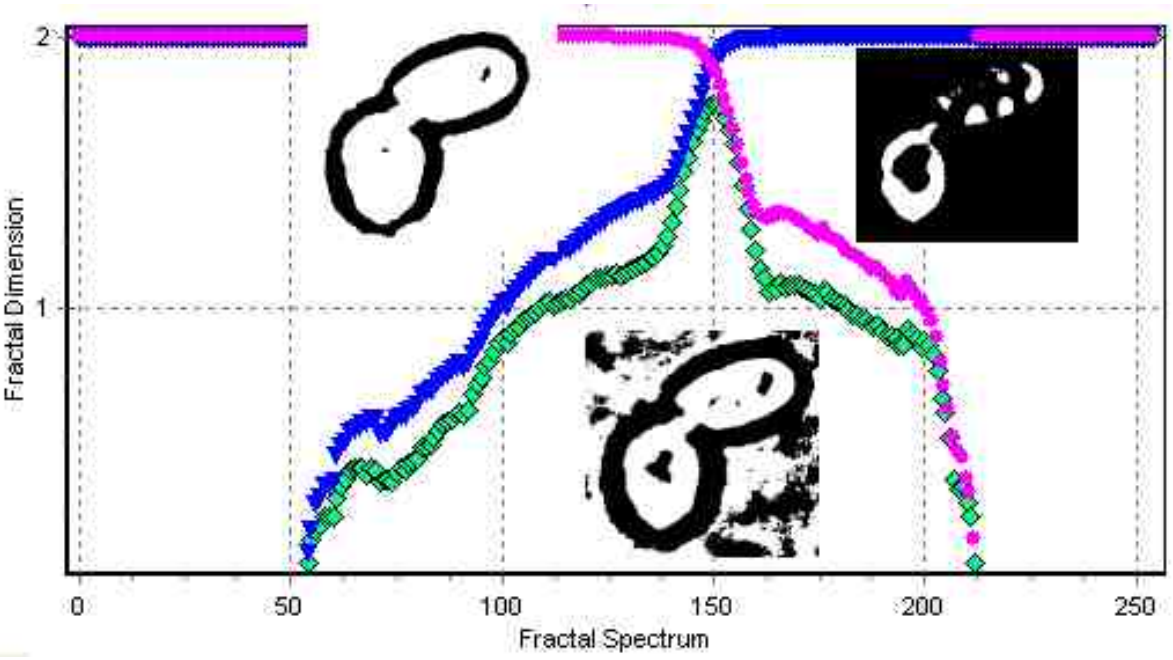

Figure 22: Fractal Dimension values at different thresholding levels in the green color space with images of the cell at levels 135, 150, 183 (left to right)

colour is predominant and all other colour bands effect is minimal. For this reason in practical applications the Red colour band values are often substituted for whole RGB.

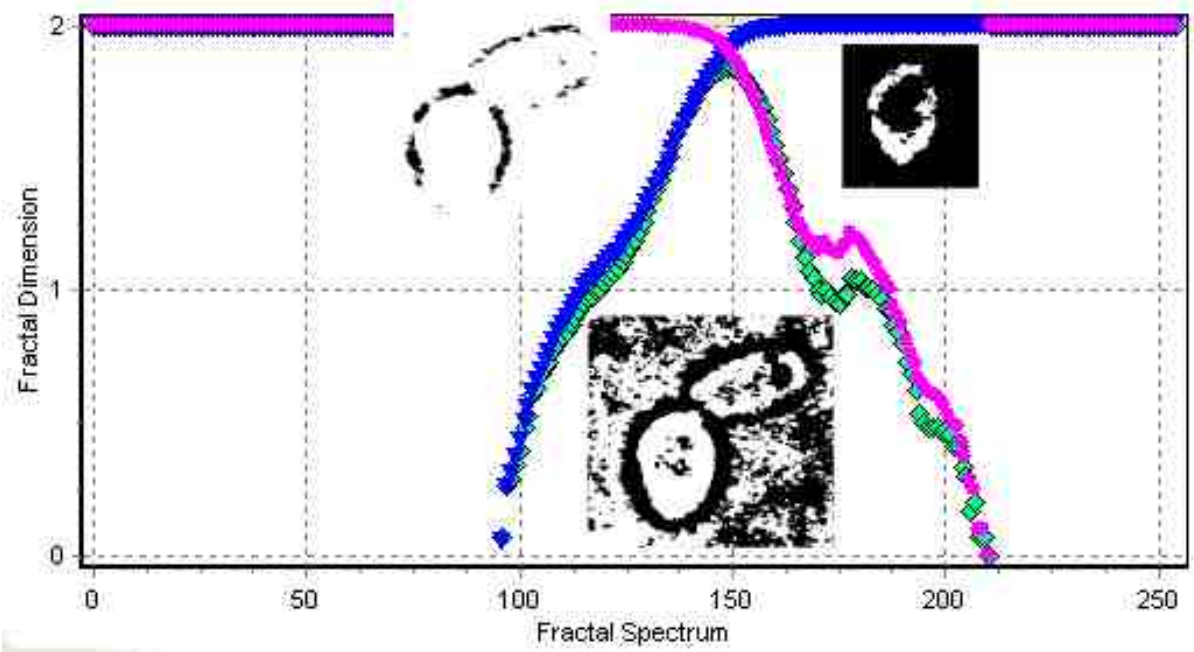

Figure 23: Fractal Dimension values at different thresholding levels in the blue color space with images of the cell at levels 126, 151, 174 (left to right)

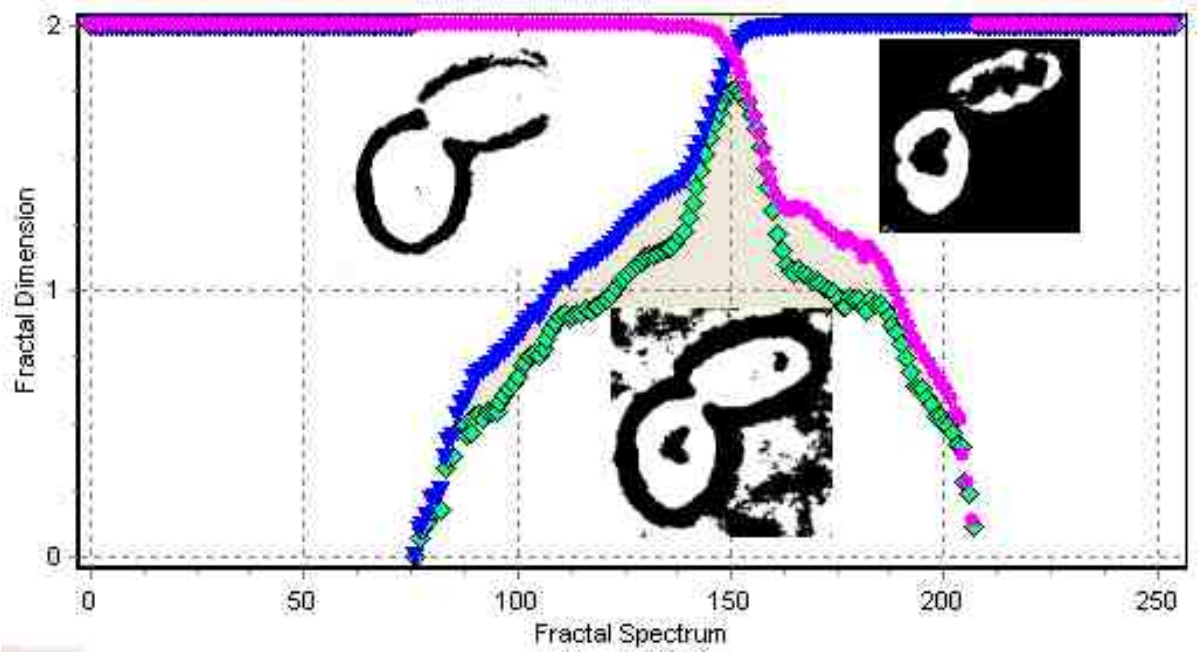

Figure 24: Fractal Dimension values at different thresholding levels in the RGB color space with images of the cell at levels 120, 178, 190 (left to right)

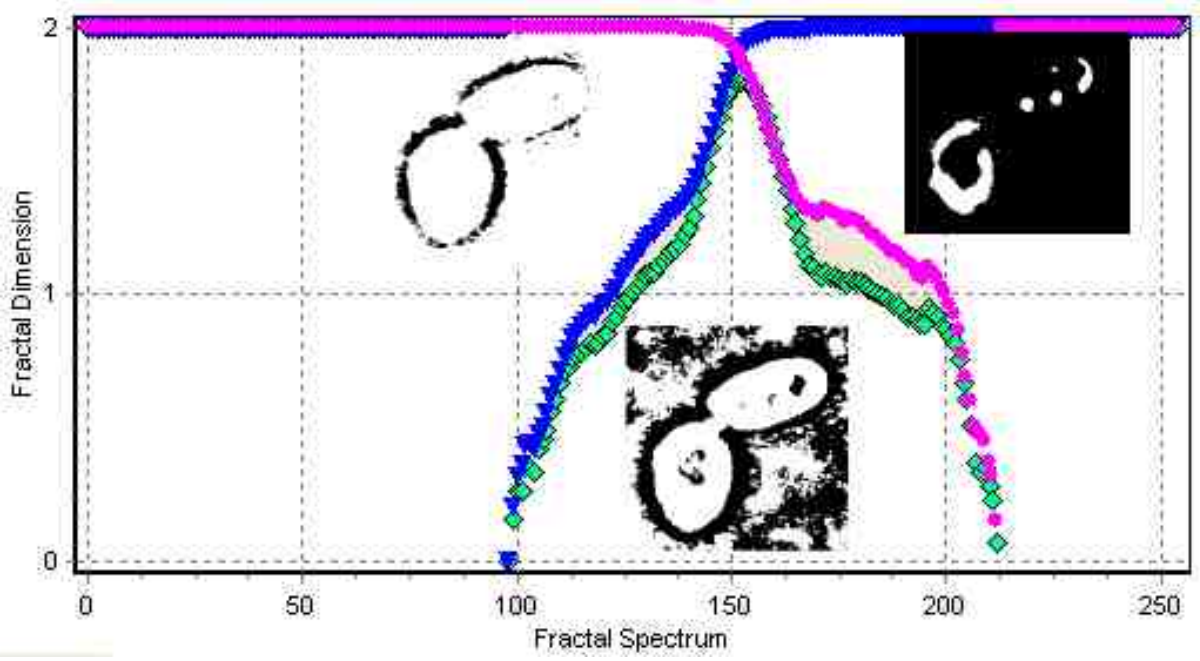

Figure 25: Fractal Dimension values at different thresholding levels in the brightness color space with images of the cell at levels 137, 153, 183 (left to right)

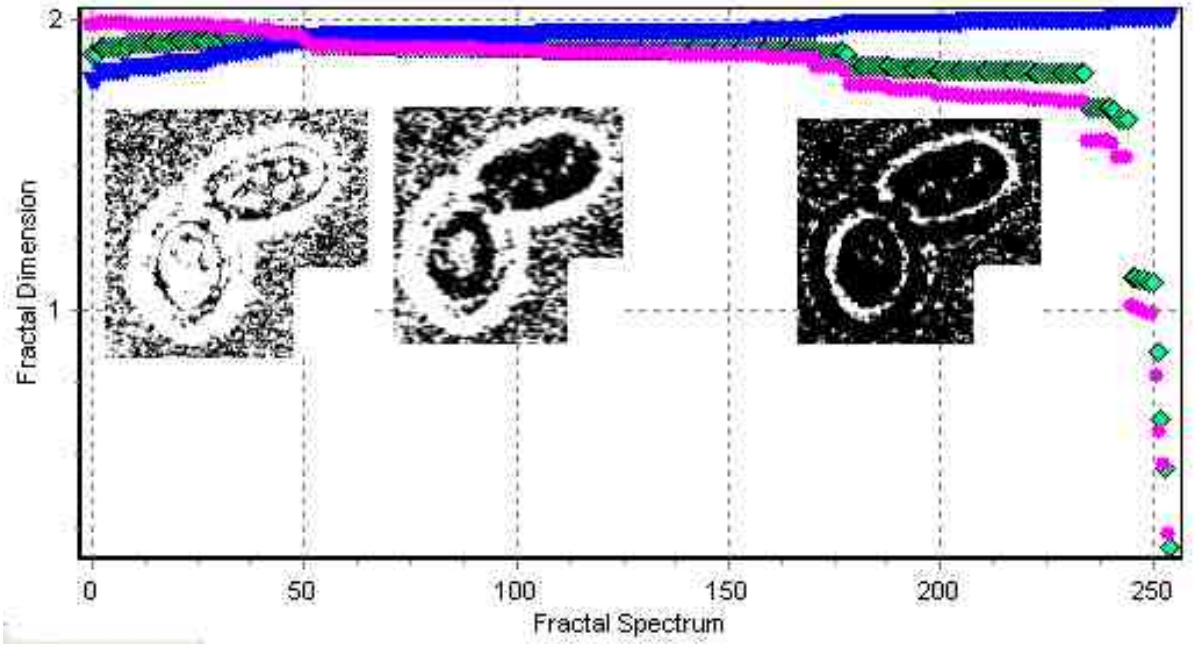

Figure 26: Fractal Dimension values at different thresholding levels in the hue color space with images of the cell at levels 50, 100, 200 (left to right)

The set of illustrations above show the same data analysed in different colour spaces and with different thresholding levels selected for those particular colour spaces.

As seen in the Figure 26 the Hue colour space is not suitable for analysing the obtained image data set. The amount of noise from the background is too high within this colour space over all thresholding levels.

All remaining analysed colour spaces provide comparative results with only slight differences. The each separate bands colour spaces are looking only at the pixels visible in given colour space. This is most often useful when working with the dyed tissue or cells allowing to observe and quantify metabolic changes happening within the cells themselves or in the surrounding environment. The main difference between RBG and the Intensity colour space is in the weight different colour bands are contributing to the final pixel. For the further analysis the intensity colour space have been chosen.

5.1.3.1 Growth quantification

While the method is not able to provide the absolute numbers of the cell sizes, this disadvantage can be mitigated by calibration. The counting chamber used to preserve the media during the experiment was known to have the size of the smallest cell 0.1 mm long. The magnification of the microscope used in the experiment have been 2400×. Hence it's size on the captured image have been equivalent to 240 mm of the image data. Due to the resolution of the camera, such image size could be also written as 750 pixels. Using this calibration data the real sizes of the cells can be obtain. However it is important to keep in mind that if changing the resolution of the camera, magnification or even a storage format of the data, the amount of pixels representing 1 mm of real size can change too.

5.1.4 Results Discussion

In total over 15 experiments concerning growth of the cells have been performed. The experiments presenting typical scenarios been chosen for more detailed explanation:

5.1.4.1 Candida vini

The cells of *Candida vini* are shown in the first data series. The experiment have been performed at temperature of 24 °C, the first budding have been observed after 1.25 hours. The next budding occurred after 3.17 hours and the next one after 4 hours. The experiment have been terminated after last budding at time 5.82 hours. The data have been captured every 2 minutes.

The Figure 27 shows the growth of the cell during the experiment. In the curve of the Fractal Measure values is possible to see little areas of lowering *K* at the beginning of the budding. This is caused by the thinning of the cellular wall at the budding site and by the growing bud being too small in comparison to the rest of the cell and it not being fully focused.. This effect is however not visible for the 3rd budding. The reason behind is that the budding occurred this time in parallel to the camera view point. Since the top of the cellular wall is not focused the thinning is not observed and doesn't show in the curve. The dip in the Fractal measure is even more pronounced when the combined Fractal measure for black areas and black&white boundary is observed. This is shown in the Figure 28.

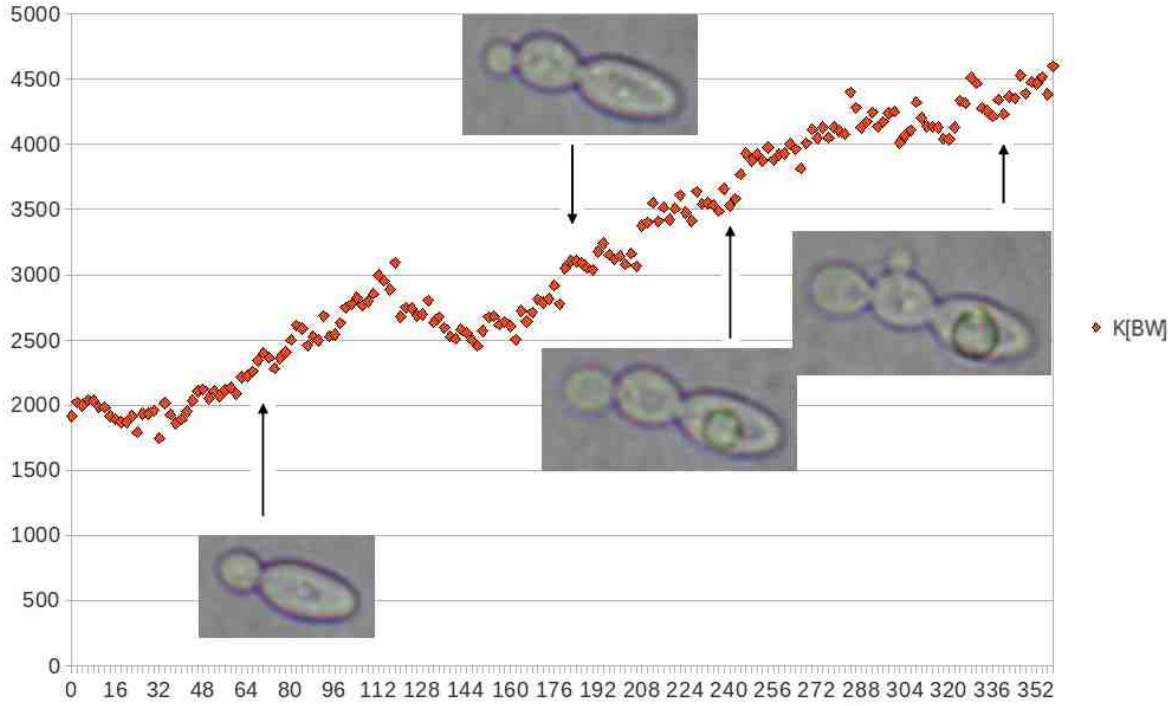

Figure 27: *Candida vini*, K_B, cell growth, cell at times 70, 190, 240 and 350 minutes

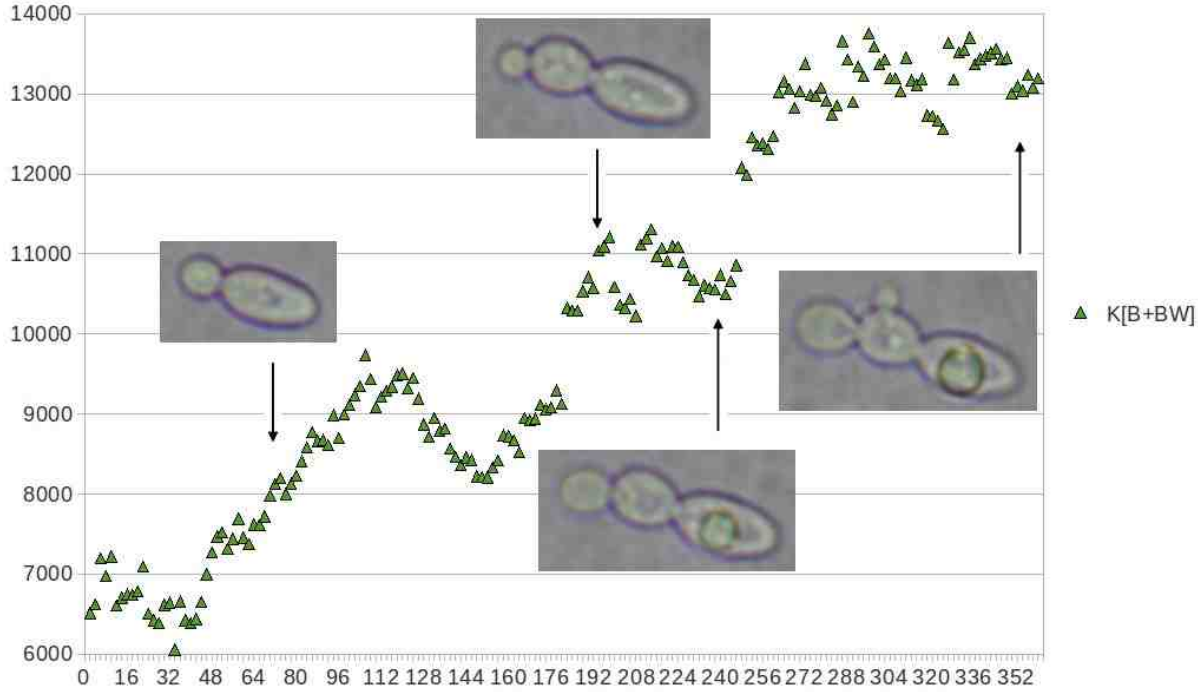

Figure 28: *Candida vini*, K_{B+BW}, cell growth, cell at times 70, 190, 240 and 350 minutes

The above described behaviour is typical for the observation of the cellular growth. The cells keep relatively constant gathering the nutrition from its surroundings. Once it has accumulated enough of resources the budding phase starts. The next lowering of the steepness of the curve is caused by another nutrition accumulation phase as well as by the slowdown of the growth of the new bud itself.

During the 3rd budding cycle, the budding started on the top of the cell. This usually caused experiment to be stopped since such bud is difficult to focus together with the mother cell itself. In this case however the growing bud have been focused and contributed to the changes of Fractal Measure same as the buds growing side ways.

By calibrating the resolution against the size of the grid cell of the counting chamber, the cell size have been found to be 23 × 13 μm at the beginning of the experiment and 48 × 19 μm towards the end.

5.1.4.2 Kloeckera apiculata

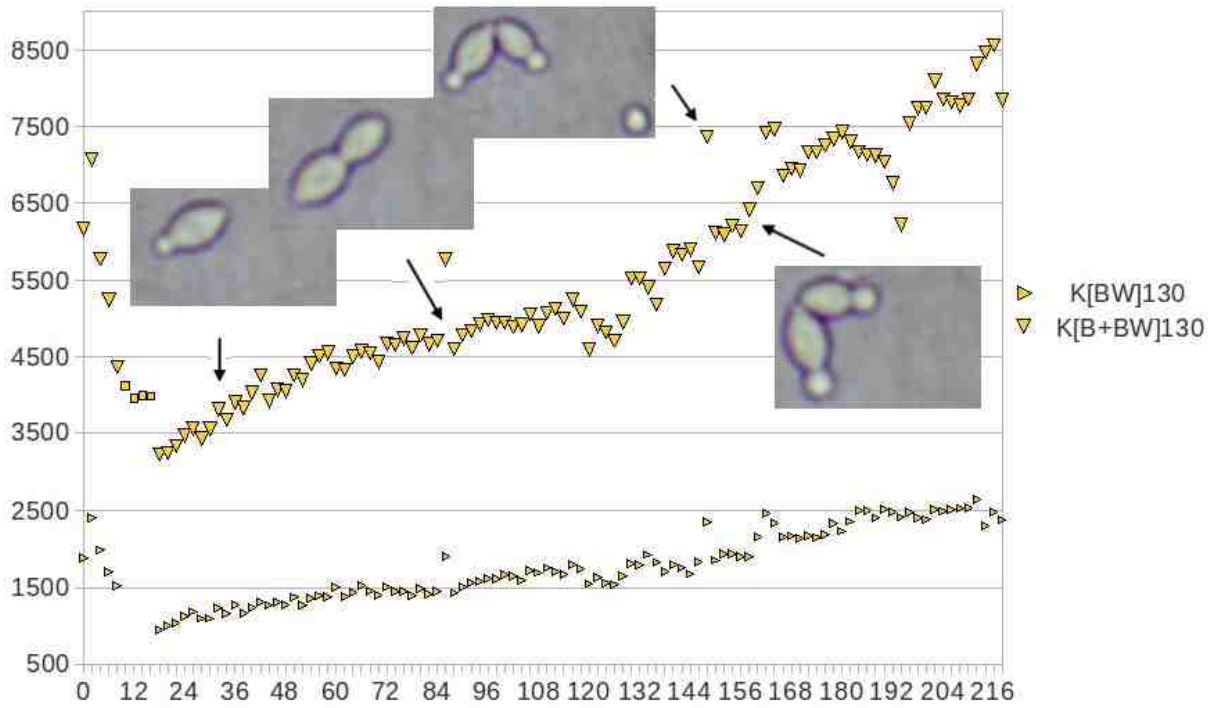

Figure 29: *Kloeckera apiculata*, K_{BW} and K_{B+BW}, cell growth, cell at times 30, 90, 144 and 160 minutes

The next series of experiments consisted of the observations of *Kloeckera apiculata* cells in the nutrient media at the temperature 23 °C. The first budding occurred 30 minutes after the start of the observation. Next two buds started to grow at time of 1.5 hours. The high growth rate is typical for this specie. Apart from growing fast the specie is also very active in the nutrient media moving around a lot. In few cases the experiment had to be terminated due to the excess movement of the cells and their disappearance from the visual field. Another property of this specie was the fact that it tend to create spiral colonies and to turn itself vertically as soon as at least 4 cells have been together. This is clearly shown in the Figure 29 at the time 160 minutes. There are also occasional errors visible in the Fractal measure curve, for example at the time 144 minutes. The errors are due to stray cells entering visual field. In most of the other experiments, this could have been reduced by choosing the area of interest for the analysis, however with this fast moving specie it was not always possible. However such erroneous frames themselves are clearly visible and sticks out so much that such data will be safely discarded from any further numerical analysis by use of conventional statistical

methods and could be removed from the results already by the software during the analysis phase if desired.

The size of the cell have been found to be 13 × 11 µm at the beginning of the experiment and 27 × 19 µm towards the end.

The measured Fractal dimension values followed similar curve to the one for fractal measure.

In comparison to *Candida vini*, the *Kloeckera apiculata* specie is faster growing due to each of the new buds accumulating nutrition rapidly and then participating on the multiplication in the next cycle. The lack of the dip in the curve at the beginning of the next multiplication cycle in this case is attributed to the smaller size of the cells and hence the smaller differences between the mother cell and its offspring. Another contributing factor is the fact that this specie tends to grow offspring from the narrow tips of the cells hence further lowering the amount of the cellular wall affected by the growth.

5.1.4.3 Saccharomyces fragilis

Growth of the *Saccharomyces fragilis* specie had been characteristic in the very quick start of the growth phase and nearly the constant speed afterwards. The experiment have been performed at the temperature 24 °C in the second type of the nutrient media. Even though the *Saccharomyces fragilis* specie tended to multiply faster then the *Kloeckera apiculata*, the Fractal Measure and Fractal Dimension curves produced by the cell multiplications bore same characteristics, and were just slightly steeper. The details of the experiment are shown in the Figure 30.

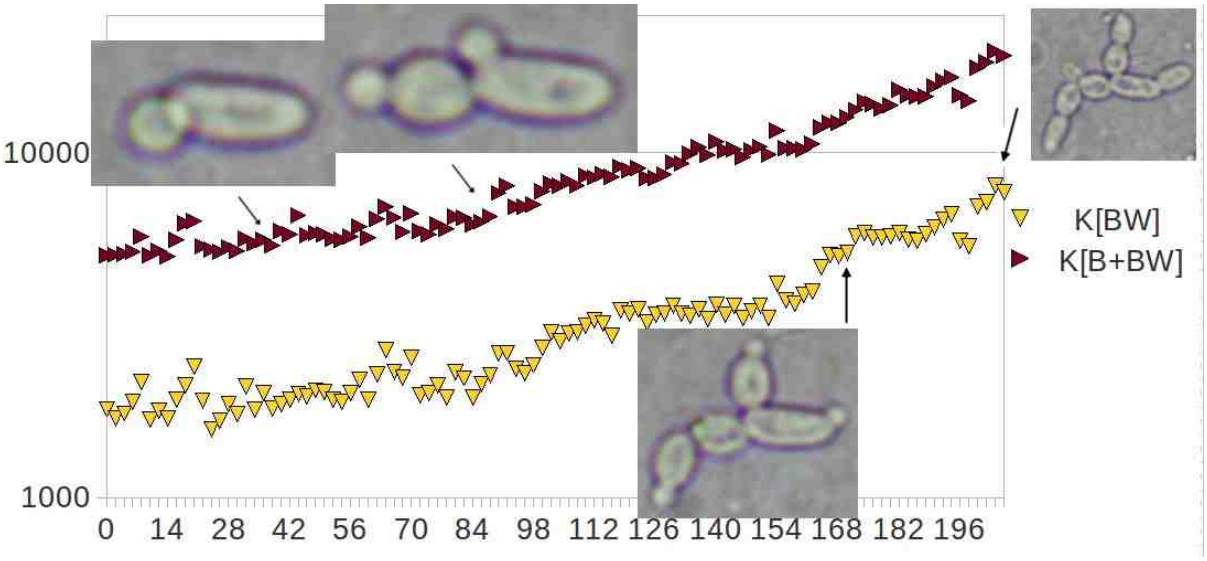

Figure 30: *Saccharomyces fragilis*, K_{BW} and K_{B+BW}, cell growth, cell at times 40, 96, 170 and 196 minutes

5.1.4.4 Geotrichum candidum

The next examined specie have been *Geotrichum candidum*. The specie doesn't multiply by budding, but by use of arthrokonids instead. With that difference came the different typical

growth Fractal measure curve. The experiment had run at temperature 24 °C. The first multiplication have been observed at the time 3.25 hours. The specie is characteristic by the thin walls which made the observation more difficult. On the other hand the cells tended to move very little or not move at all during the experiment which made it easier to choose the area of interest for automated analysis.

The size of the cell have been determined to be 34 × 11 μm at the beginning of the experiment and 85 × 13 μm towards the end.

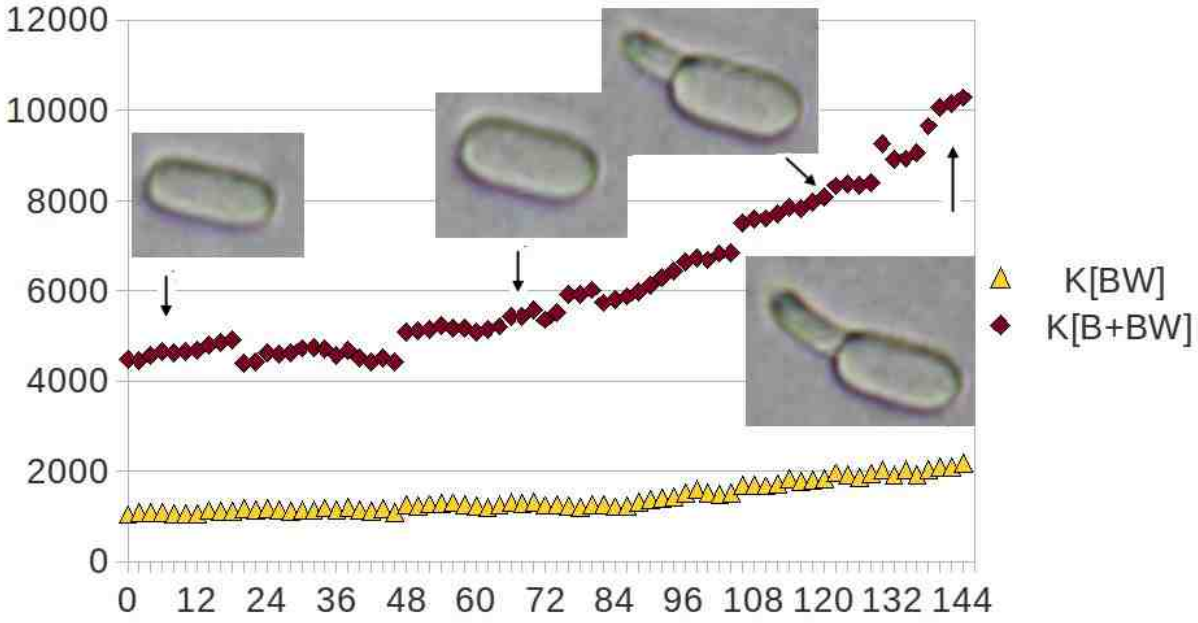

Figure 31: *Geotrichum candidum*, K_{BW}, K_{BWB}, cell growth, cells at time 10, 70, 120 and 140 minutes

5.1.4.5 Dipodascus magnusii

The last observed yeast specie have been *Dipodascus magnusii*. This specie divides the same way as above mentioned *Geotrichum candidum*. The experiment have been made using the first nutrient media and ran at temperature 24 °C. Same as before the growth is nearly linear without any significant build ups and relaxation phases. The size of the cell have been determined to be 27 × 18 μm at the beginning of the experiment and 65 × 23 μm towards the end.

The analysed data described above have been obtained as a part of experiments performed for study [43].

5.1.5 Comparison of selected method conventional methods

One of the most common methods is calculation of the cells using counting chamber. Counting chamber is a specially designed glass chamber with a net of squares dividing the compartment into small segments (usually of size 0.1 mm)[35]. The cells or any particles visible under microscope can then be counted for each of the cells in the net covering the

compartment. This can be done either on the fly or later from captured image of the microscopic view of the chamber at given time. Same as in case of our analysis this method can be used for any kind of particles, not only living cells and is completely unobtrusive to the experiment. The disadvantage of the method in comparison to fractal analysis is the need to manually count amount of particles in each selected cell of the chamber and then use the statistical methods to estimate the total amount. The fractal analysis is able to provide the count over the whole colony as long as this is in the visible field of the microscope and can be captured in the image.

Other available method is Indirect Cultivation Method. This methods is operates on the assumption that from each of the cells will grow another colony if it is put into nutrition rich environment. The concentration of cells in the initial sample is drastically lowered by mixing it with water. Such very low concentration suspension is then cultivated again and newly grown colonies are counted. From the amount of cultivated colonies the amount of cells in the original colony is estimated backwards. This is an obtrusive method as it ultimately interrupts observed experiment. Due to requirement on growth of cells into colonies, method is suitable only for suspensions of living organisms and of those only for organisms that are relatively easily and without health hazards cultivated and grow quickly enough. This method have been developed into various variations, based on amount of time that is available for obtaining results and based on estimated concentration of cells in the sample. Method is very simple and not very expensive to perform. Since in the industry most of the quality control operations assume collecting of small samples from relatively big amounts of main suspension, method obtrusiveness is not an issue.

More modern methods are represented by membrane filter method that is based on capturing cells on the sterile membrane followed by cultivation of the captured cells. Method can be also used for certain non-living suspensions with limiting factors being size of the particle to be captured by the membrane and observed using microscope.

Another family of methods are electronic methods that operate on measuring conductivity of the suspension. The main problem of those methods is high sensitivity to conductive dirt and therefore requiring extremely clean environment during calibration as well as during the measurement itself. Electronic methods based on counting signal change while transferring suspension through set of electrodes suffer from yet another kind of error due to their inability to distinguish signal generated by passing single cell from those generated by passing aggregate of cells.

The main difference of the approach used here and the previous works focused on use of the fractal based analysis [29] was a complete automation of the data processing without any manual steps. All the previously manually performed operation have been now done autonomously. The automation of the operations have introduced the new category of issues that had to be dealt with. The following problems need to be considered when planning to use fully automated data processing:

- the baseline of the image data sets. The differences in the lightening conditions when taking the images, require different base-lining. In order to perform such automatically, the assumption of the continuity of the experimental data have to be made. After that the image data can be auto-corrected by ensuring the change of the fractal properties stays within predefined range in comparison to changes between previous and following frames.

- the positioning and the movement of the observed elements. The movement itself doesn't pose the problem as long as the observed object stays in the visual field throughout the whole

experiment. The issues can however occur if other stray objects enter the visual field intermittently. Apart from that the only requirement is to select area of interest for the analysis big enough to cover the object of the interest all the time.

- random noise. The constant noise, such as dirt on the observation apparatus or the edges of the experimental area are of no consequence. Although such items introduce the error into obtained Fractal Measure and Dimension, this error is systematic and it's effect is only in shifting the curve up or down on the horizontal axis. It can be also easily offset by base-lining the data against empty apparatus prior to starting the experiment.

5.2 Distribution Studies

5.2.1 Algorithms

The following algorithm attempts to describe process of distribution based analysis.

1. Select area of interest
2. Decide on direction of the analysis (not unidirectional, direction top-down or left-right)
3. Perform 1D Wavelet Analysis of the area of interest (ROI) in the image
4. Create distribution graph of Fractal Measure *K* values over the ROI
5. Repeat the above for an image with known distribution to obtain a calibration curve
6. Determine count and distribution of the objects in analysed area by comparison of the results from analysed area with the results obtained for the calibration curve.

The describe method is relative (to the calibration image data) and its main advantages and disadvantages are related closely to this fact:

- The limiting factor for the use of the method is its ability to only analyse imaging data for the systems where calibration data can be generated.
- The advantage of the method is ability to choose sensitivity in selected area by providing the right set of calibration data.

5.2.2 Programing

The functionality to perform one dimensional wavelet analysis over two dimensional data such as image in the direction of interest (top-to-down or left-to-right) have been incorporated in the latest version of Harmonic Fractal Analyser (HarFA) software building on the previously implemented, more general wavelet and harmonic analysis functionality. The programing language used for implementation is Delphi. HarFA can be therefore now used to generate distribution data sets from analysed images as well as the sets from calibration data. The output from the analysis is suitable for further processing in the common spreadsheets such as Excel.

5.2.3 Data Processing

The following set of images shows the images of cells from the experiment studying the decay and cell destruction. Typically in such an experiment the enzyme secretion sensitive dye is used to colour the cells. The change in the colour is interpreted as a change in the cells

life cycle. In our experiment, as shown in the set of the images of the yeast cells below the dye used changes colour of the cells to green when alive and to red when dead.

The cell distribution in this experiment is fairly uniform with all the cells being of almost same size. Therefore the using the algorithm for determination of the distribution of cells described above we can directly determine total count of the cells without need for defining multiple distribution calibration curves.

Each of the images in the set will be analysed three times in different colour spaces. First, in the intensity colour space to obtain a total count of the cells in the analysed image. Secondly in the green colour space to determine total count of alive cells, and lastly in the red colour space to determine the amount of dead cells.

Radiation of *Candida vini* at 10 minutes intervals

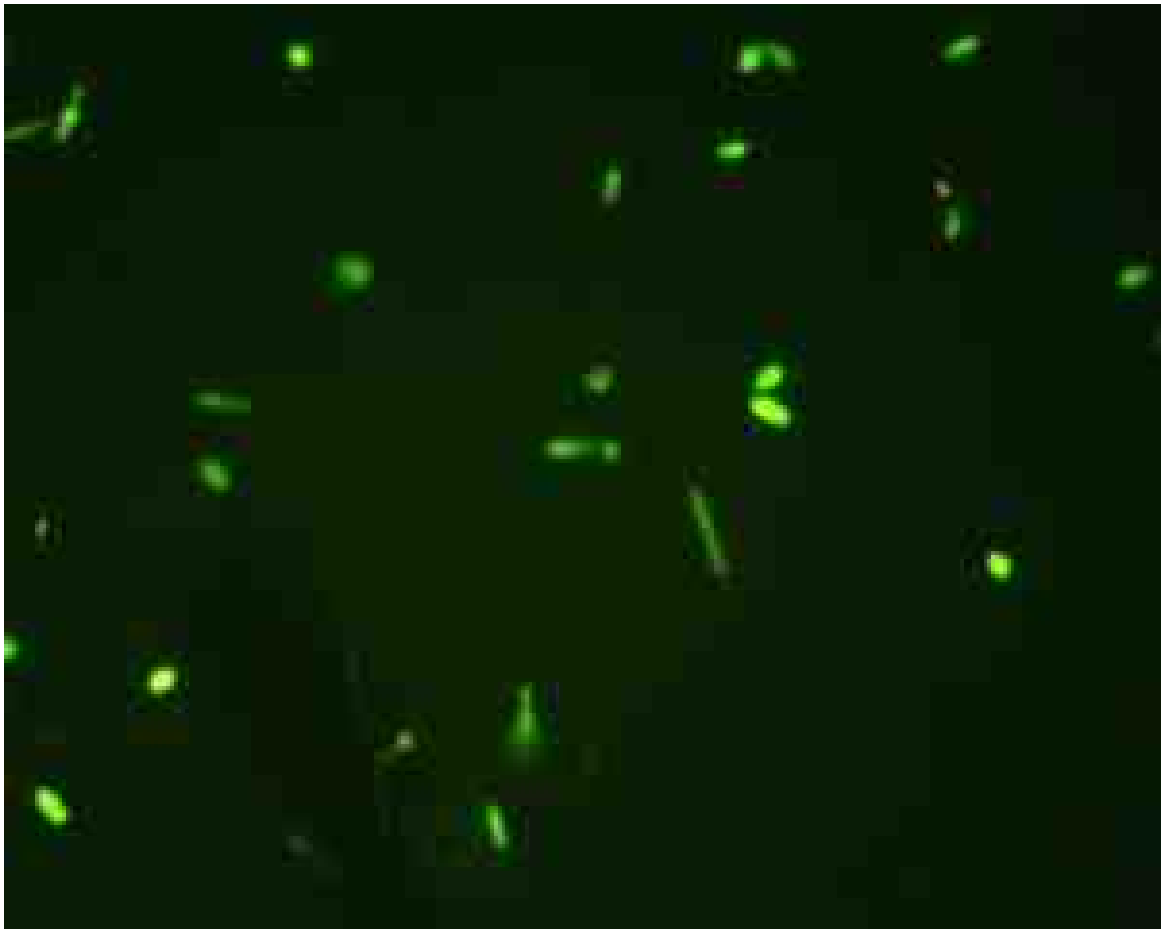

Figure 32: *Candida vini*, time 0 min

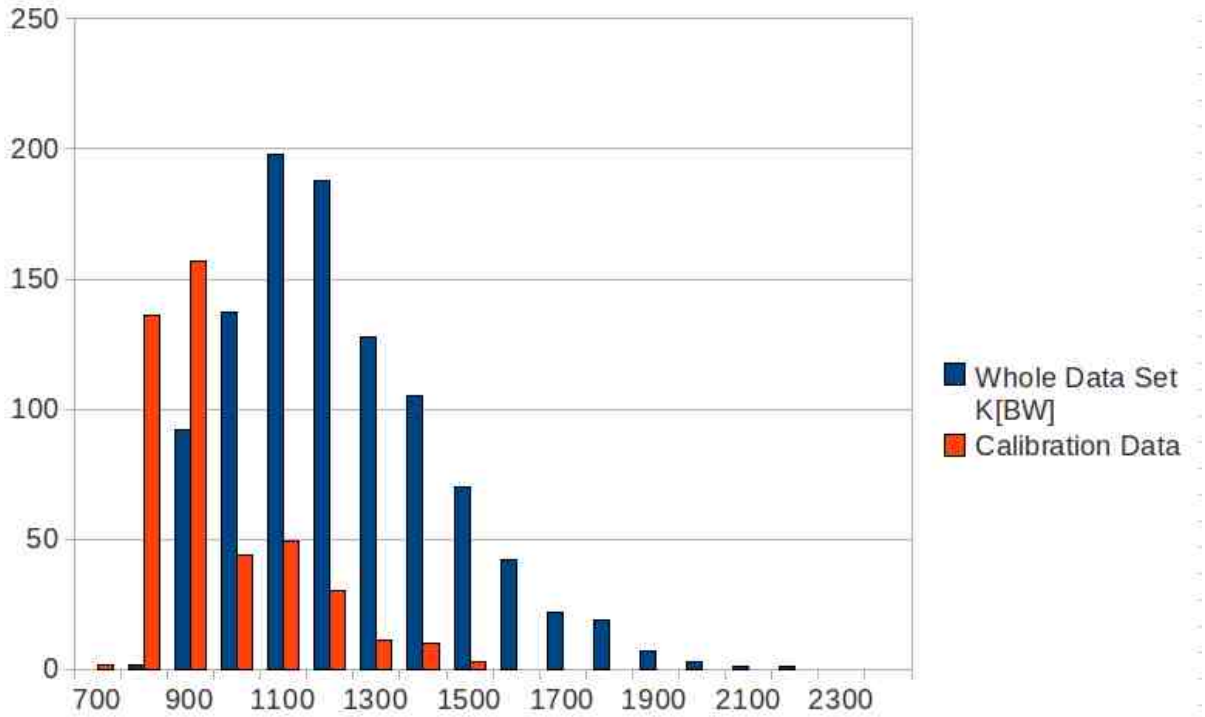

Figure 33: Distribution of Fractal Measure for single cell

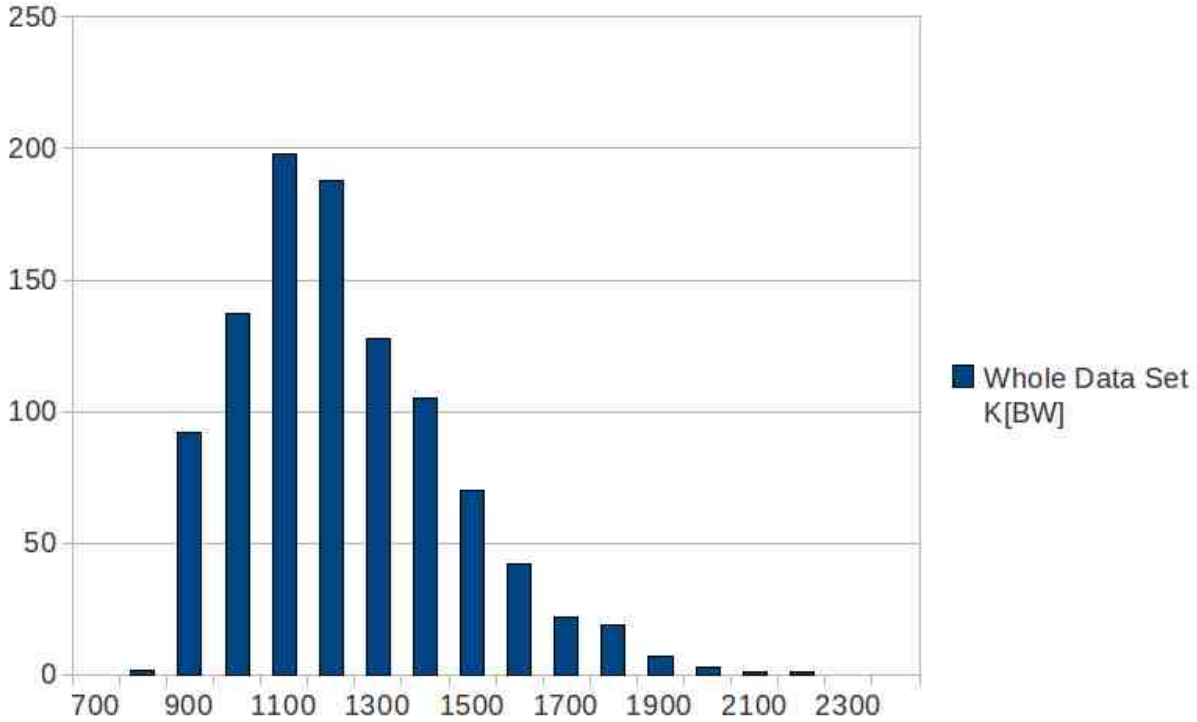

Figure 34: *Candida vini*, intensity color space, Fractal Measure Frequency

The single cell Fractal measure frequencies have been measured in the same image, but using a smaller area (¼). This accounts for the shift in measured frequencies and by multiplication of measured frequency by 4, this will be adjusted to the frequencies collected while measuring whole image.

The value of the Fractal Measure is in direct correlation with the surface covered by the measured object. Therefore by comparing Fractal Measure values from the frequency distribution for one cell the total of the cells in analysed image can be found.

$$c_t = \frac{\sum K_{bw_t} \cdot w_t}{\sum K_{bw_n} \cdot w_n} \cdot n$$

where c_t is total count of cells in analysed image,

K_{BWt} is a Fractal Measure of the Black-White interface,

w_t is a total width of the analysis run (the power of 2 for 1D wavelet analysis),

the K_{BWn} is a Fractal Measure of the Black-White interface in the calibration image,

the w_n is the width of the analysed area in the calibration image and

n is a total count of cells in the calibration image.

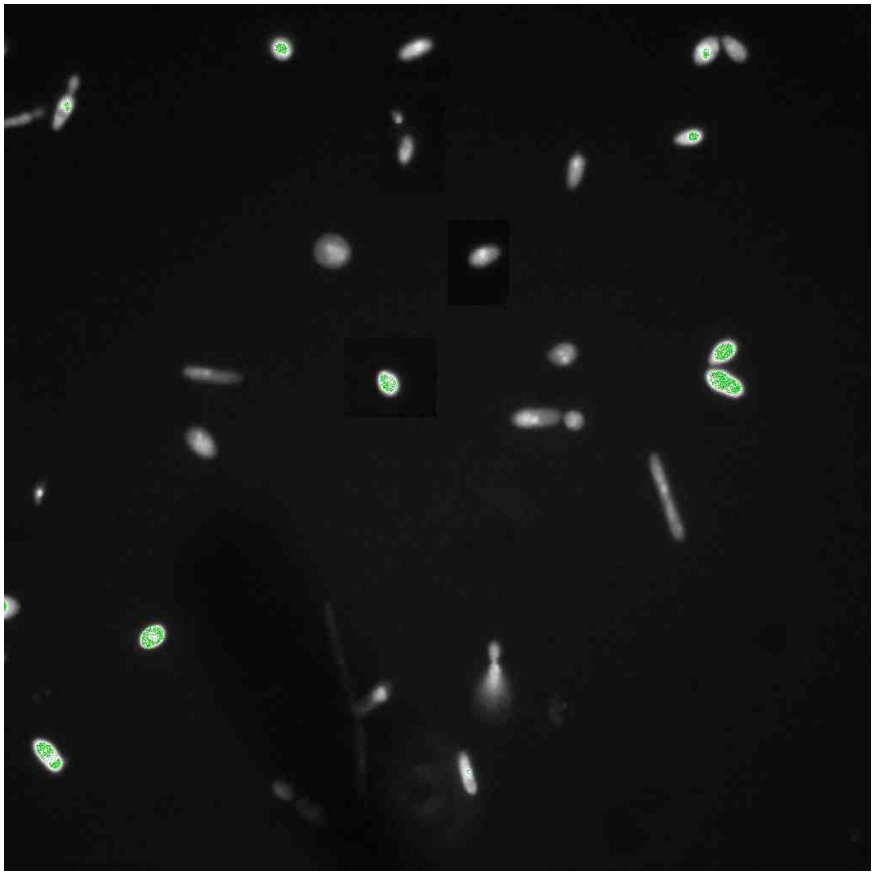

Figure 35: *Candida Vini*, time 0, green color space

In this case the single cell was present in the area of the image used for the calibration since the analysed cells had fairly uniform distribution. However in other cases where more cells of different sizes and shapes are present in the analysed area it might be necessary to choose such an area for calibration that contains more then one cell, or more exactly at number of cells of each shape and size to represent same distribution as observed in the analysed image. The more closely matches the distribution of cells in calibration area the analysed area the lower error is introduced by the calibration.

Using the formula described above the total of the cells calculated in the analysed image have been found to be 39.

The same image but in green colour space only looks like shown in Figure 35. Since the intensity of the green colour and the life power of the cells are in the correlation, it is clearly visible, that when the interference of the other colours is removed, not all cells show same amount of live power. The cluster of very healthy cells in the top right corner have been chosen for calibration this time. Using the calibration data generated from the cluster the total amount of healthy cells in the image have been calculated to be 22. The difference to the previously observed count are the cells that are either already dead or dying. This is normal for the living environment as all the cells go through their life cycle. Further below it will be observed that the amount of the dead cells increases progressively with the amount of radiation the cells have been exposed to.

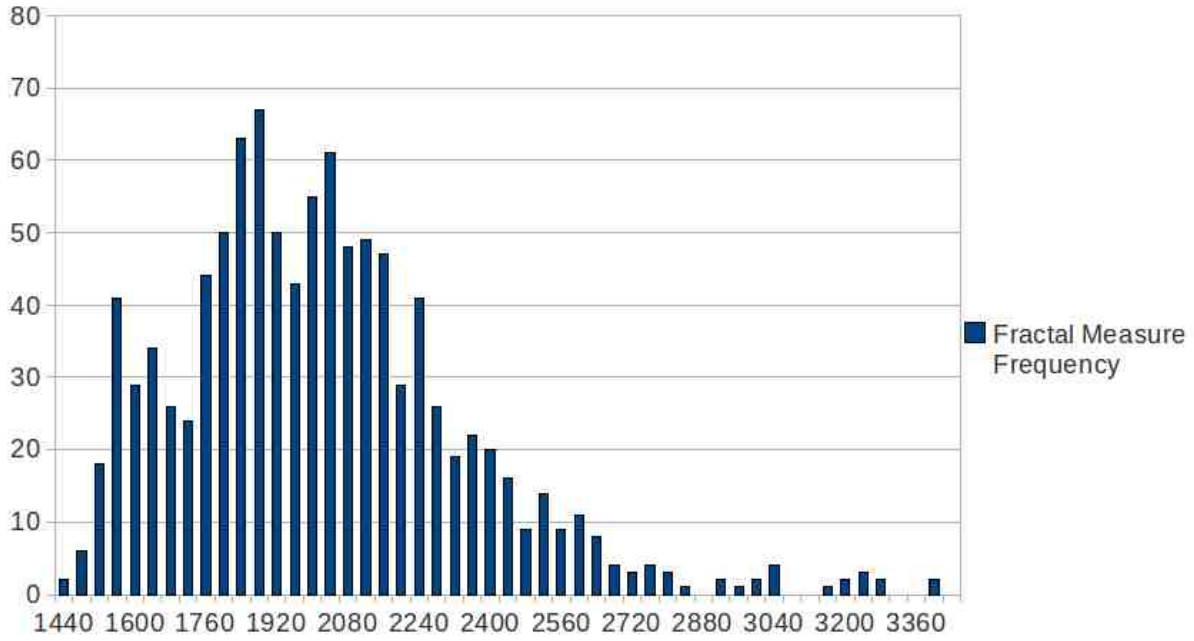

Figure 36: *Candida vini*, time 0 min, green color space

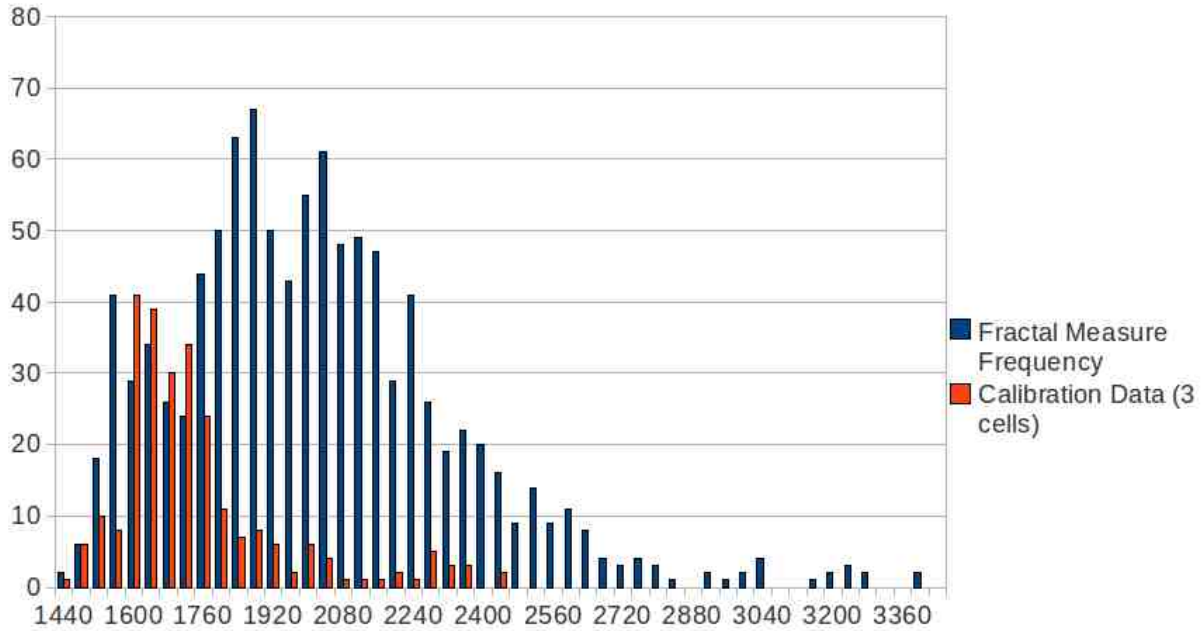

Figure 37: *Candida vini*, time 0 min, green color space, calibration

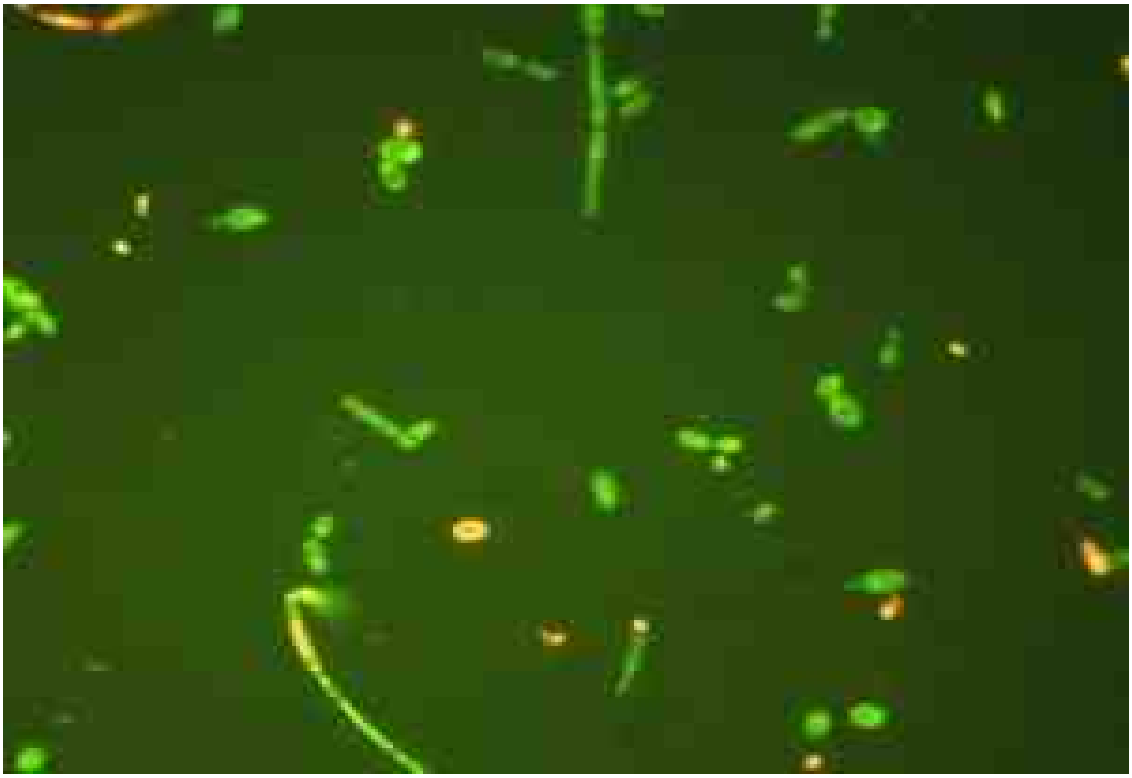

Figure 38: *Candida vini*, time 70 min

After running the experiment for 70 minutes and repeatedly exposing the cells to radiation, another set of images have been taken and as can be seen in Figure 38 the amount of dead or dying cells have increased. Using the above described method with the same set of calibration data as in the images taken at time 0, the total amount of cells (measured in the intensity space) at time 70 minutes have been found to be 38 (in comparison to 39 at time 0)

showing the colony didn't grow too much in size and the amount of living cells (visible in green colour space) have been found to be 21 (in comparison to 22 at time 0).

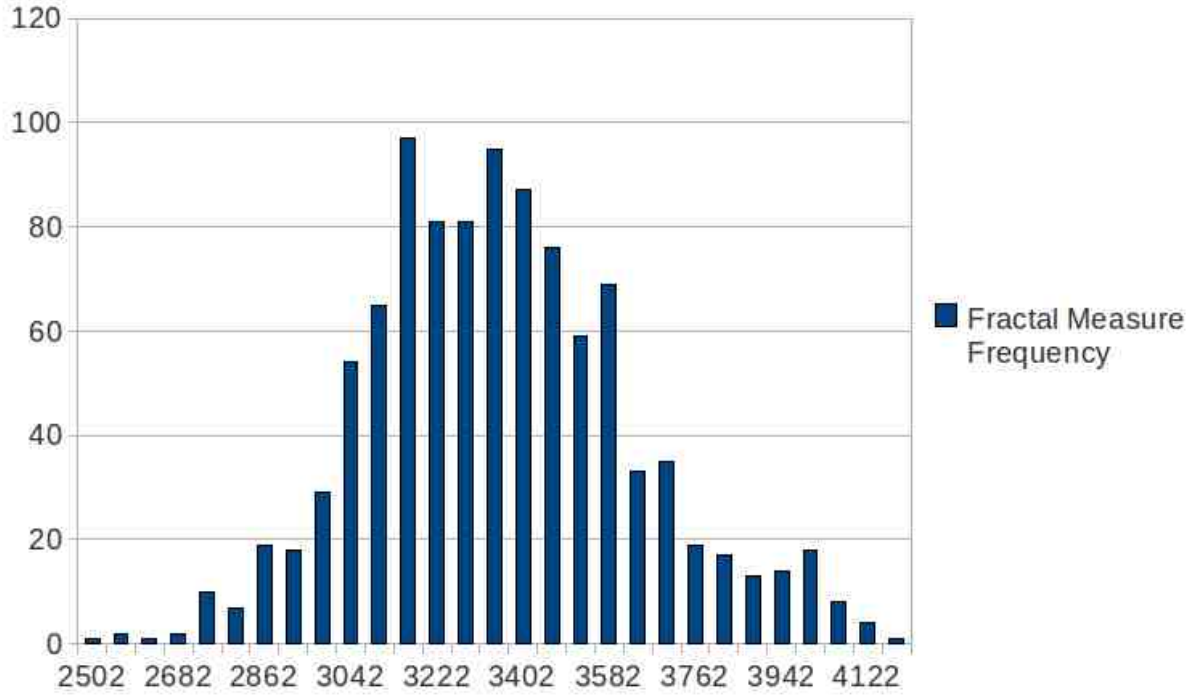

Figure 39: *Candida vini*, time 70 min, intensity color space

Clearly, the healthy *Candida vini* cells in this experiment have not been affected much by level of radiation to which the cells have been exposed during the experiment. However the amount of completely dead cells (those with high visibility in red colour space) have increased from 9 in the image taken at time 0 to 25 in the image taken at time 70 minutes. The overlap between the total amount of the cells and the sum of alive (green) and dead (red) cells is caused by the fact that the proteins responsible for green colour remain in the body of the cells shortly after the dying so at certain point (shortly before cell's final moments) it is possible to observe both the red and green colours in the cells. This is unfortunately not visible for the human eye directly, but to show this effect the image of the cell has to be shown in different colour spaces as shown in Figure 40.

Among other things it also shows how concentrating only on one factor (visibility in green colour space) can be deceiving. Another result that can be devised from the data analysis, is that in fact the colony of *Candida vini* have been affected adversely by the radiation, but the effect was just becoming visible at the time when the experiment have been stopped. Performing such analysis can be completely automated and if it had been so, images could be analysed within a second after being taken and system can suggest prolongation of the experiment and continuation of the observation even though on first sight there is no significantly higher amount of dead cells visible yet.

Looking at the Fractal Measure Frequency distribution curve at Figure 41 it can be seen that new element is becoming clearly visible. The frequency curve shows two distinct peaks. Each of the peaks signifies one distinct shape of the cells present. From the height and width

of the peak we can also estimate that the amount of elongated dead cells (second peak) in just a slightly smaller then the amount of cells with circular shape (the first peak). This feature shows for yet another unexplored feature of the one dimensional wavelet analysis as a way for determining and classifying shapes of objects in the analysed image data.

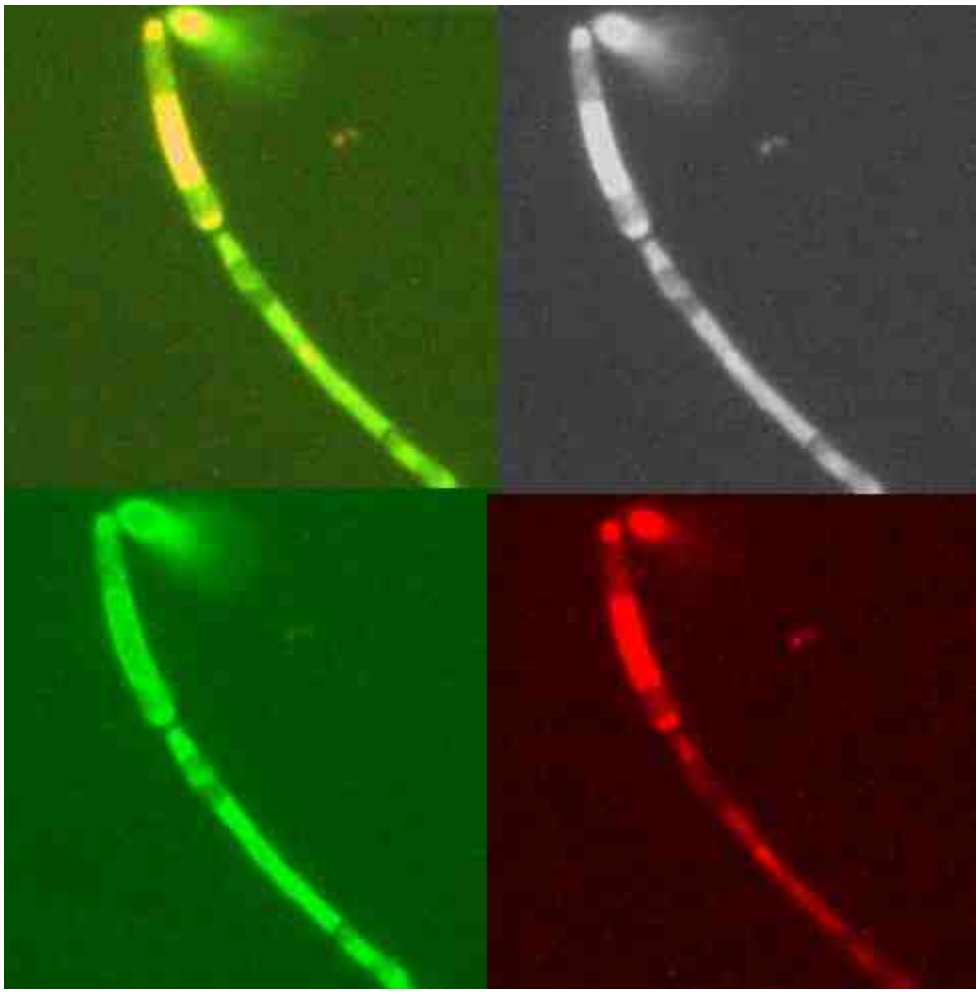

Figure 40: Dying cell. From top-left to bottom-right: Original, Intensity, Green, Red color spaces

The same analysis have been performed also for other species of yeast to confirm the method works in general and is not limited to only one shape of cells. See Appendix A – Distribution studies for more details. The analysed data described in this part have been obtained as part of the experiments performed for study [44].

The Figure 42 shows then differences when analysing frequencies in different colour spaces. Towards the end of the experiment the Fractal Measure visible in the red colour space is growing while the one in the green colour space is becoming less dominant. Still in this particular experiment there have been only few dead (visible in the red colour space) cells.

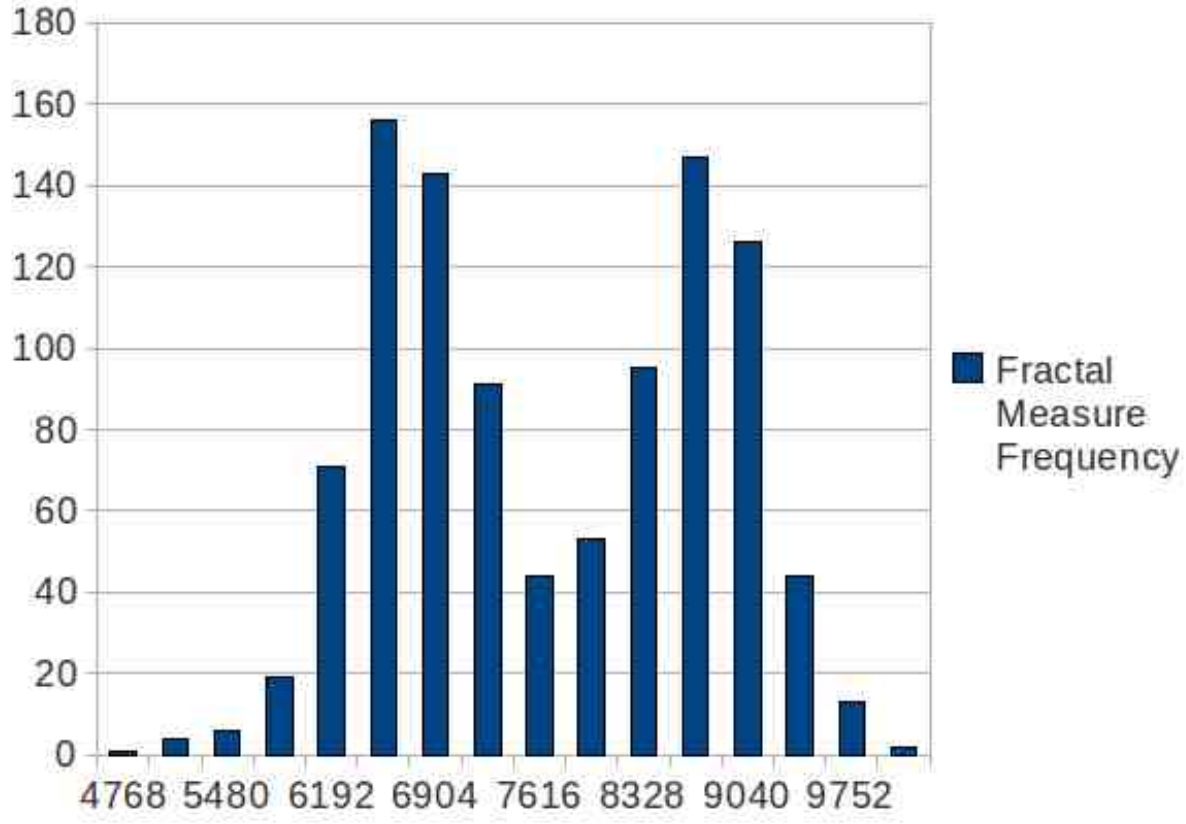

Figure 41: *Candida vini*, time 70 minutes, K_{BW} Frequency in red color space

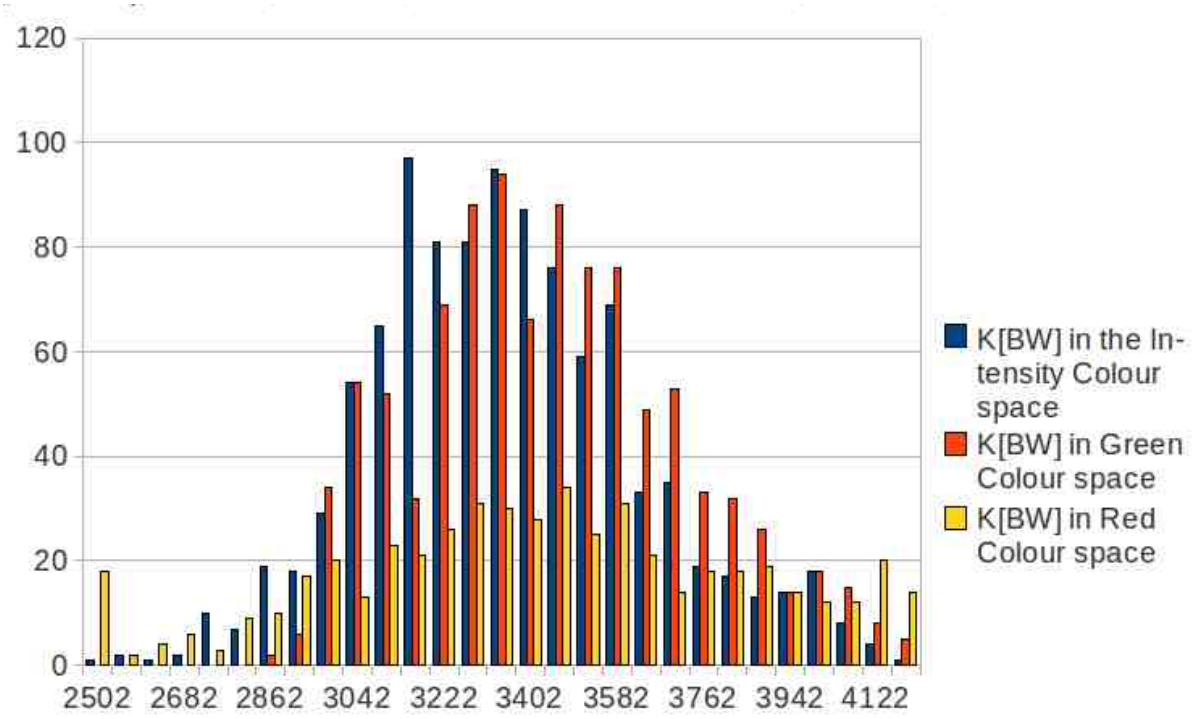

Figure 42: *Candida vini*, 70 minutes, K_{BW} Frequency in all color spaces

5.2.4 The effect of the shape on the distribution and importance of the calibration

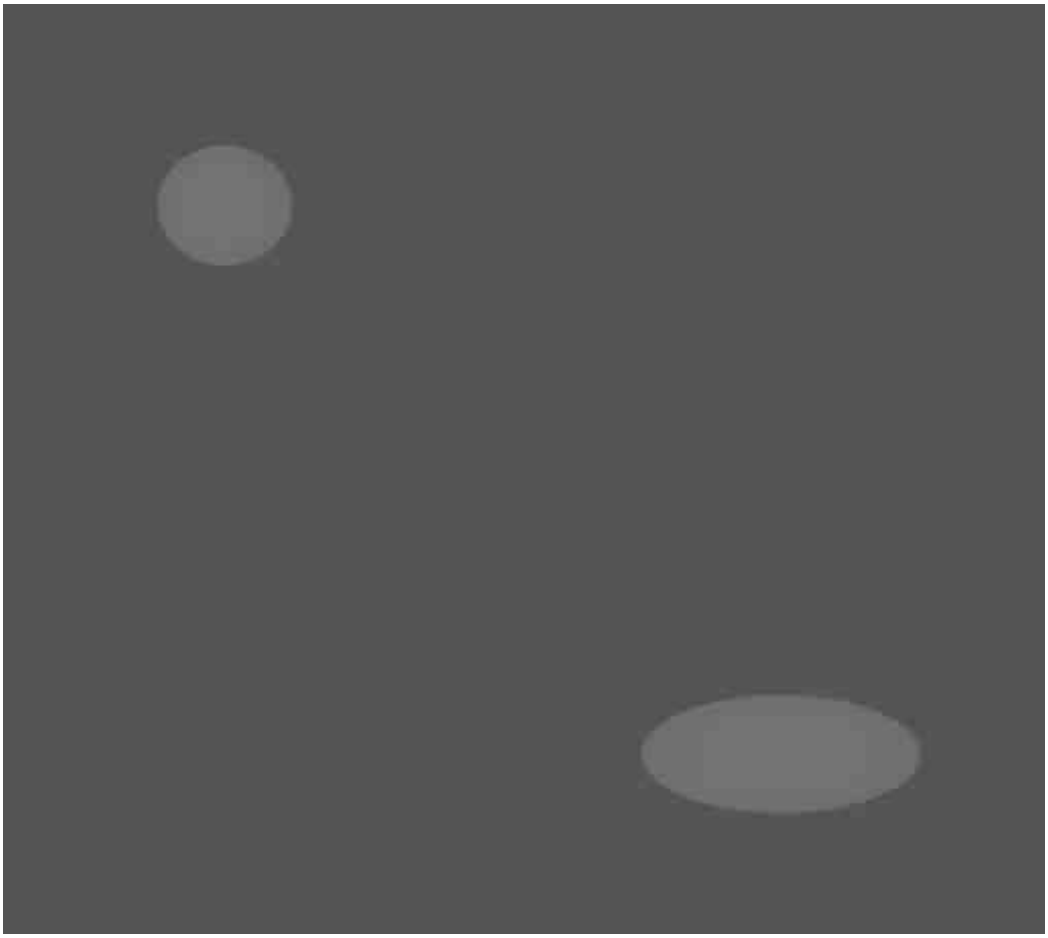

Figure 43: Circular and elliptical cell models

Using the model shown in the Figure 43 the effect of the shape of the analysed object (cell in this case) will be evaluated. First the left side of the model containing only the round shaped cell will be analysed, then the analysis of the right side of the model containing elliptically shaped cell will be performed. In the end the whole model will be analysed showing the combined effect on the Fractal Measure frequencies and providing leads in how to compute in such variations when performing general image analysis using the method described above. The model, in difference from the real measurements, doesn't contain any background noise (i.e. the background is made of the shade of the gray rather then nearly black-grey noise). For this reason the frequency bands (Fractal Measure values of 1) are omitted from the diagrams created from model. This has no effect on the final shape of the objects and is artificial artefact introduced by using ideal model.

Throughout the model, cells have been created using the gradients rather then simple white blobs in order to get important (from the analysis point of view) model parts as close to reality as possible. The gradient in the round model part is linear in all directions from the centre. If shown in the three dimensional view (Z direction representing the gradient itself) the round model would look like a cone. The elliptical part of the model have been created using the shaped angular gradient pattern. Again in 3D model this would look like a deformed (elongated in direction of X axis) cone.

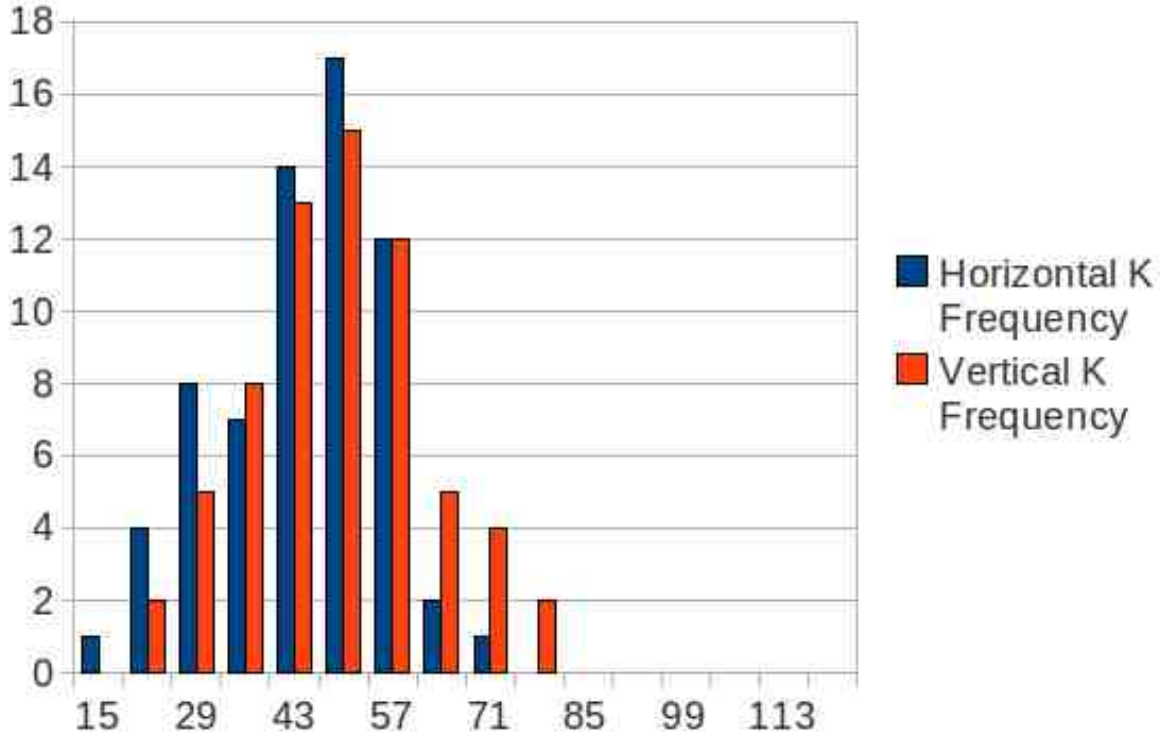

Figure 44: Round Cell Model, Fractal Measure Frequencies

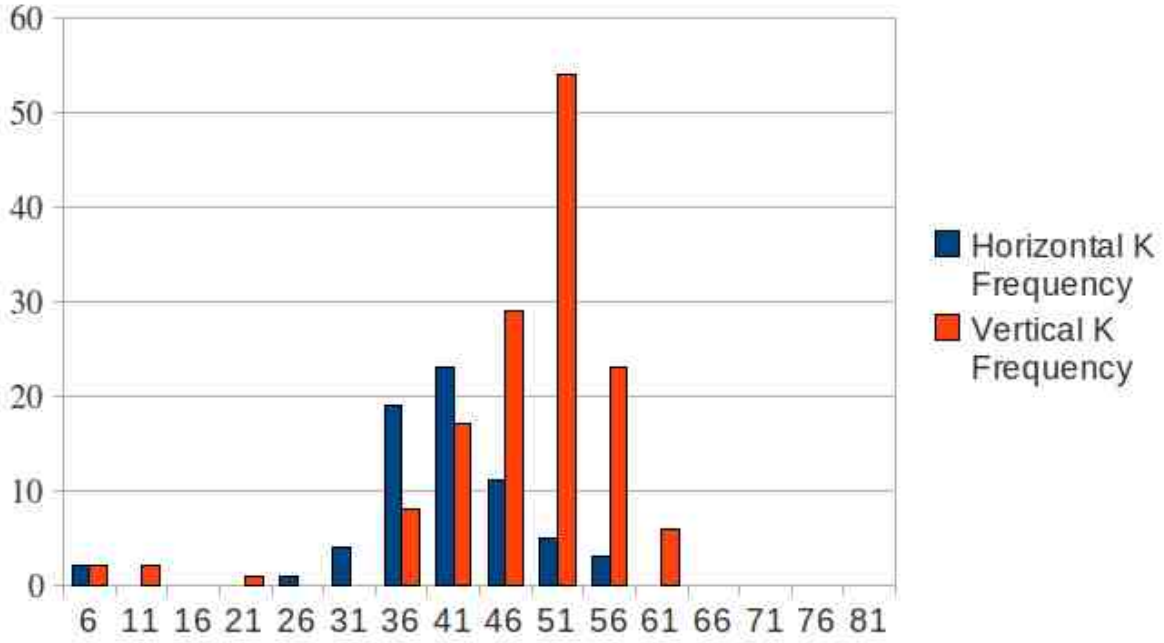

Figure 45: Elliptical Cell Model, Fractal Measure Frequencies

Analysing the round model the Fractal Measure Frequency profile shown in Figure 44 have been obtained. The chart shown the distribution of Fractal Measure close to normal Gaussian bell curve. The differences between results when analysed horizontally and

vertically are in the range of single units and caused by the differences of the gradient distribution of the generated circle when looked at from different direction.

Figure 45 shows Fractal Measure Frequencies distribution for the elliptically shaped model cell. While the distribution is nearly identical no matter if measured in horizontal or vertical direction for circular shape, it is not so for the elliptical one. This is due to uniformity of the circle. The Frequency distribution measured around Y axis is wider and produces higher numbers then the same frequency measured along X axis which has shape close to the Frequency distribution produced by the circle. This opens possibility of devising the analysis method that by measuring frequencies from different directions device the predominant shape or orientation of the measured objects.

The Figure 46 shows the Fractal Measure Frequencies for both circle and ellipse alongside and shows that even when shape of the distribution is similar along the axis in which the measurement have been made, the mass covered by the Frequencies is higher for the ellipse as it covers bigger surface area in the image.

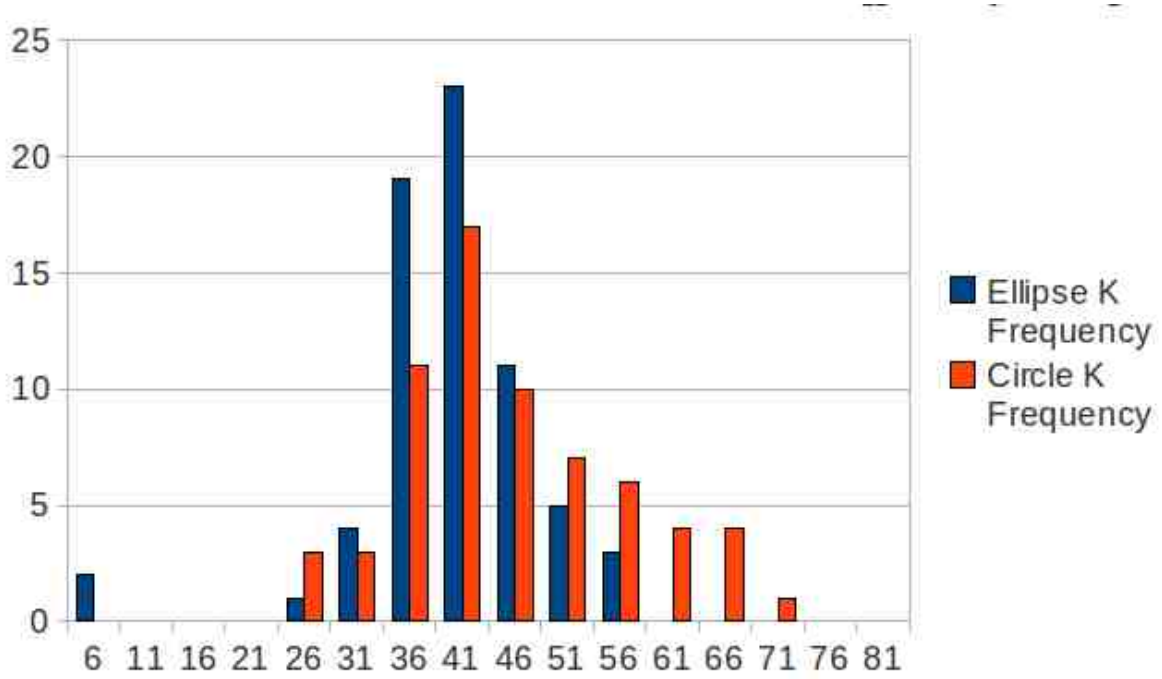

Figure 46: Circle and Elliptical Model Fractal Measure Frequencies

In the Figure 47 we look at the total distribution for combined round and elliptical cell model. The combined graph resembles more the round rather then elliptical one. This is attributed to the fact that round model contributes more values to the total and is therefore more significant. Also even though the shape of the cells is different in the model and the elliptically shaped cell has lower total intensity, the ratio of the intensities is quite similar (the Fractal Measure Frequencies are in the same area) so rather then shifting the graph to the left or the graph the intensities of the elliptically shaped cell contribute to the total in exactly same area. In general it is possible to say that the effect of the shape of the cell is very little relevant as long as the total area covered by the cell and its intensity is comparable.

Even though the effect of different shape cells on the total frequencies distribution is minimal, the importance of the shape of the cells can't be underestimated and shapes have to

be taken in account when looking for calibration data. In the model above, using the only round cell as a calibration the total of cells will be calculated to be 1,15; while using the elliptical cell as a calibration the total will be 2,1. The result obtained via round cell calibration underestimates the total due to higher intensity of the round cell. The over estimation using the elliptical cell can be attributed to the same reason – the cell has lower intensity then the round one and therefore appears to be "bigger". The calibration data for real experiments have to be chosen so the distribution of sizes, shapes and intensity of the cells in the calibration set is as close as possible to the distribution in the whole analysed image or image sets to minimize the errors.

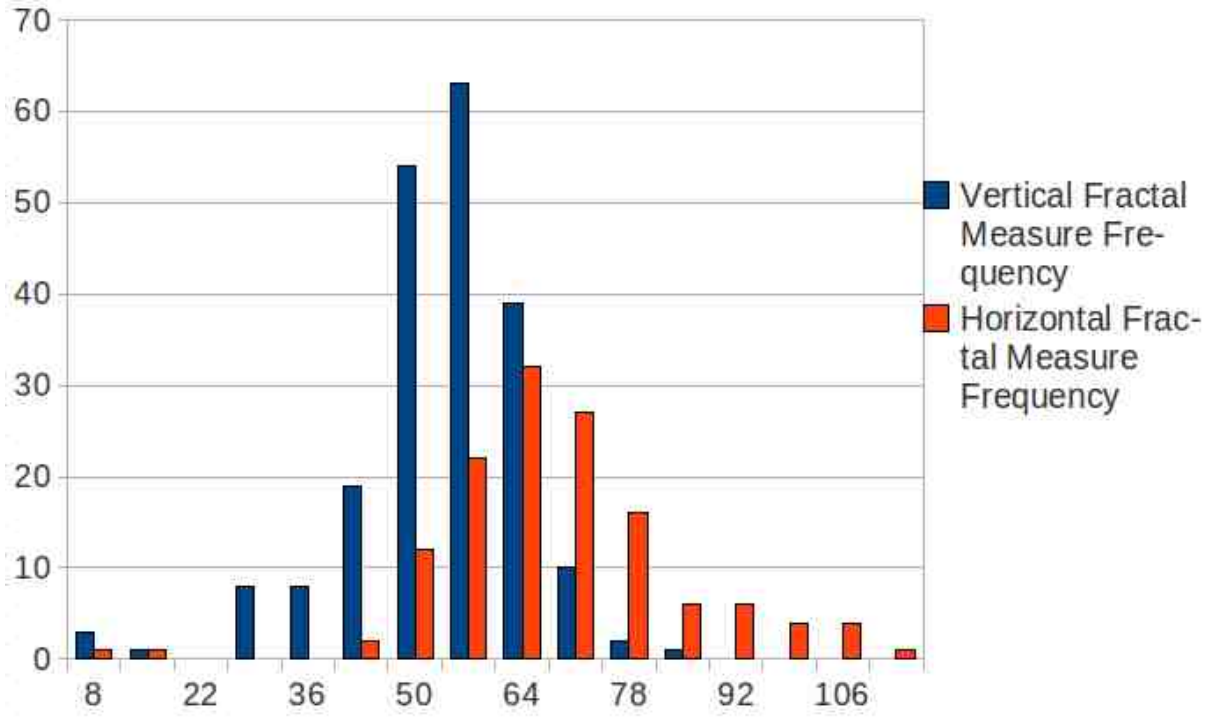

Figure 47: Round and Elliptical Cell Model, Fractal Measure Frequencies Distribution

6. CONCLUSIONS

It has been shown that the Fractal Analysis is fully suitable for analysing disperse systems such as a colony of cells in the nutrient media. It has been also shown that the use of Fractal measure and its relation to the surface area of the cells can be successfully used to obtain the exact counts of the cells or more generally of the any elements under the observation. Using the Fractal Measure distributions it is also possible to create a calibrations for the distributions of the cell or other element sizes and count those in the environment. The previous works[29] based on the use of Fractal Analysis had imposed many preprocessing steps into the analysis to clean out the data, re-position the elements to ensure their location to be the same throughout the analysis and to remove any noise from the data. This works has shown, and the results have been already incorporated in the HarFA software, that the noise effect is insignificant in most of the cases, and when it bears any significance to the performed analysis, rather then manual removal, it can be removed systematically by base-lining the analysis against the image of empty experiment area. It have been also shown that the location information itself bears no significance in the kinetic (growth) experiments and as such can be safely ignored. The fact of changing location together with the automation of the analysis and choosing overall area of interest instead of choosing the the analysed area par frame independently only imposes the requirement of choosing the bigger area to ensure the analysed cell stays within the chosen area throughout the whole analysis.

The distribution studies hinted at the possibility of using Harmonic Fractal Analysis to obtain the exact counts of the cells against the calibrated cell(s) size. When dealing with the distributions of the cells of different sizes or even of different shapes and species, using the right calibration data it will still be possible to obtain counts even for such heterogeneous systems. The counting algorithm could be used also in the growth studies, in which case the resulting counts would be giving real numbers throughout the experiments due to small sizes of the budding cells. The fraction in this case would be growing until the growing bud becomes of the size of the original cell. Due to this technique depending heavily on the Fractal Measure value, which itself is a function of the analysed surface area, the best results are achieved when analysing dyed or otherwise coloured cells (elements) to increase the surface area and obtain results with higher precision. The differences between output from the model and the experimental data also show that it is necessary to choose the data for calibration that are related to the environment in which experiment occurs and contain the same noise as the experimental data rather then trying to find correlation between the model and real data which would only result in quantification of the background noise related to the experimental setup.

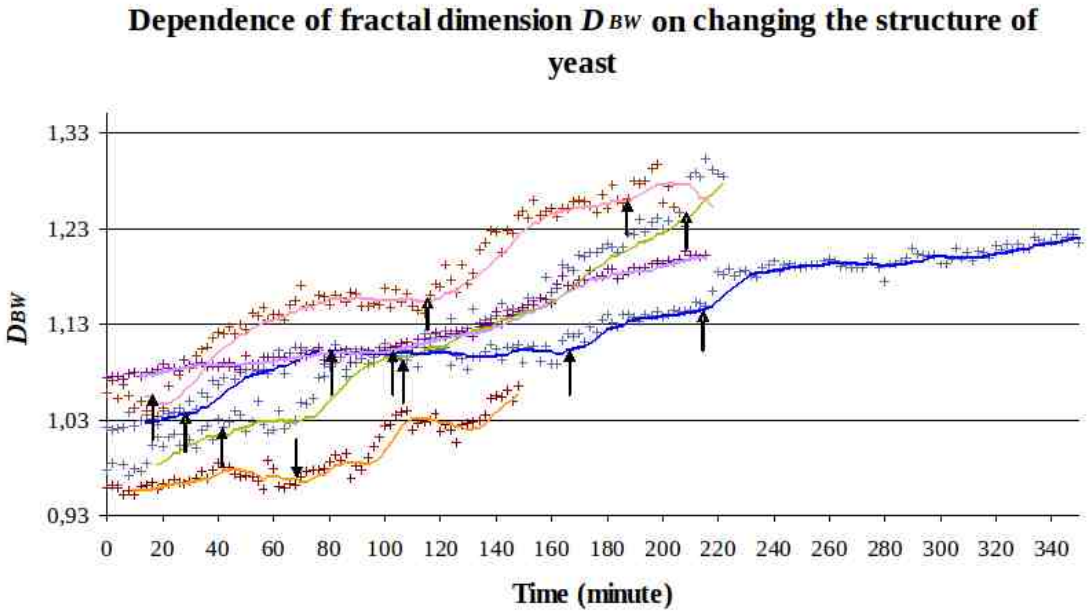

Figure 48: Growth of the yeast, by color: *Candida vini,* *Kloeckera apiculata,* *Saccharomyces fragilis,* *Geotrichum candidum,* *Dipodascus magnusii* [43]

Figure 48 Shows the summarized results from all growth experiments. This chart highlights the differences in the growth curves of different yeast species which. The differences are caused by different dynamics of the growth rather then the differences in the size and shape of the cells which have been abstracted from measured data by use of fractal based image analysis. Method thus provides basic instrumentation for automated comparisons of growth dynamics of different species as well as measurement of differences in growth of the same species in different environments. Similarly the method can be applied to measure dynamic changes in any kind of disperse system.

The Figure 49 and Figure 50 then show the summary of the results for all analysed yeast families. It appears that only the *Hansenula anomala* shows any real sensitivity to the radiation with quantifiable decline in population. The *Candida vini* and *Saccharomyces pastorians* are largely unaffected by the radiation with their populations not growing but keeping steady. The *Rhodotorula glutinis* family shows on the other the signs of slow expansion with the increased number of live cells in the population. The important thing to consider when looking at the results is the fact that the analysed system is dynamic and changing during the experiment. The dead cells are dissolving and disappearing from the view and the living cells are multiplying and of course dying. So rather then seeing absolute numbers we see only changes and trends in the dynamic balance of the system.

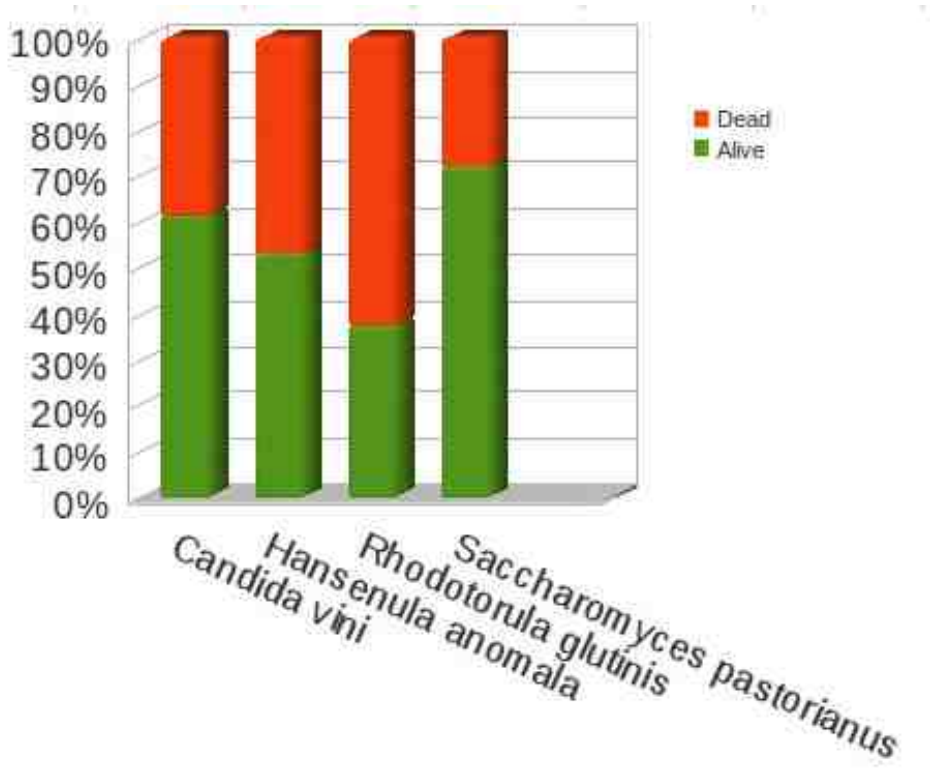

Figure 49: Live vs. Dead cells at Time 0 minutes

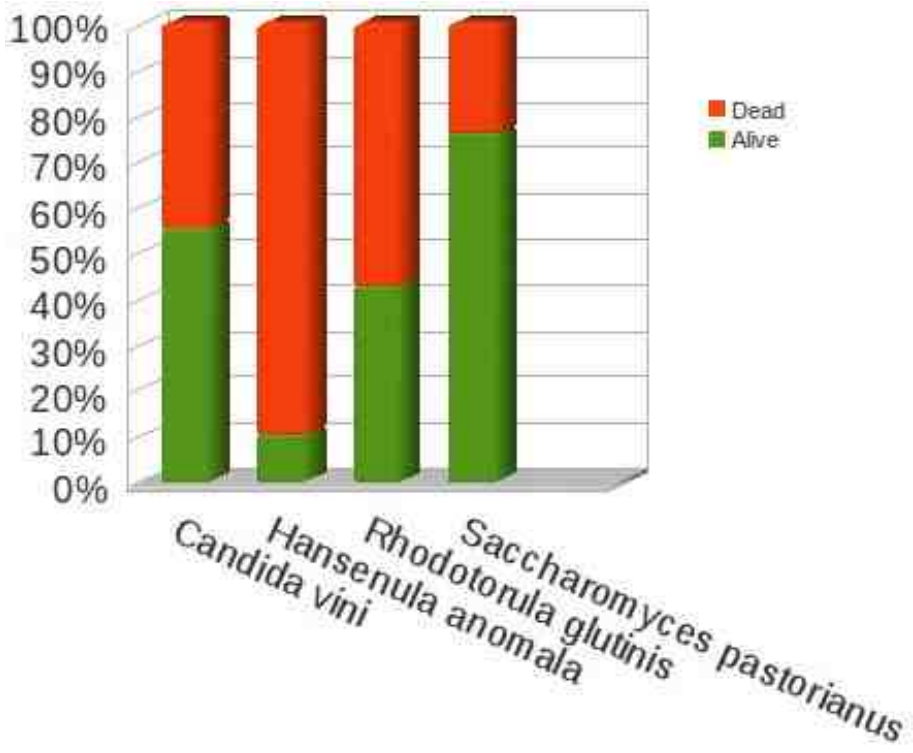

Figure 50: Live vs. Dead cells at Time 70 minutes

7. LITERATURE

[1] Hunter, R.J.: *Foundations of Colloid Science*, Oxford University Press, 1989

[2] Russel, W.B., Saville, D.A., Schowalter, W.R.: *Colloidal Dispersions*, Cambridge University Press,1989

[3] Hackley, V.A., Ferraris, C.F.: *The Use of Nomenclature in Dispersion Science and Technology*, NIST, special publication 960-3, 2001

[4] Myers, D.: *Surfaces Interfaces And Colloids*, Wiley-VCH Publications, ISBN 0471330604.

[5] Madigan, M., Martinko, J. (editors): *Brock Biology of Microorganisms*, 11th ed., Prentice Hall., 2006, ISBN 0-13-144329-1

[6] Lichtman, M. A., Williams, W. J., Beutler, E., Kaushansky, K., Kipps, T. J., Seligsohn, U., Prchal, J.: *Williams hematology*, 7th. Edition, ISBN 0-07-143591-3

[7] Pharm Eur. 2006. 5.1.6 : *Alternative Methods for Control of Microbiological Quality*, Pharm Eur vol.5.5 pp 4131-4142.

[8] Zmeškal, O., Komendová, B., Bžatek, T., Julínek, M.: *Hodnocení kvality tiskových bodů metodami obrazové (waveletové) analýzy*

[9] Barnsley, M.: *Fractals Everywhere*, Second Edition, Morgan-Kaufmann Publishing

[10] Weisstein, E. W.: *CRC Concise Encyclopedia of Mathematics, Second Edition,* ASIN:1584883472

[11] Zmeškal, O., Nežádal, M., Komendová, B., Julínek, M., Bžatek, T.: *Fraktální analýza obrazů tiskových struktur*, Conf. Of Wood, Pulp and Paper. 1st de. FCHPT STU Bratislava, 2003 p. 57 – 59, ISBN 80–901250–8–5, (Czech version PDF).

[12] Zmeškal, O., Nežádal, Bžatek, T.: *Fractal-Cantorian geometry, Hausdorff dimension and the fundamental laws of physics*, Chaos, Solitons and Fractals 17, 2003, pp 113-119

[13] Hausdorff, F.: *Dimension und äußeres Maß*, Mathematische Annalen 79(1–2) (March 1919) pp. 157–179

[14] Besicovitch, A. S.: *On Linear Sets of Points of Fractional Dimensions*, Mathematische Annalen 101 (1929)

[15] Wei-Bin Han, Gui-Xi Yi, Hua Xin: *Study on correlativity among capacity dimension D0, information dimension D1, algorithmic complexity C (n) and b value*, Acta Seismologica Sinica, Volume 11, Number 4, pages 507-510, July 1998, ISSN:1000-9116

[16] Maggi, F., Mietta, F., Winterwerp, J. C. : *Effect of variable fractal dimension on the floc size distribution of suspended cohesive sediment*, Journal of hydrology, 2007, vol. 343, no1-2, pp. 43-55, ISSN 0022-1694

[17] Halmos, P.: *Measure theory*, Van Nostrand and Co, 1950

[18] Dobrushin R. L.: *Gaussian and their subordinated self-similar random generalized fields*, Ann. Probab., 7(1), 1–28, 1979.

[19] Biermé, H. and Estrade, A.: *Poisson random balls: self-similarity and X-ray images*, Adv. Appl. Prob., 38, 1–20, 2006

[20] Biermé H., Estrade A. and Kaj I.: *About scaling behavior of random balls models*, S 4 G 6th Int. Conference, published by Union of Czech mathematicians and physicists, 63–68, 2006.

[21] Nakayama T., Yakubo K.: *Fractal concepts in condensed matter*, 2003, ISBN 3-540-05044-2
[22] Federer, H.: *Geometric Measure Theory*, Springer-Verlag, 1969 , ISBN 3-540-60656-4
[23] Klíma, Bernáš, Hozman, Dvořák: *Zpracování obrazové informace*, 1 vyd. Praha: ČVUT 1996.
[24] Častová, N., Vlček, J.: *Funkce komplexní proměnné a integrální transformace*. 1 vyd. Ostrava: VŠ Báňská, 1992
[25] Polák, J.: *Integrální a diskrétní transformace*. 1 vyd. Plzeň: VŠSE, 1991
[26] Zmeškal, O., Julínek, M., Bžatek, T.: *Obrazová analýza povrchu potiskovaných materiálů a potištěných ploch*. Conf. Pardubice, V. Polygraphic conf. University of Pardubice, September 12 – 13., 2003, ISBN 80–7194-372-X, (Czech version PDF).
[27] Dickinson, C.: *An Evaluation of the Current State of Digital Photography*, bachelor's thesis, Rochester Institute of Technology, 1999
[28] Holman, P, Najzar, K.: *Wavelets*. Pokroky matematiky, fyziky a astronomie, Praha: číslo 4, ročník 44, 1999.
[29] Tománková, K.: *Studium vlastností hrubě disperzních soustav pomocí metod obrazové analýzy*, (Czech version)
[30] Kocková – Kratochvílová, A.: *Taxonómia kvasiniek a kvasinkovitých mikroorganizmov*, 1 vyd. Bratislava: Alfa 1990, ISBN 80-05-00644-6.
[31] Maturin, L., Peeler, J. T.: FDA Bacteriological Analytical Manual, Edition 8, Revision A, 1998.
[32] Jarvis, B., Lach, V.H., Wood, J.M.: *Evaluation of the spiral plate maker for the enumeration of microorganisms in foods,* 1977, J. Appl. Bacteriol., 43:149-157.
[33] Donnelly, C.B., Gilchrist, J.E., Peeler, J.T., Campbell, J.E.:*Spiral plate count method for the examination of raw and pasteurized milk,* 1976 Appl. Environ. Microbiol. 32:21-27.
[34] Zipkes, M.R., J.E. Gilchrist, and J.T. Peeler.*Comparison of yeast and mold counts by spiral, pour, and streak plate methods,* 1981, J. Assoc. Off. Anal. Chem. 64:1465-1469.
[35] American Public Health Association: *Compendium of Methods for the Microbiological Examination of Foods*, 1984, 2nd ed. APHA, Washington, DC
[36] Association of Official Analytical Chemists: *Official Methods of Analysis*, 1990 , 15th ed. AOAC, Arlington, VA.
[37] American Public Health Association: *Standard Methods for the Examination of Dairy Products*, 1993, 16th ed. APHA, Washington, DC.
[38] Caprette D. R.: *Experimental Biosciences Introductory Laboratory* – Bios 211, Rice University
[39] Lattuada M. ,Wu H., Morbidelli M.: *Estimation of Fractal Dimension of colloidal gels in presence of multiple scattering,* ETH-Zurich
[40] Dekker, M.: *Handbook of industrial automation*, ISBN: 0-8247-0373-1
[41] Sobh, T., Elleithy, K., Mahmood, A., Karim, M. (editors): *Inovative Algorithms and Techniques in Automation, Industrial Electronics and Telecommunications*, ISBN 978-4020-6265-0

[42] Harmonic and Fractal Analyzer - HarFA software home page http://www.fch.vutbr.cz/lectures/imagesci/includes/harfa_introduction.inc.php

[43] Tomankova, K., Jerabkova, P., Zmeskal, O., Vesela, M., Haderka J.: *Use of the Image Analysis to study growth and division of yeast cells*

[44] Jeřábková, P.; Zmeškal, O.; Veselá, M.; Haderka, J. Využití waveletové transformace v mikrobiologii. In Digitální zobrazování v biologii a medicíně. Nezařazené články. České Budějovice: Entomologický ústav AV ČR, 2005. s. 30 (1 s.). ISBN: 80-86668-03-7

8. APPENDICES

8.1 Appendix A – Distribution studies

8.1.1 Hansenula Anomala

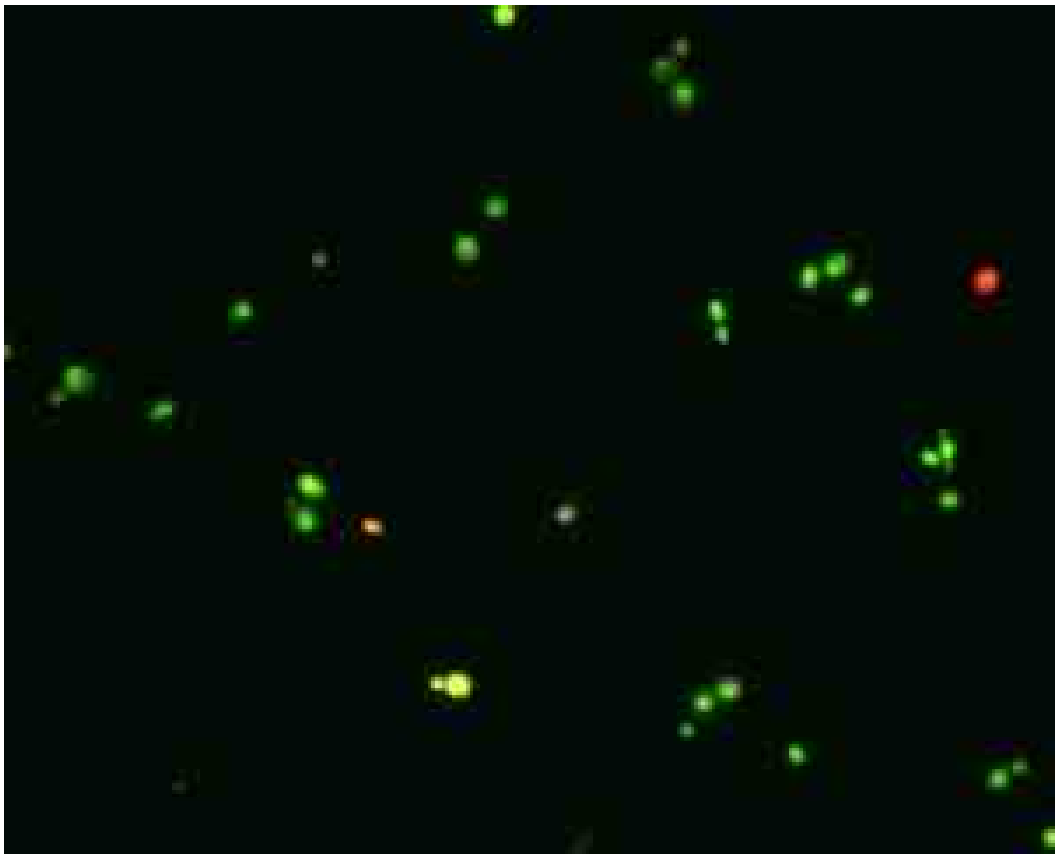

Figure 51: Hansenula Anomala, time 10 min

Following are the image data from the radiation experiment explained earlier, but performed on yeast cells of *Hansenula Anomala* family.

While the *Hansenula* colony in the Figure 51 seems to be still very healthy at this point of the experiment with only the 2 cells completely death at first sight, the analysis uncover the reality to be a bit different.

Based on the intensity based analysis, the total amount of cells have been determined to be 34. The Fractal Measure frequencies for the whole image and for the calibration data set are shown in Figure 52 and Figure 53 respectively.

The analysis in the red colour space, however shows that the destruction of the cells have been already triggered and is in progress more less over the whole colony. Analysing the image in the red colour space, it have been found that total of 16 cells (nearly a half of the cells in the colony) are already dying. The Fractal Measure frequencies for the analysed data and for the calibration are shown in Figure 54 and Figure 55 respectively.

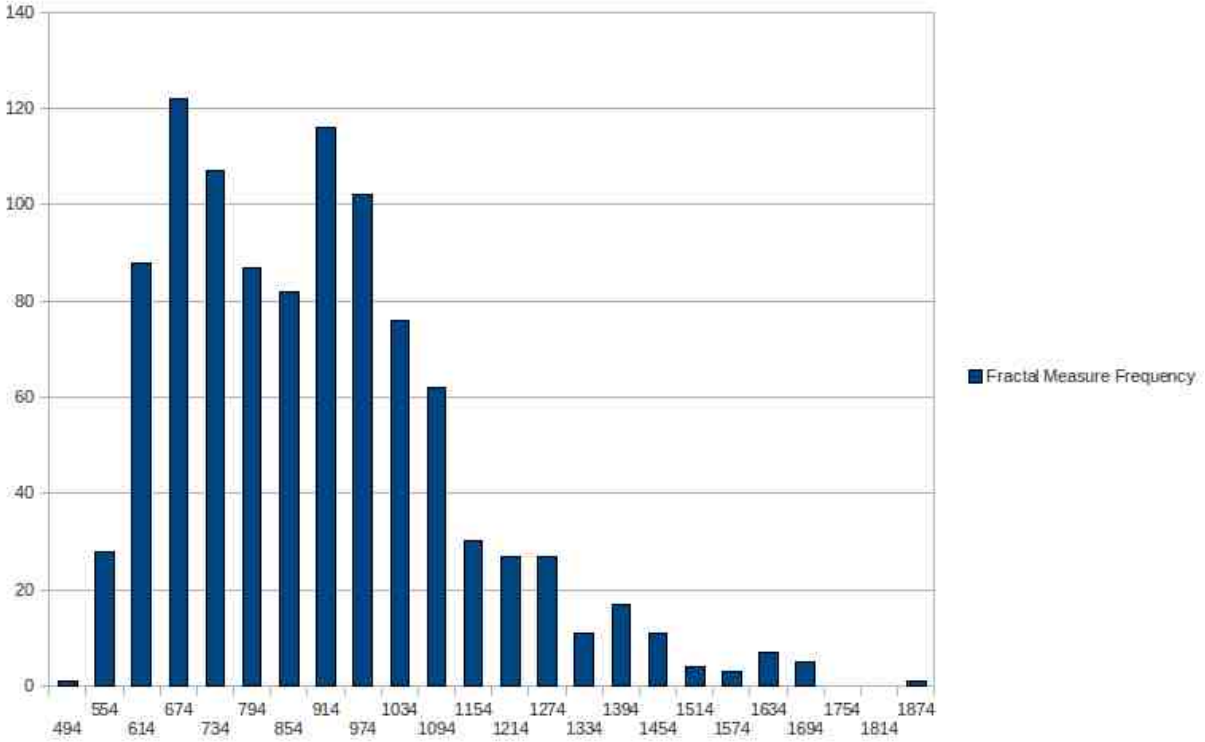

Figure 52: Hansenula Anomala, time 10 min, Fractal Measure Frequencies in the Intensity space

The same colony after the 70 minutes of radiation looks as shown in the Figure 56. Even without detailed analysis it is clearly visible that most of the cells are completely death. The only cells remaining alive are those born later during the experiment and not present at the beginning. The data analysis in the red colour space shows there are 35 dead cells present.

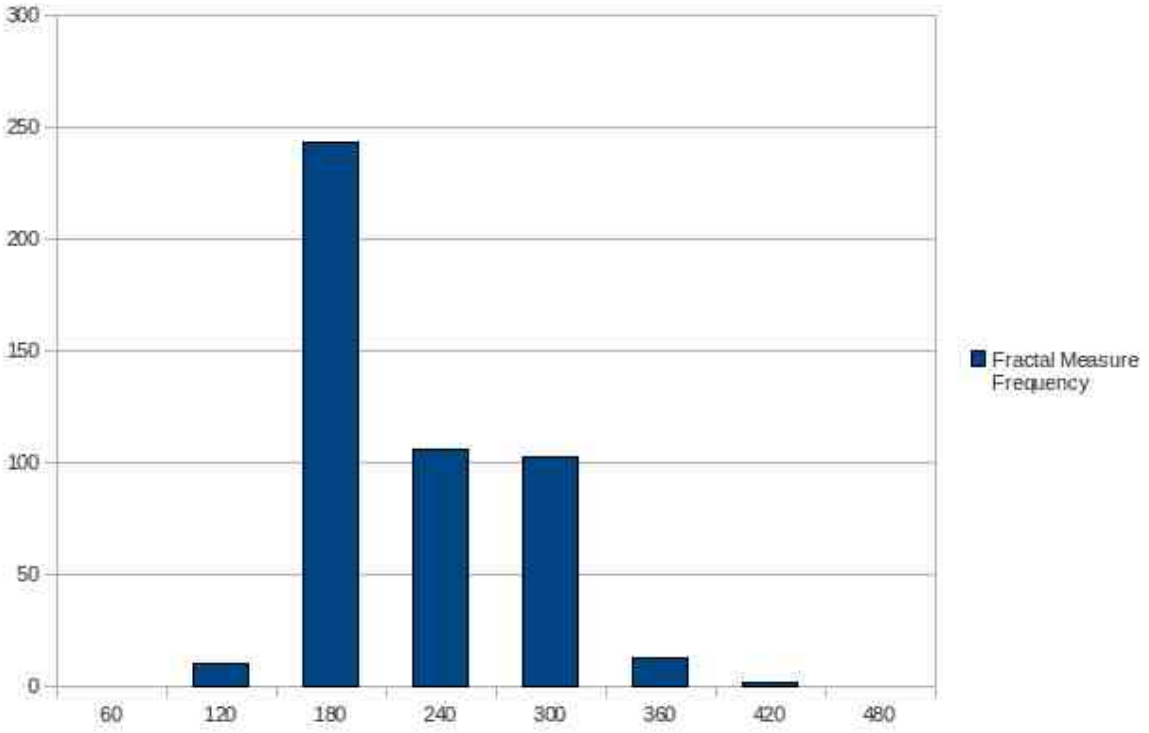

Figure 53: Hansenula Anomala, time 10 min, Fractal Measure Frequencies in the Intensity space, calibration data set

The Fractal Measure frequencies are shown in Figure 57 and the Fractal Measure frequencies for the calibration data are at Figure 58.

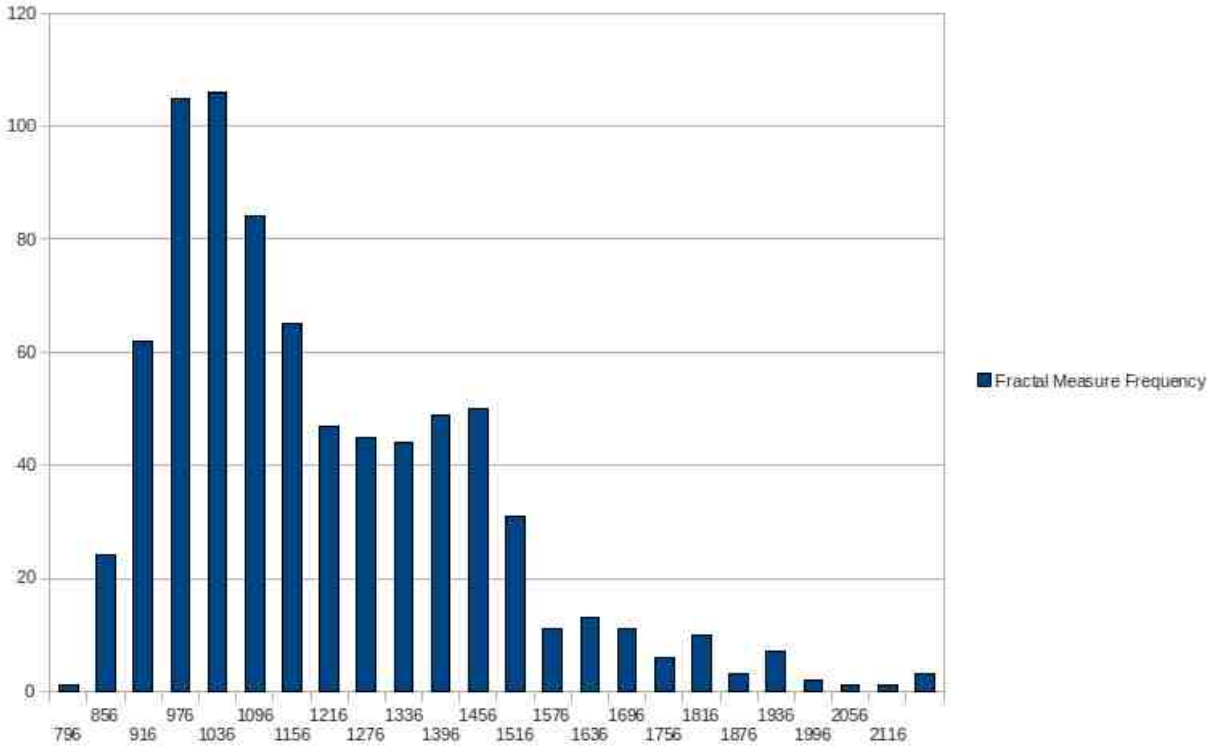

Figure 54: Hansenula Anomala, time 10 min, Fractal Measure Frequencies in the red color space

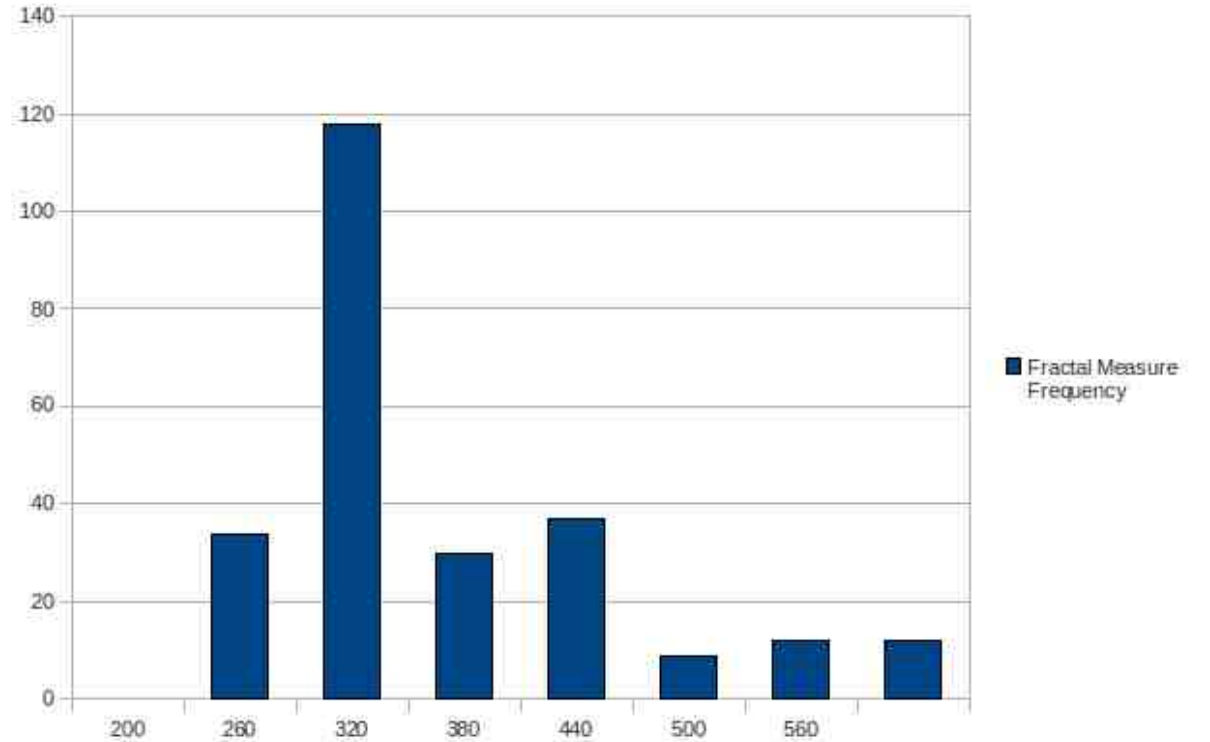

Figure 55: Hansenula Anomala, time 10 min, Fractal Measure Frequencies in the red color space, calibration data

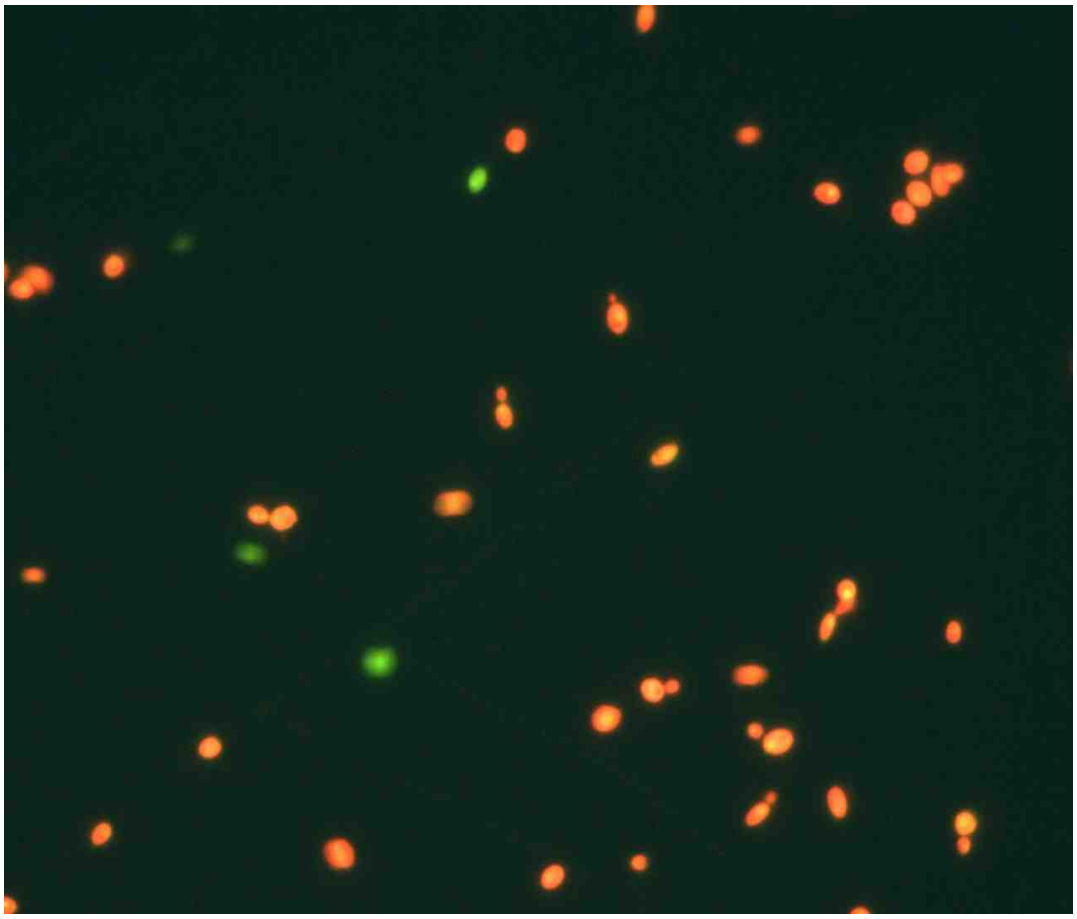

Figure 56: Hansenula Anomala, time 70 minutes

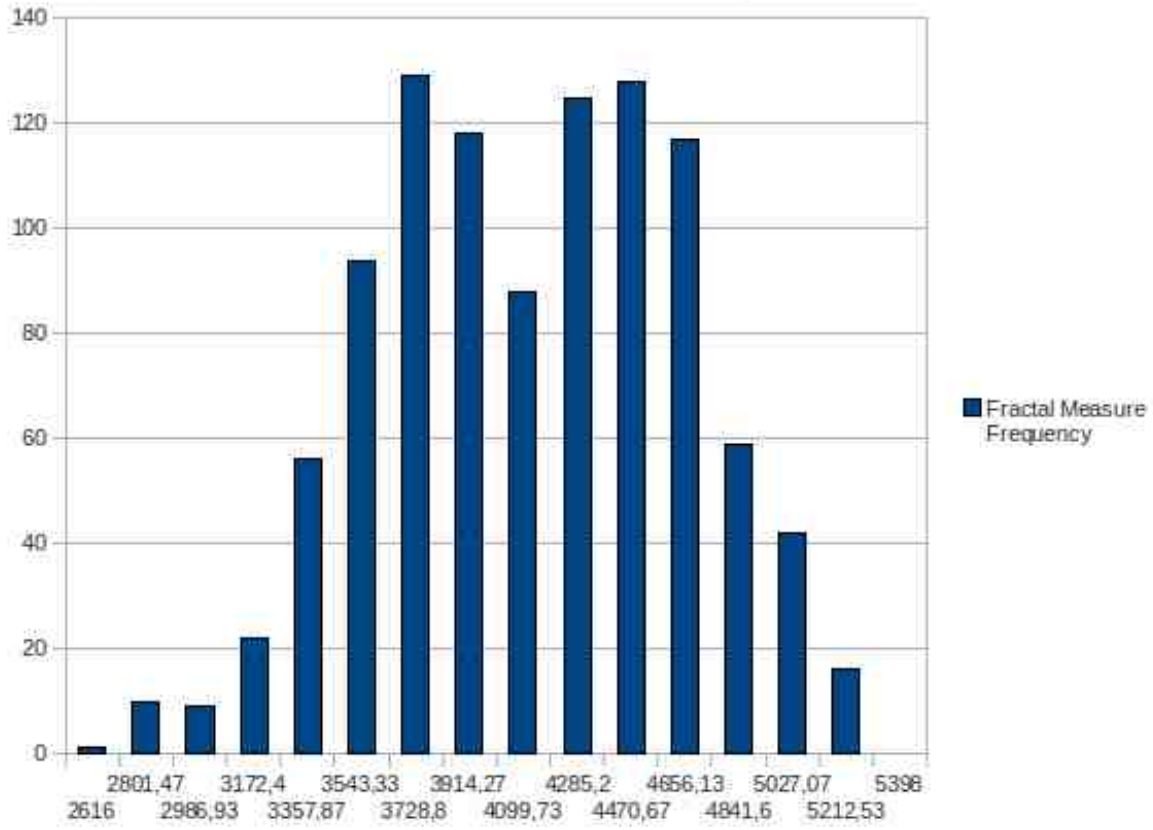

Figure 57: Hansenula Anomala, time 70 min, Fractal Measure Frequencies

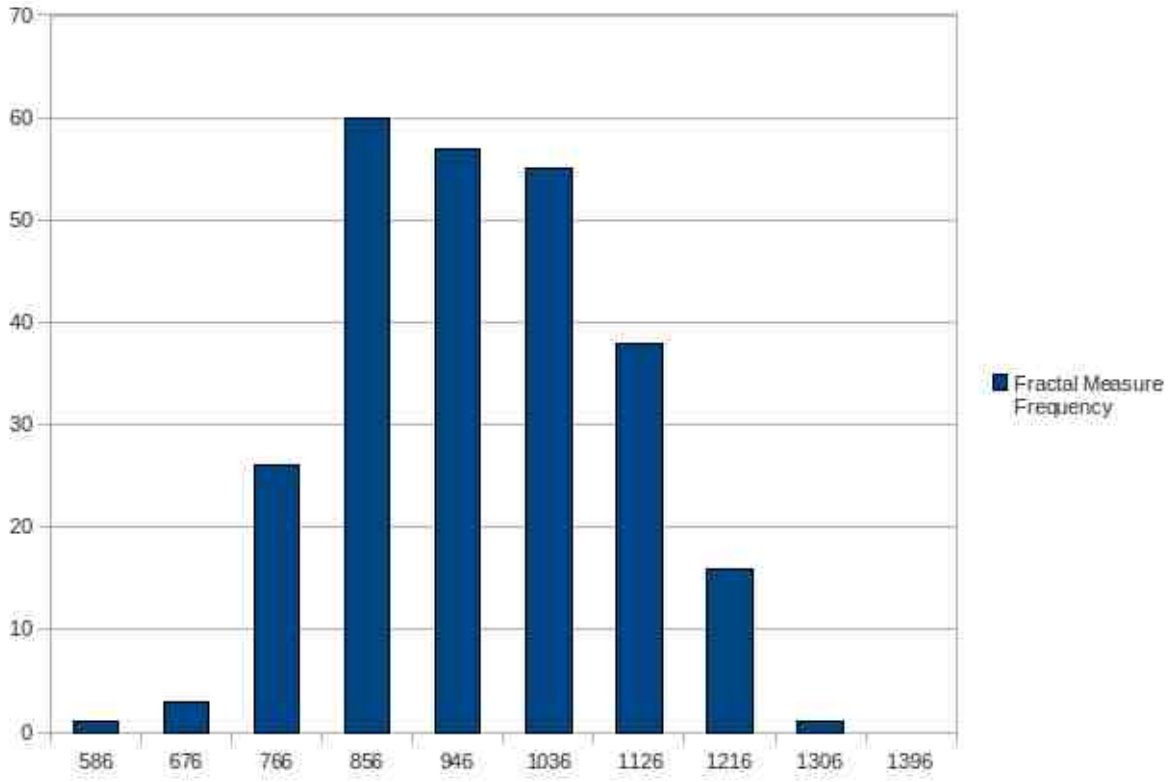

Figure 58: Hansenula Anomala, time 70 min, Fractal Measure Frequencies calibration data

8.1.2 Rhodotorula glutinis

The results of radiation experiment performed on yeast cell colony of the Rhodotorula glutinis family. The Figure 59 shows the colony at the 10 minutes after beginning of the experiment. The total amount of cells in the intensity colour space have been determined to be 28. The Fractal Measure Frequencies in the intensity colour space are shown in Figure 60 and the Fractal Measure Frequencies for the calibration data in same colour space are shown in Figure 61.

The analysis of the same data in red colour space show more dead or dying cells in the comparison to the population size then in the experiment with Hansenula Anomala species. The total amount of dead or dying cells have been determined to be 20 . The Fractal Measure Frequencies of the image data in the red colour space are shown in Figure 62 and the Fractal Measure Frequencies of the calibration data in the same colour space are shown in Figure 63.

The image data captured at the time 70 minutes (Figure 64), shows the total amount of cells in the colony to be 35. The Fractal Measure Frequencies are shown in Figure 65 and the calibration data Fractal Measure Frequencies are shown in Figure 66. The analysis of the same data in the red colour space shows the total of 20 cells dying or dead. Those are the nearly same numbers as at the beginning of the experiment, showing that while this colony was not in perfectly healthy state at the beginning, it is in same shape towards the end of the experiment. It might be possible that the reproduction rate of this specie allows for replacing the dying cells by their offspring before the radiation or it might be just simply immune to the level of the radiation used in the experiment. The Fractal Measure Frequencies in the red

colour space for the image data as well as for the calibration data are shown in the Figure 67 and Figure 68 respectively.

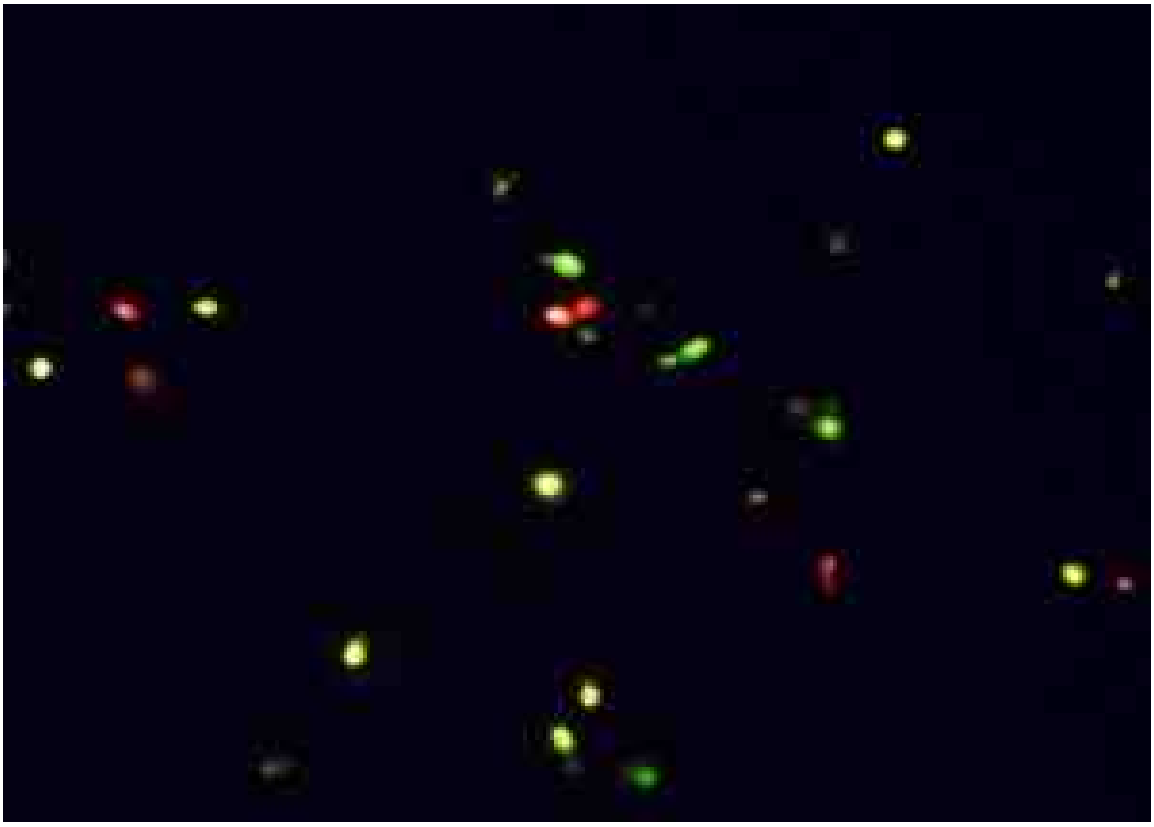

Figure 59: Rhodotorula glutinis, time 10 minutes

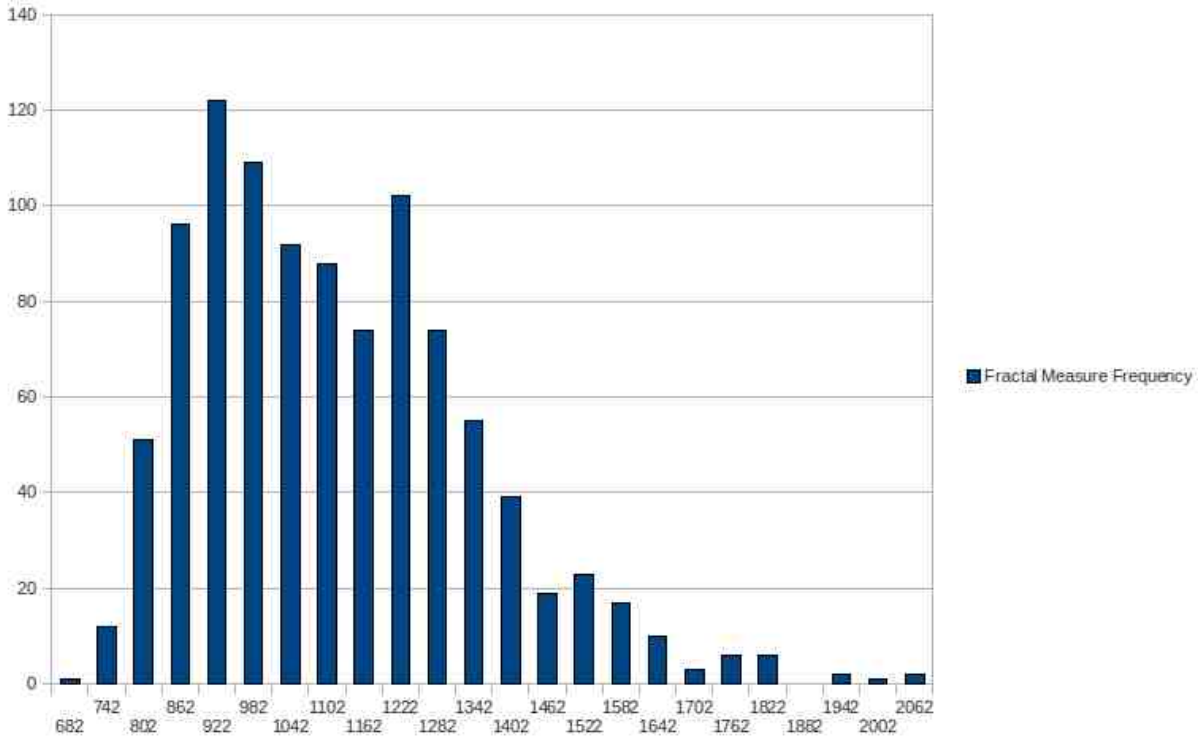

Figure 60: Rhodotorula Glutinis, time 10 minutes, intensity color space

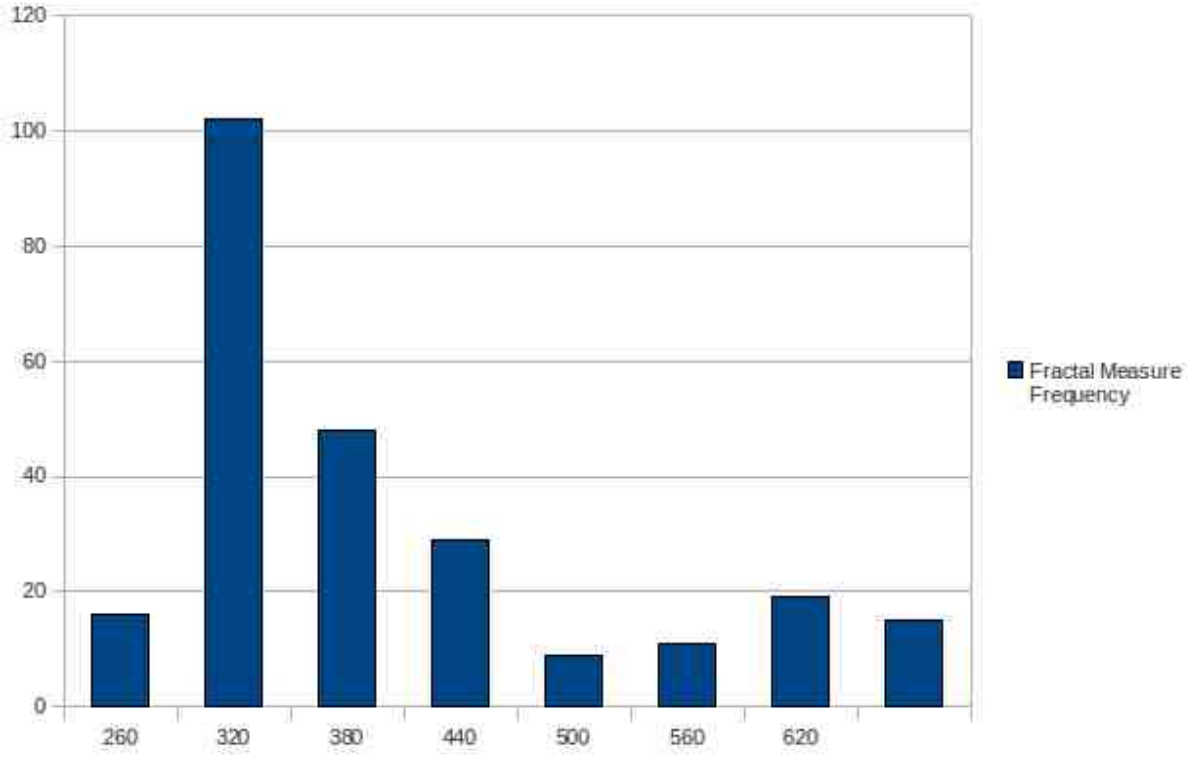

Figure 61: Rhodotorula Glutinis, time 10 min, intensity color space, calibration data

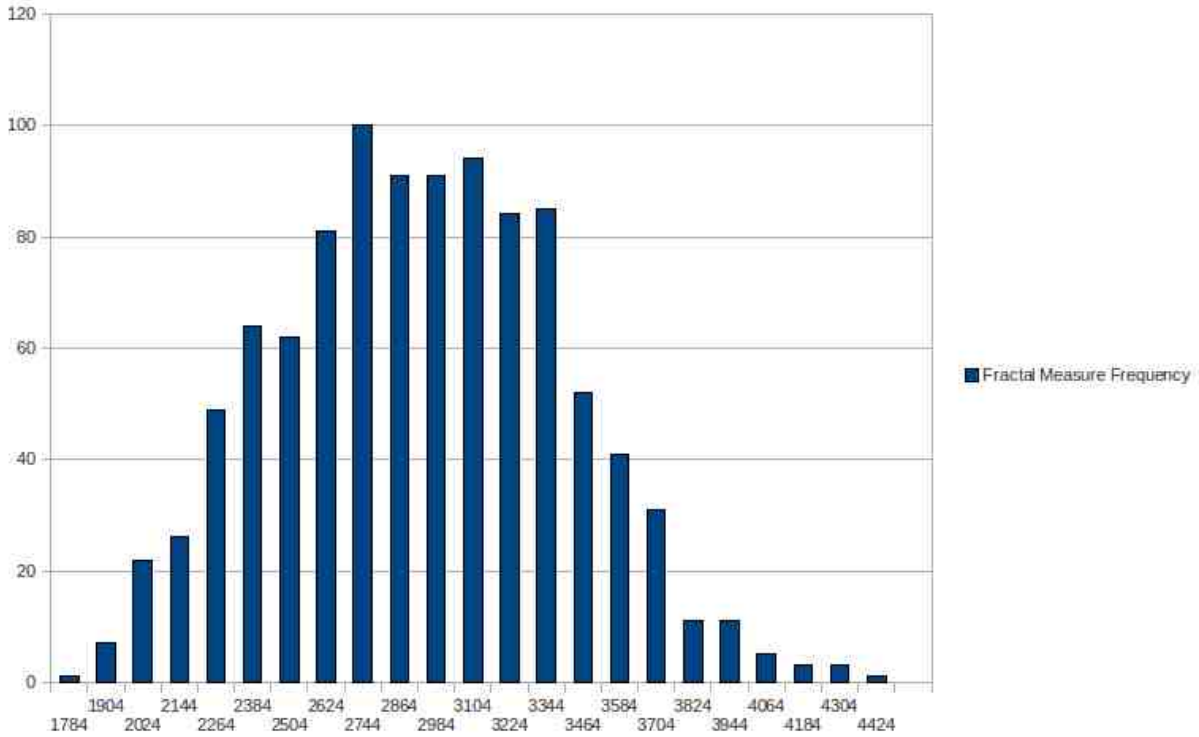

Figure 62: Rhodotorula Glutinis, time 10 minutes, red color space

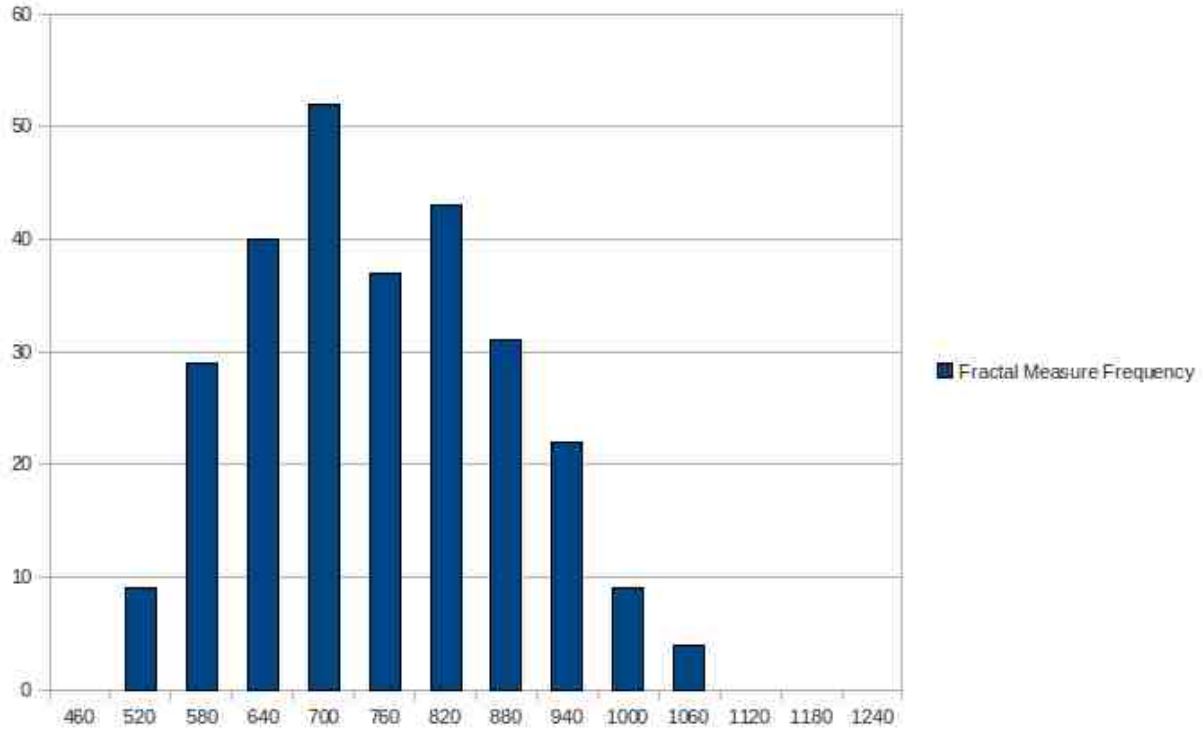

Figure 63: Rhodotorula Glutinis, time 10 minutes, red color space, calibration data

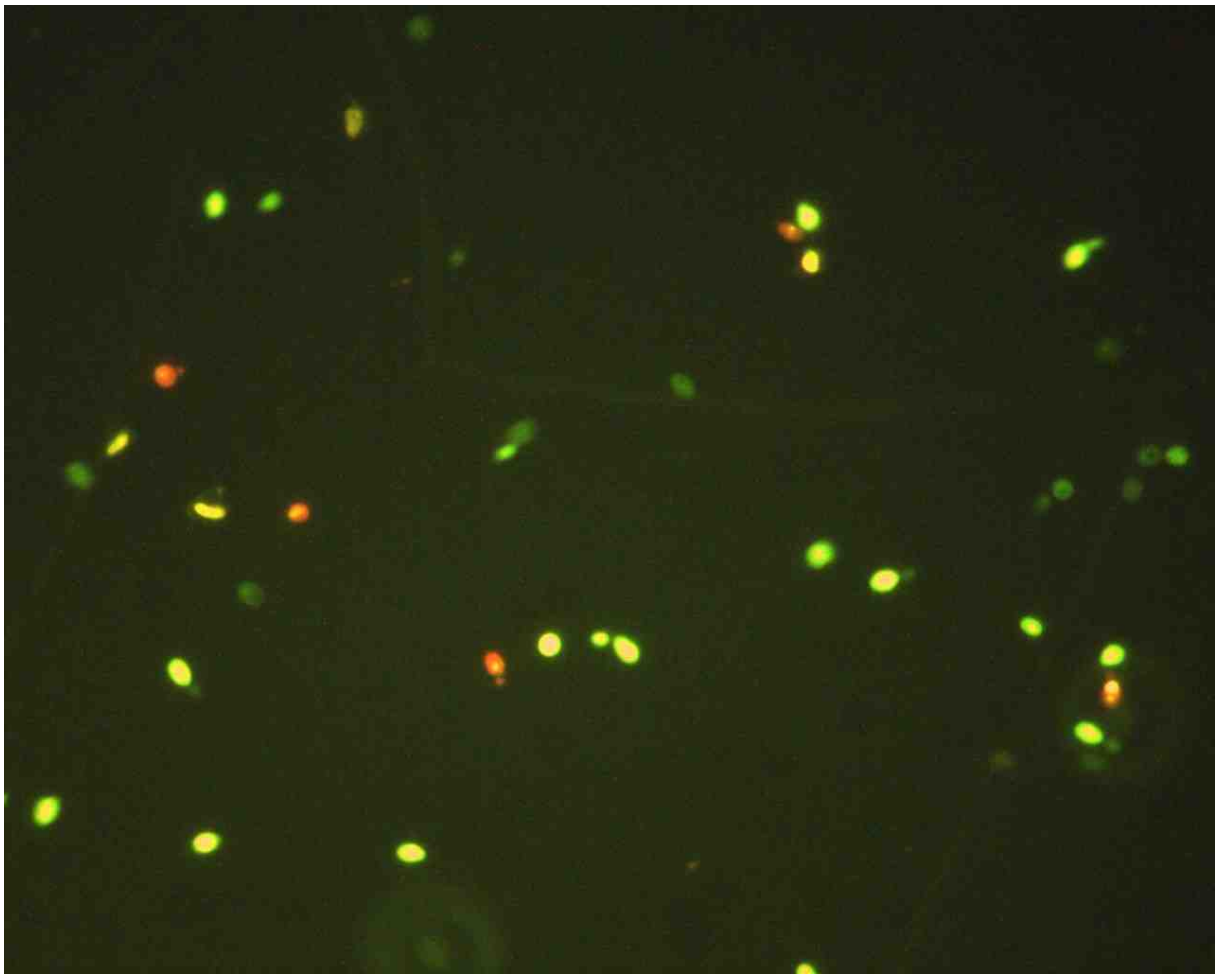

Figure 64: Rhodotorula Glutinis, time 70 minutes

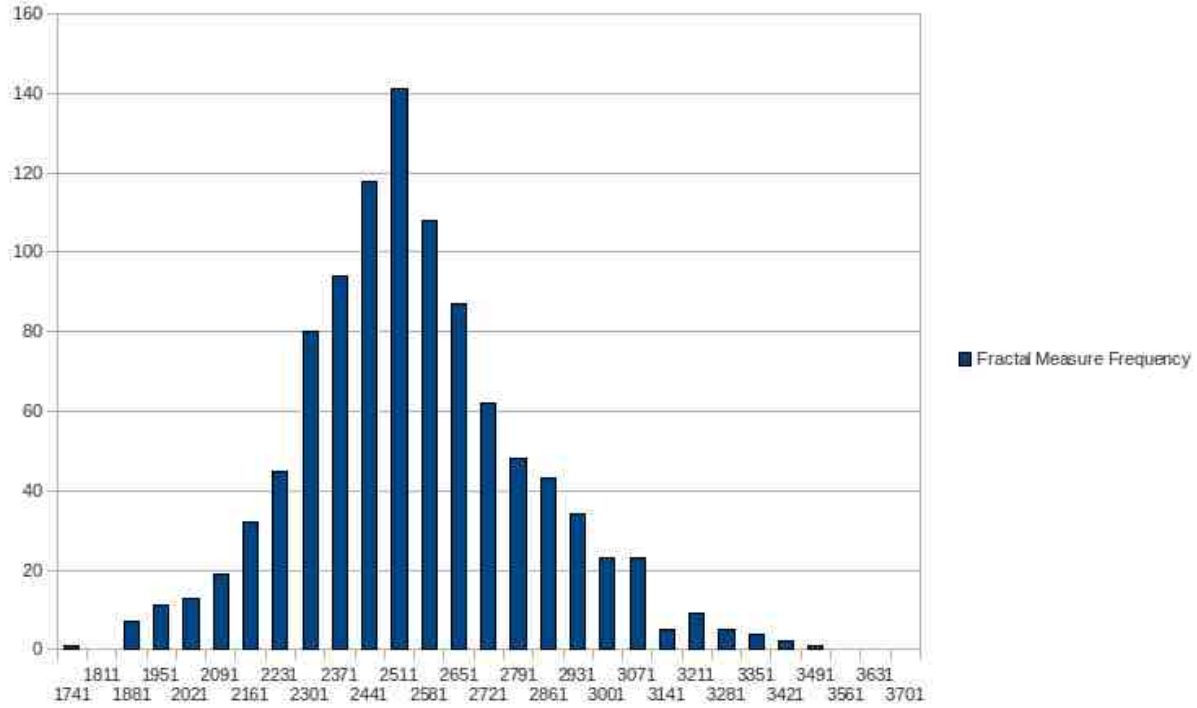

Figure 65: Rhodotorula Glutinis, time 70 minutes, Intensity color space

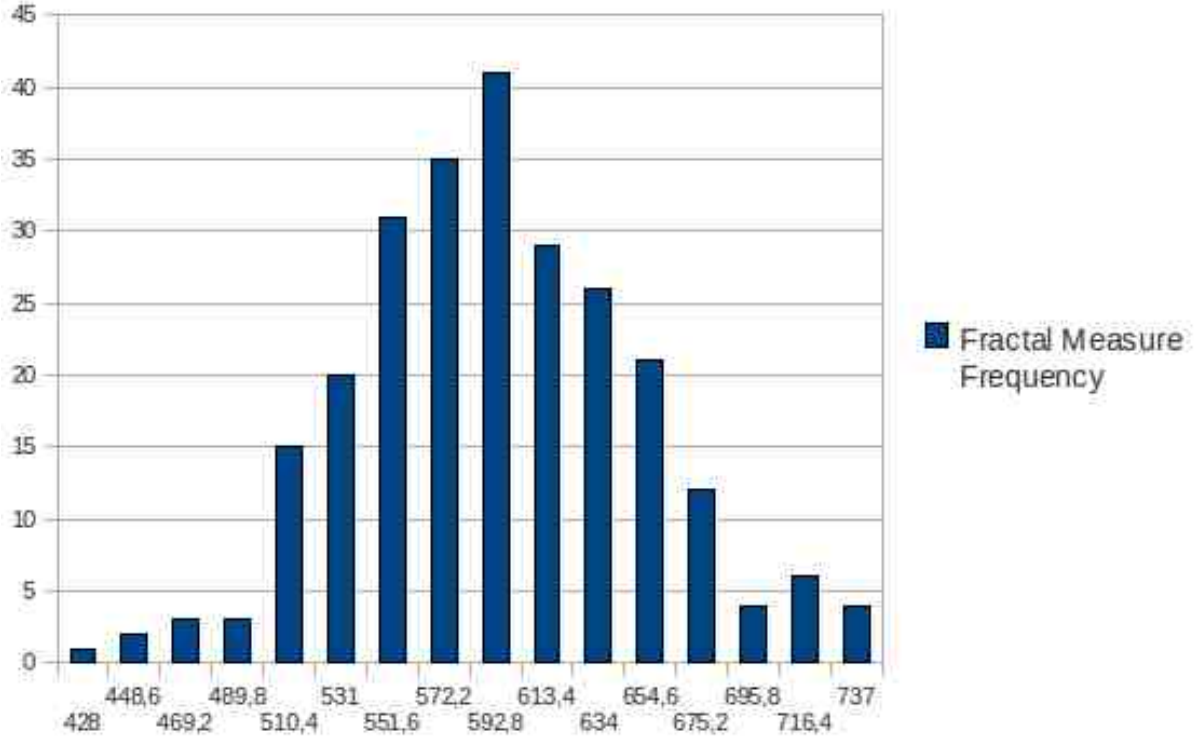

Figure 66: Rhodotorula Glutinis, time 70 min, Intensity color space, calibration data

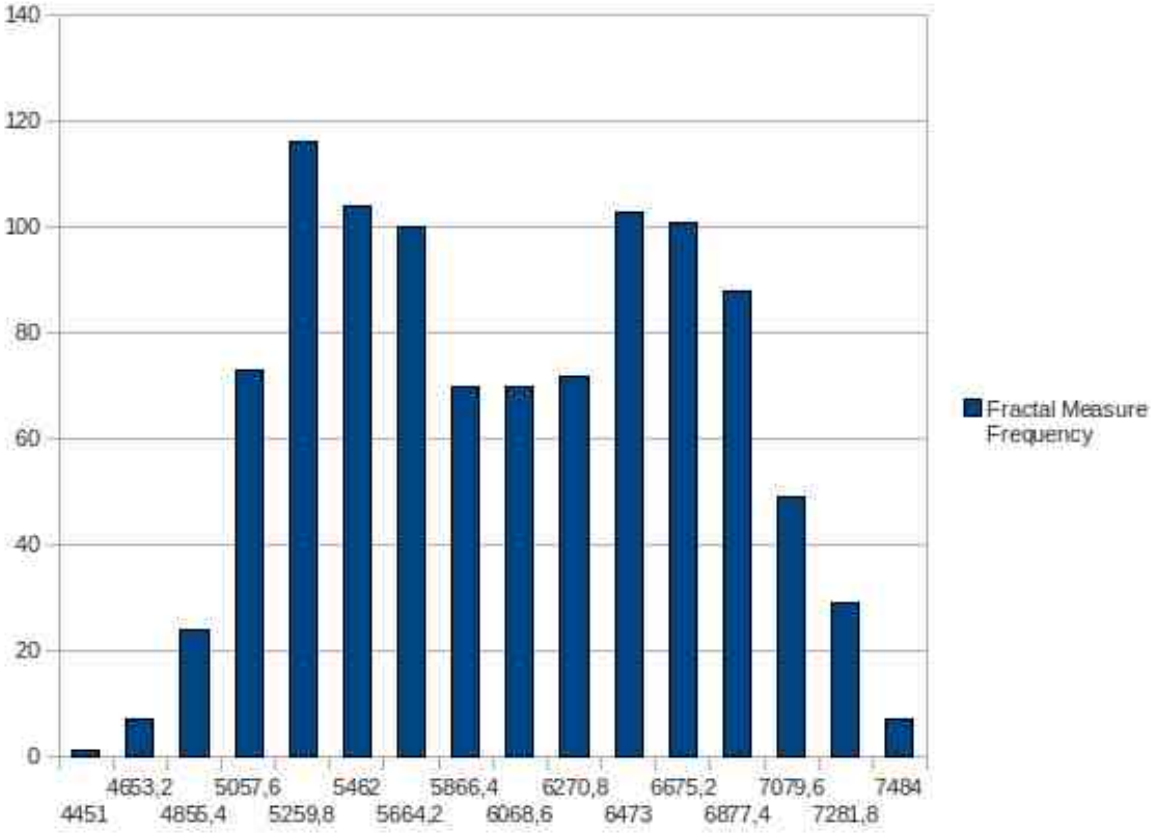

Figure 67: Rhodotorula Glutinis, time 70 minutes, red color space

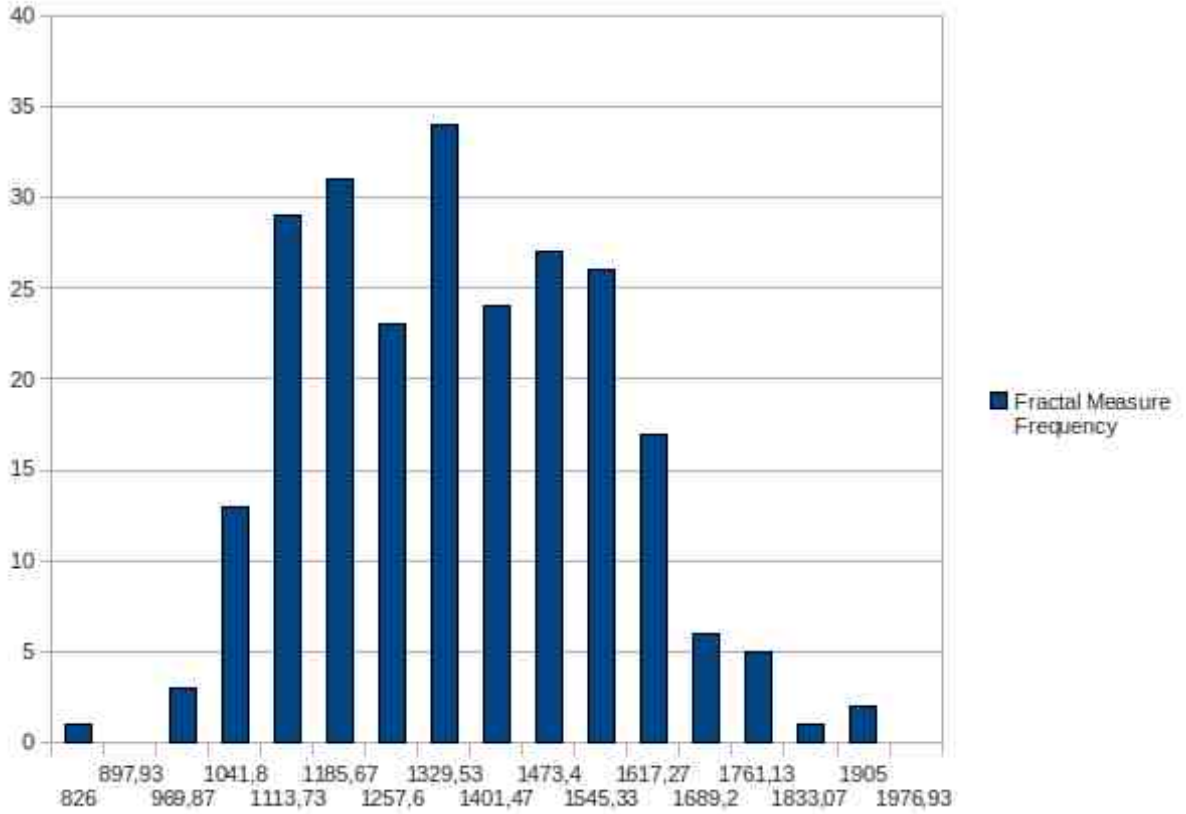

Figure 68: Rhodotorula Glutinis, time 70 minutes, red color space

8.1.3 Saccharomyces pastorianus

The last of the radiation experiments have been performed on the large *Saccharomyces Pastorians* colony as shown in Figure 69. The colony size have been estimated by measurement of the Fractal Measure Frequencies in the intensity colour space (Figure 70). The size have been found to be on 125 cells. The calibration data Fractal Measure Frequencies are shown in Figure 71.

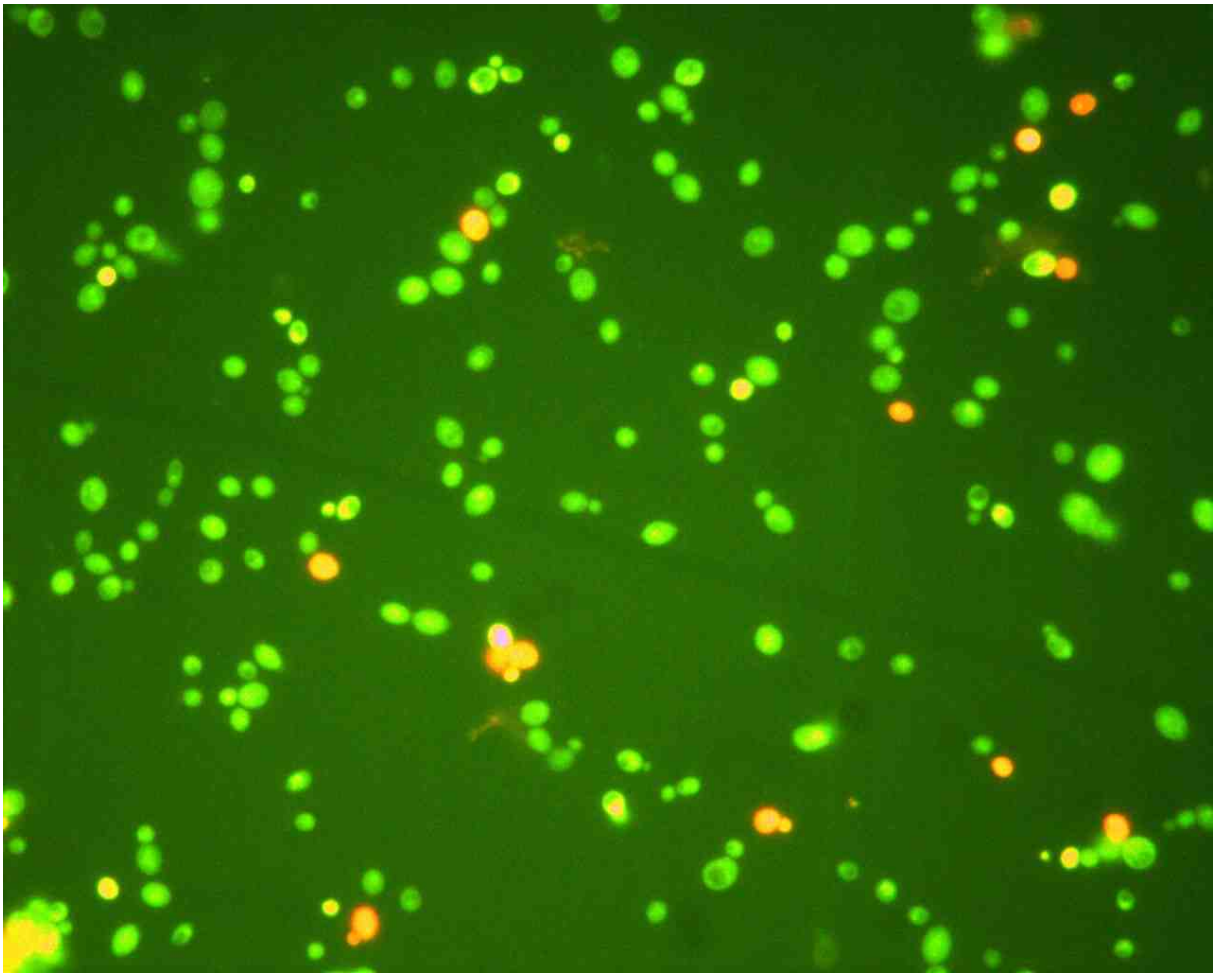

Figure 69: *Saccharomyces Pastorianus*, time 10 minutes

The analysis in the red colour space have shown there are already 36 cells dead or dying at this time. The Fractal Measure Frequencies for the image data and for the calibration set are shown in the Figure 72 and Figure 73 respectively.

The image data collected at the end of the experiment, in time 70 minutes (Figure 74), show that that the total amount of cells is nearly unchanged. Measured based on the Fractal Measure Frequencies in the intensity colour space (Figure 75) using the calibration data set containing single cell (Figure 76) shows the total amount of cells in the image to be 180.

The analysis in the red colour space revealed 43 of the cells to be already dead or dying. The Figure 77 shows Fractal Measure Frequencies for the image data in the red colour space and Figure 78 shows the frequencies for the calibration data set.

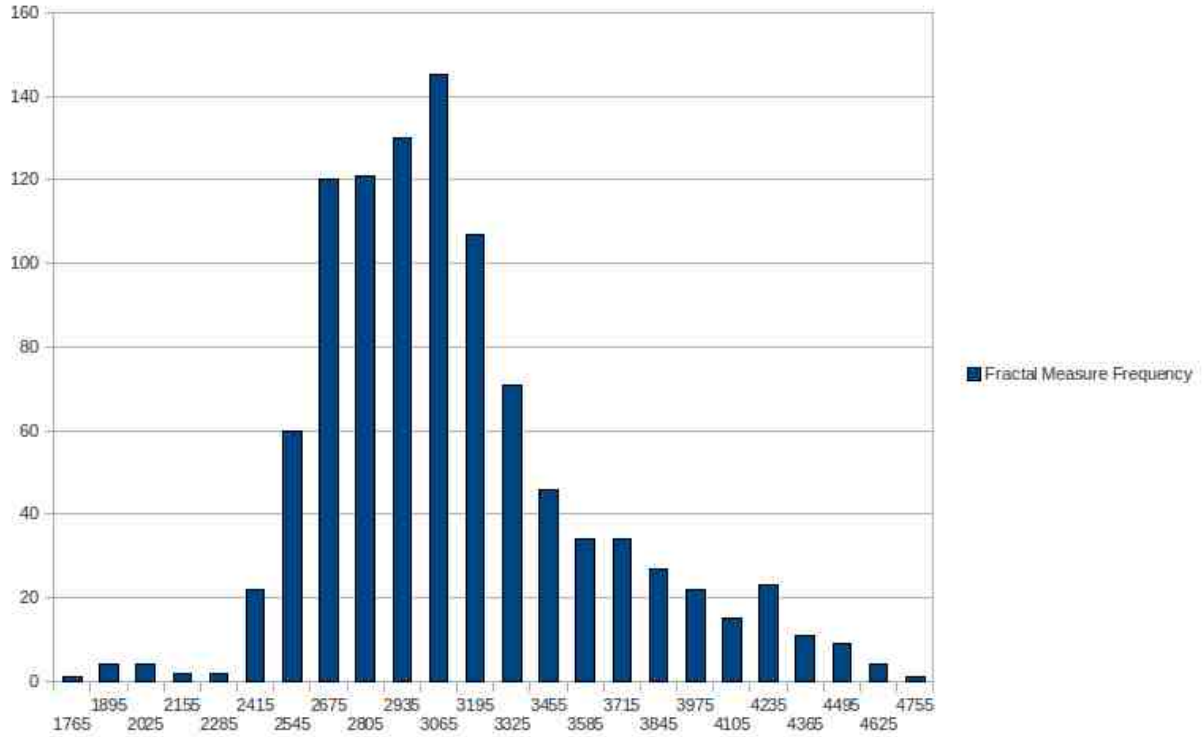

Figure 70: *Saccharomyces Pastorianus*, time 10 minutes, intensity color space

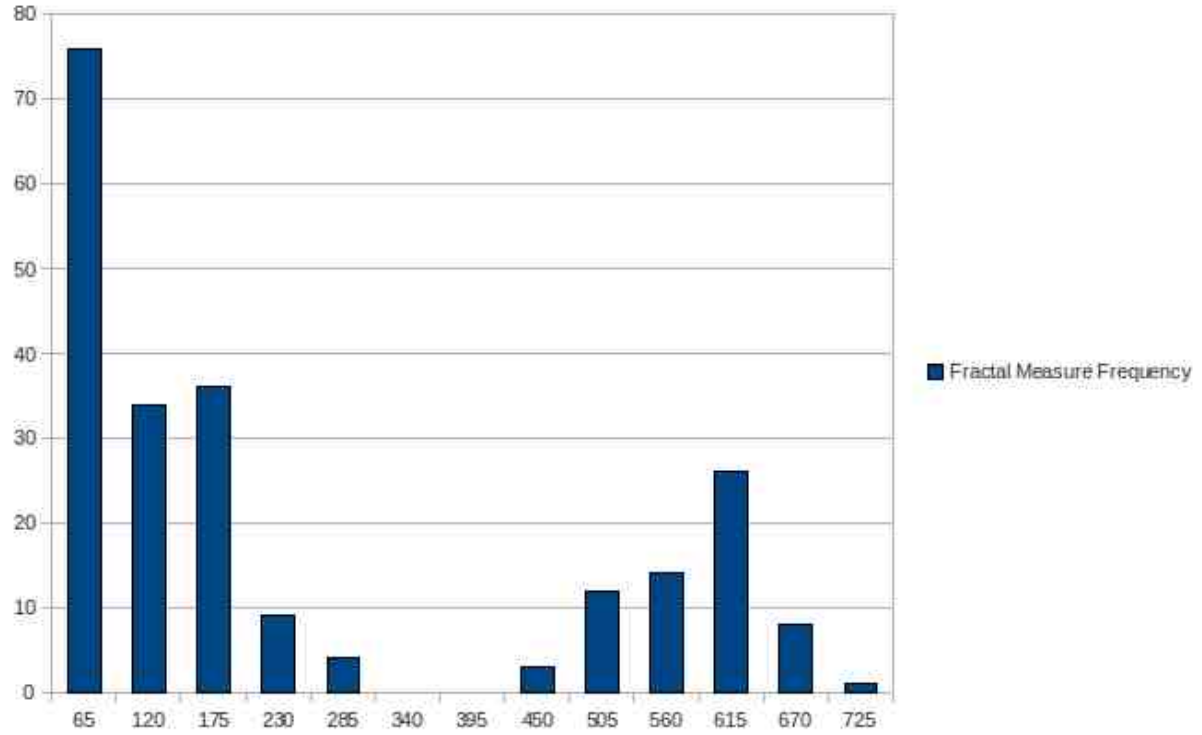

Figure 71: *Saccharomyces Pastorianus*, time 10 minutes, intensity color space, calibration data

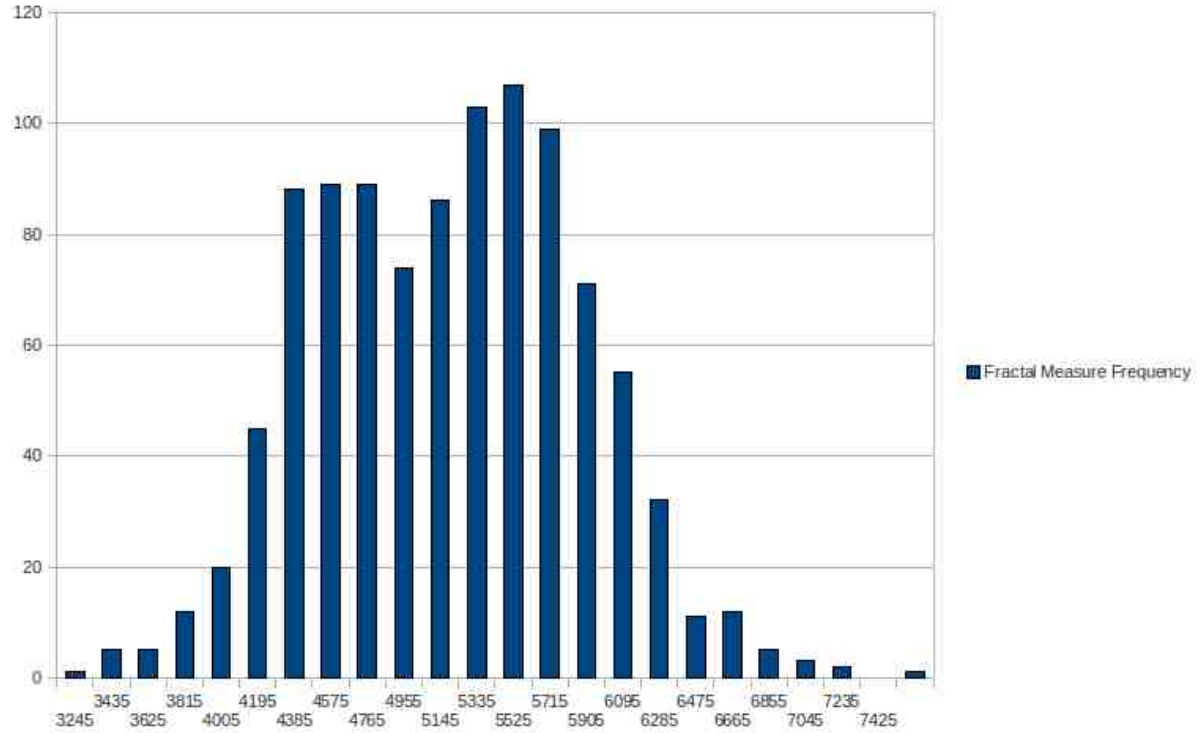

Figure 72: *Saccharomyces Pastorianus*, Fractal Measure Frequencies at time 10 minutes, red color space

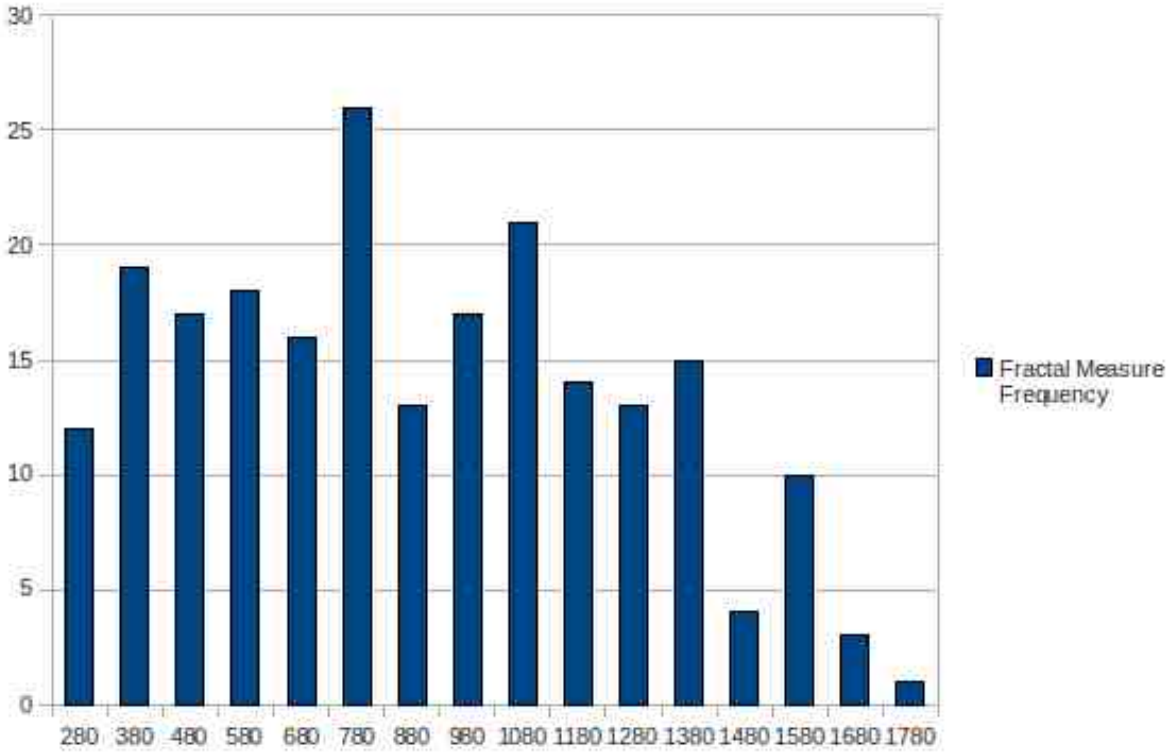

Figure 73: *Saccharomyces Pastorianus*, Fractal Measure Frequencies at time 10 minutes, red color space, calibration data

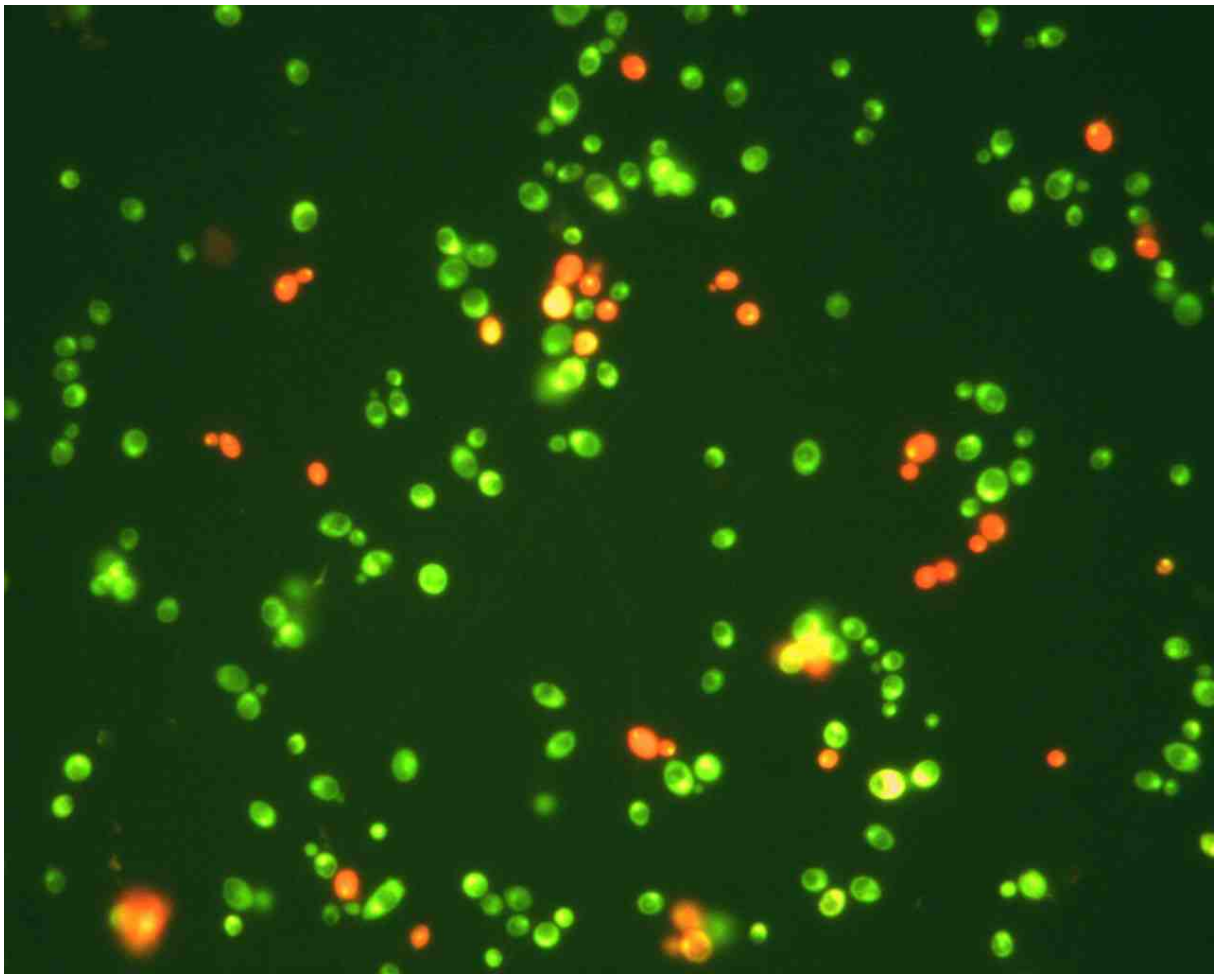

Figure 74: ***Saccharomyces Pastorianus*****, time 70 minutes**

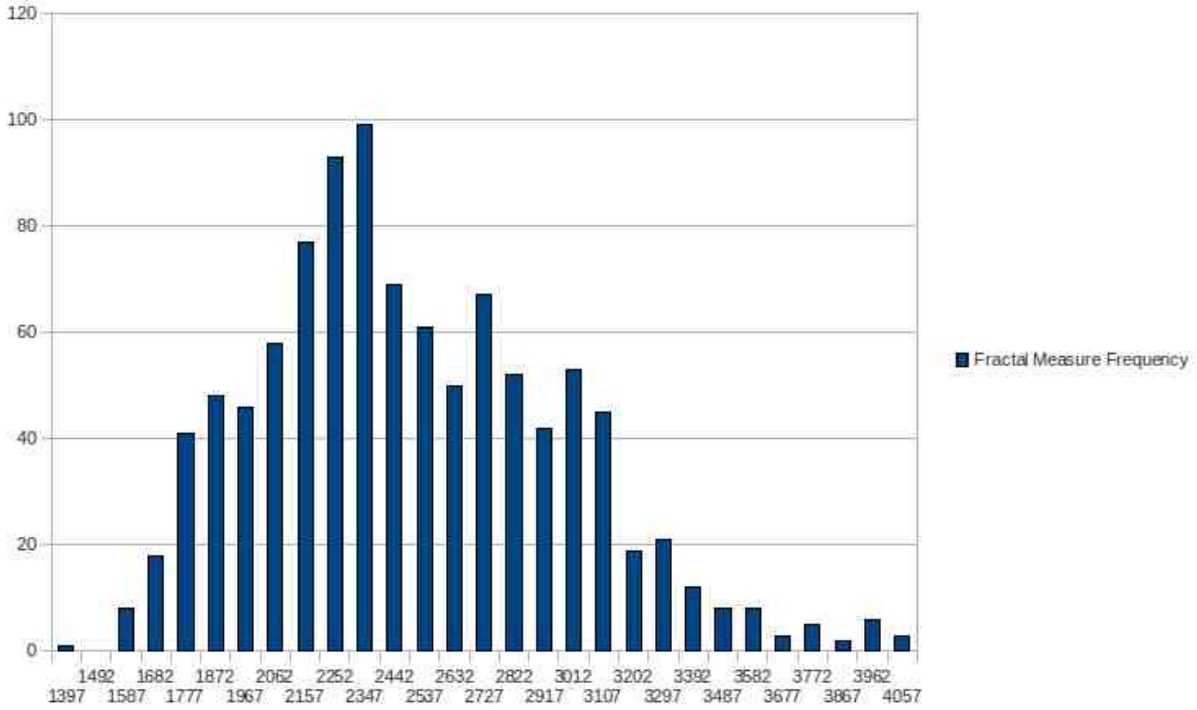

Figure 75: ***Saccharomyces Pastorianus*****, Fractal Measure Frequencies, time 70 minutes, intensity color space**

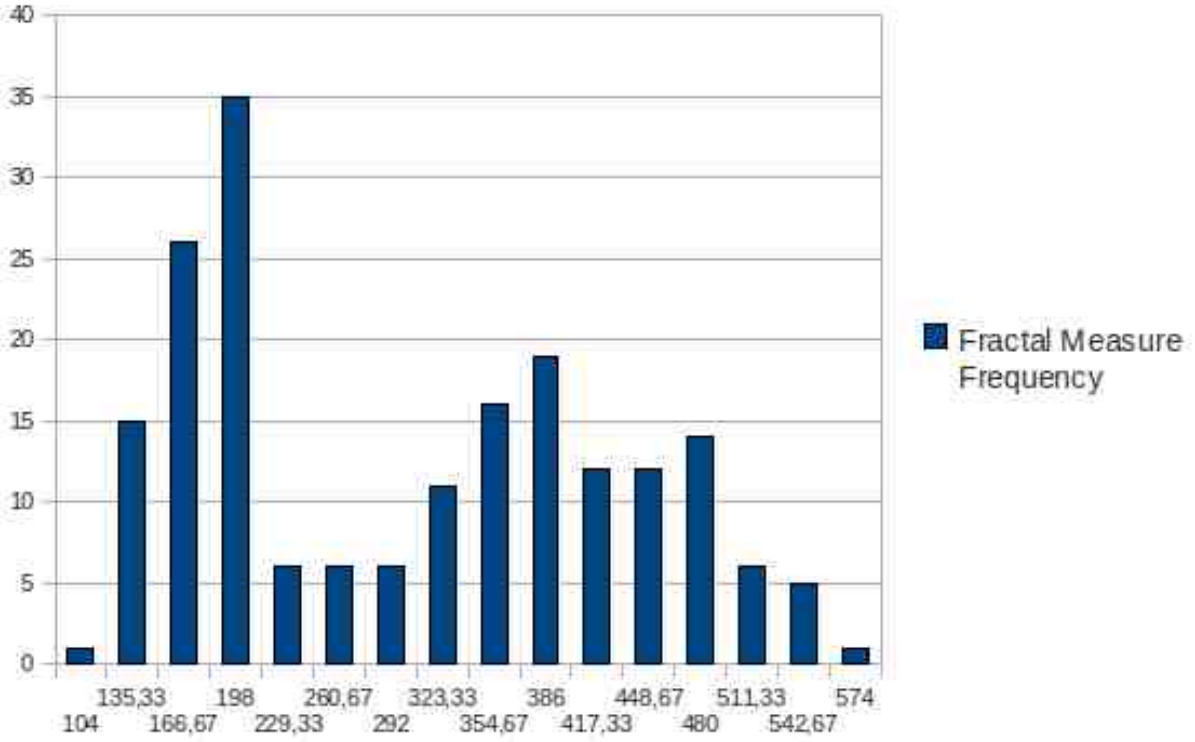

Figure 76: *Saccharomyces Pastorianus*, Fractal Measure Frequencies, time 70 minutes, intensity color space, calibration data

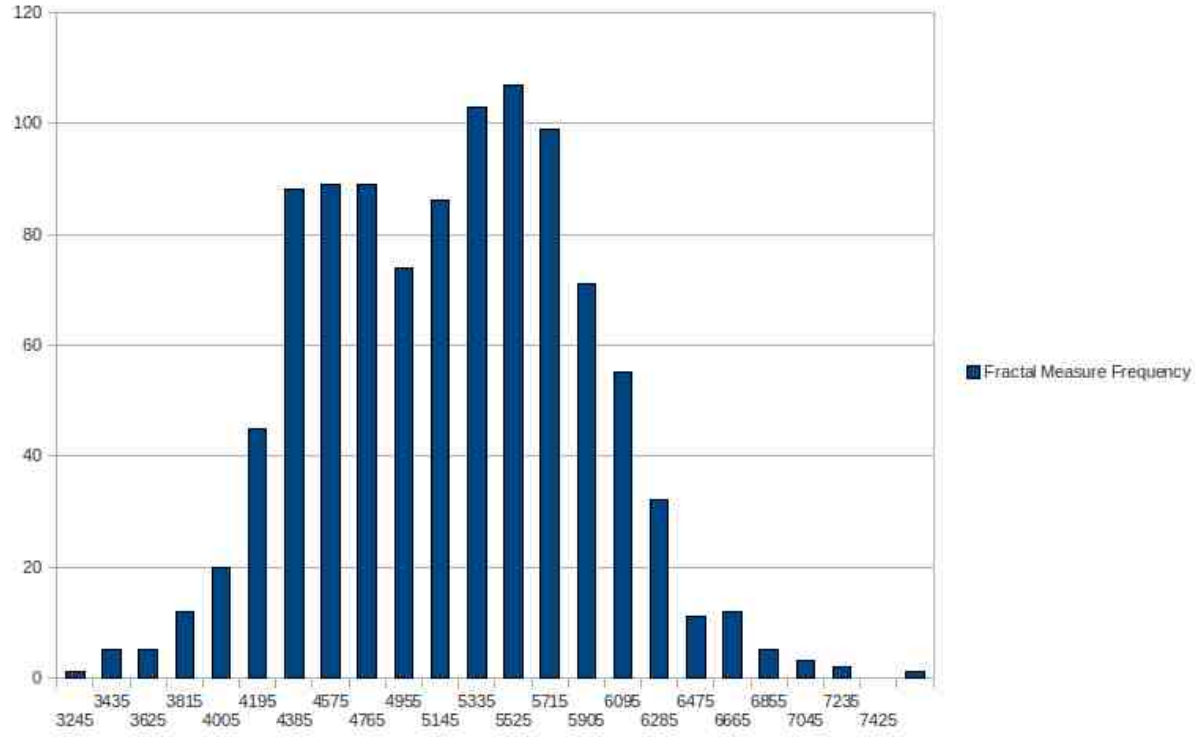

Figure 77: *Saccharomyces Pastorianus*, time 70 minutes, red color space

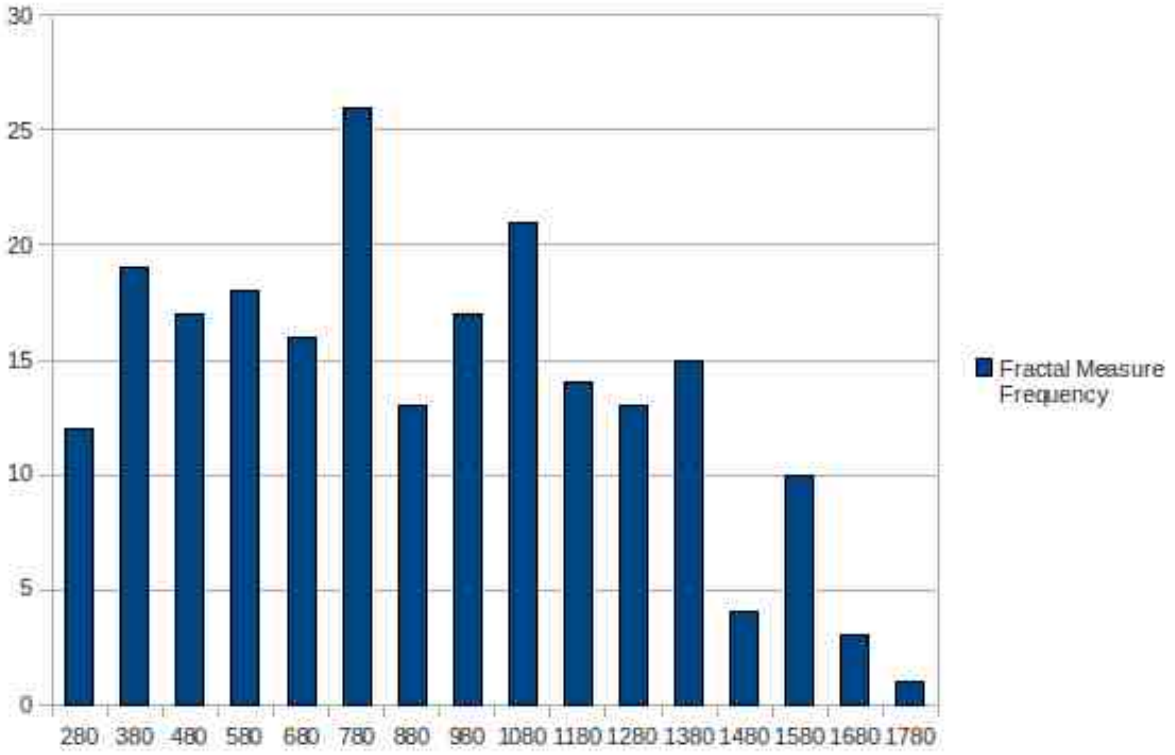

Figure 78: ***Saccharomyces Pastorianus*****, time 70 minutes, red color space, calibration data**

8.2 Appendix B - Articles